Synthesis, characterization and evaluation of ruthenium(II) polypyridyl complexes as sensitizer for dye sensitized solar cells

University of Fort Hare
Together in Excellence

By

Mkhohlakali Andile Cyril (200909133)
B. Sc., B. Sc. (Honours) Chemistry (UFH)

Being a dissertation submitted to the Faculty of Science and Agriculture in fulfilment of the requirements for the award of the degree of

Master of Science in Chemistry

of the

University of Fort Hare,

Supervisor: Professor P. A. Ajibade

January

DECLARATION BY CANDIDATE

I hereby declare that this dissertation submitted for MSc degree in Chemistry, at the University of Fort Hare, is my own original work and has not been previously submitted to any other institution of higher learning. I further declare that all sources cited or quoted are indicated and acknowledged by means of comprehensive list of references.

_____

Date

CERTIFICATION

This is to certify that this research is a record of original work carried out by Mkhohlakali Andile Cyril under my supervision in the Inorganic Materials Research laboratory of the Department of Chemistry, University of Fort Hare in fulfilment of the requirements for the award of Master of Science degree in Chemistry.

_____ _____

Date

Supervisor

P. A. Ajibade

Professor of Inorganic Materials Chemistry

B. Sc (Hons), MSc (Ibadan);

PhD (UniZul); MRSC (London)

DEDICATION

I dedicate this dissertation to my mother Miss Nozisile Bongiwe Mkhohlakali, my late grandparents Mr Hebelele Mkhohlakali and Miss Nophicile Mkhohlakali. Your undying spirit and faith in me from my young age has always being my motivation.

ACKNOWLEDGEMENT

Firstly, I would like to thank God 'The Almighty' for the gift of life, with Him anything is possible. I am deeply grateful to my supervisor, Prof P. A. Ajibade for his guidance, encouragement and thoughtful, fruitful discussion towards my work, and also his tolerance, patience with my mistakes. This work would not have been possible without his support. I thank him for his confidence and believe in me to work on DSSCs project, and for his consistence encouragement that help me pull through courses in chemistry.

I am immensely grateful to Dr. Taziwa for his assistance in fabrication of my solar cells, Dr. Le Roux, and Miss Mphahlele for their assistance in solar cell efficiency and electrochemical studies, for their contributions to this project has gone above and beyond the call of duty. I would like to appreciate Mr Mcako, for the instrumental analysis. I thank you for your assistance and for sacrificing your time. I offer my heartiest gratitude to my parents Nozisile Bongiwe Mkhohlakali and Dumisa Mkhohlakali for their love and the support from my brother Nceba Attwell Mkhohlakali. My family has always been my pillar of support and show unyielding support and care. Without them this uphill task would have been made impossible.

I would hereby like to express my sincere thanks to: Department of Chemistry, University of Fort Hare for admission, and the space to carry out the study. Sasol Inzalo Foundation, National research foundation for financial support. CSIR for giving me a chance for solar cell characterization and efficiency test. My fellow colleagues in the Inorganic materials chemistry group for their criticism, support and kindness.

I appreciate Miss Noxolo for her love, patience and endless support.

TABLE OF CONTENTS

CHAPTER TWO

CHAPTER THREE

CHAPTER FOUR

CHAPTER FIVE

LIST OF FIGURES

CHAPTER ONE

CHAPTER TWO

CHAPTER THREE

CHAPER FOUR

LIST OF SCHEMES

CHAPTER ONE

CHAPTER TWO

LIST OF TABLES

CHAPTER THREE

ABREVIATIONS AND SYMBOLS

LUMO - Lowest Unoccupied Molecular Orbital

HOMO¬¬- Highest Occupied Molecular Orbital

DSSCs - Dye-Sensitized Solar Cells

MLCT- Metal to ligand charge transfer

MC- Metal cantered

LC- Ligand cantered

DMSO- Dimethyl sulphoxide

UV-Vis -Ultra Violet-Visible Spectroscopy

PV- Photovoltaic

FF- Fill factor

η(%)- Overall conversion efficiency

DMF- N,N dimethyl formamide

$[Ru(dmso)_4Cl_2]$- Tetrakis(dimethylsulfoxide)dichlororuthenium(II)

UV-Vi - Ultraviolet visible region

PL- Photoluminescence

Dsphen- 4,7-disulphonic acid-1,10-phenanthroline

Dcaldphen- 2,9-dicarboxaldehyde-1,10-phenanthroline

Dcbpy- 4,4'dicarboxylic acid-2,2-bipyridine

Phen- 1.10-phenanthroline

Bpy- 2,2'-bipyridine

C.V- Cyclic voltammetry

A.M - Air mass

Calc. - Calculated

Min - Minutes

HTM- Hole transporting material

J_{SC}- Short circuit current density

V_{OC} - Open circuit voltage

ABSTRACT

Dye sensitized solar cell is the device that is made up of metal oxide semiconductor, electrolyte and ruthenium complexes as sensitizer. This device harvest sun light and convert it to electricity, the first ruthenium complex dye used was N3. In this study, ruthenium(II) polypyridyl complexes formulated as $[(RuLXLY)(NCS)_2]$, where Lx and Ly are different types of ligands comprising bpy or phen as ancillary ligands were synthesized and characterized by FT-IR and ^{1}H-NMR spectroscopy. The complexes were further characterized with UV-Vis, and photoluminescence (PL) spectroscopy. These dyes showed good photophysical properties, with absorption spectra dominated by metal to ligand charge transfer (MLCT) transitions in the visible region and part of the near IR (NIR) region of the electromagnetic spectrum. The solar cell fabrication with these complexes was done, using doctor blade technique, and these cells were further characterized for current- voltages (J-V) curve and solar cell efficiency test. The solar cells based on these ruthenium complexes using TiO_2 as semiconductor gave good (J-V) curve, with overall efficiency (η) between 0,2%- 1.02 %, with JSC = 0. 776-3.44 mA cm^{-2}, V_{OC} = +/-0.59 V and FF = 0.5-0.6 under global air mass (1.5AM) illumination using potassium iodide in acetonitrile as electrolyte.

Key words: Ruthenium(II) polypyridyl complexes, photophysical properties, dye sensitized solar cells, fabrication, solar cell efficiency, current- voltage curve.

CHAPTER 1

INTRODUCTION AND LITERATURE REVIEW

1.0 Introduction

Energy is very vital to the economic and social development of the world and it improves the quality of life in all countries, therefore the world is conscious about consumption, generation, distribution, efficiency and sustainable type of energy source [1]. The major concern is the need of controlling the atmosphere, which is the basic need in quality of life [2]. Recently, the utilization of energy has increased due to increase in demand, and has also resulted in considerable interest in the conversion of energy to electricity [3–5]. There are two different kind of energy sources is available into two different alternative energy sources [6–8]. Non-renewable energy source and renewable energy source. Non-renewable energy source uses fossil fuels which include; coal, natural gas, and nuclear power [9] .

Theconsumption of non-renewable energy sources lead to its depletion and it is not replaced or renewed. The conversion of energy to electricity using fossil fuels, can lead to the emission of unwanted materials to the atmosphere, such as carbon dioxide, nitrous oxides and carbon monoxide that leads to atmospheric pollution, increase in greenhouse gases and global warming [10]. This emission which also causes pollution and global warming, affects the planet's ambient temperatures. Temperature increase caused by global warming could probably result in floods, droughts, glacier melting and serious disruption in agriculture and ecosystem if the actions are not taken to reduce their emission. As result of the consequences of no-renewable energy source development of the alternative and sustainable energy is an attractive area of research [8].

1.0 **Renewable energy**

Renewable energy is the energy that is generated from natural resources, which includes the biomass energy, wind energy, geothermal energy, hydropower, solar energy/photovoltaic energy [4-5].

1.1 **Wind energy**

Figure 1: The picture of turbines that are used for the generation of wind energy

In ancient years, the wind energy has been used for milling grain, mostly in rural areas, it was known to be used from windmill for pumping water and sailing boat [5], but recently there are several attempts to build large scale wind power system to generate electricity [4-5]. Since the 10^{th} century, wind has been used for the above uses and other low power applications, but there were several attempts to build large scale wind power system for the generation of electricity [8]. In recent years wind farm commonly employs turbines, these turbines can be located either on

land, near-shore and offshore to control and make wind energy for electricity generation[5-8]. Wind turbine uses either horizontal axis or vertical axis turbines to convert wind energy into electricity, whereby kinetic energy is converted to mechanical energy [4].

1.2 **Biomass energy**

Another recognized source of energy for the electricity generation is biomass, which has become a considerable interest, because its zero carbon emission to the atmosphere. It is also known as a source of chemical energy [11-12]. Biomass is the term used for material originating from plants (including algae), trees and crops, and is essential for the collection of sun's energy through photosynthesis [12]. Biomass can be converted into useful forms of energy such as heat, electricity and liquid fuels [13].

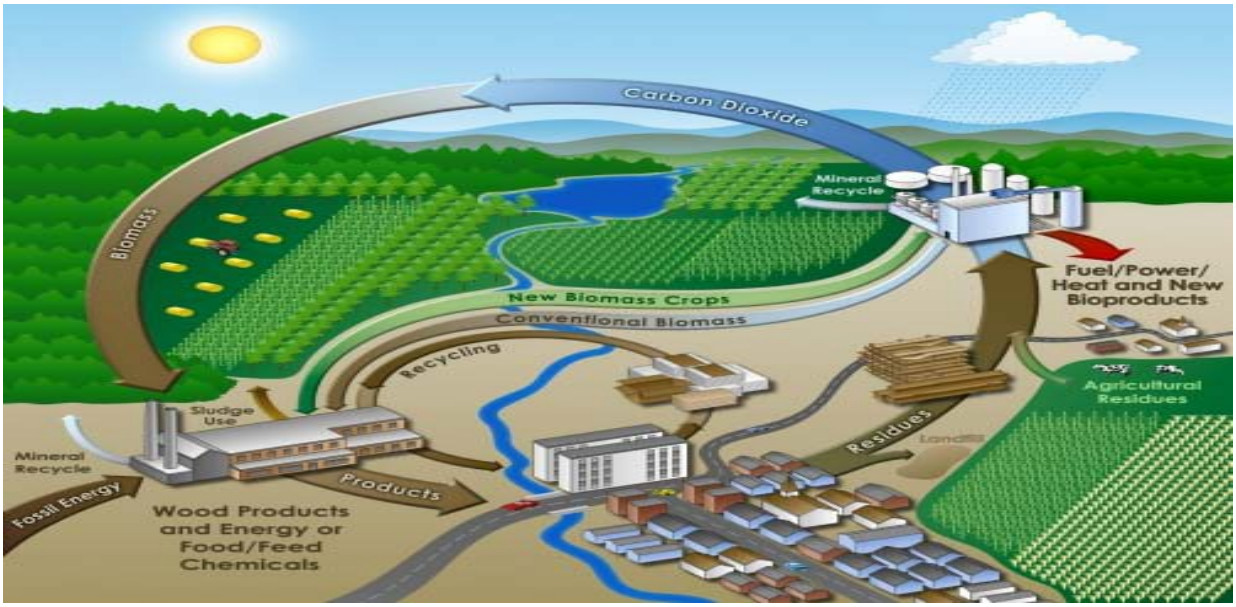

Figure 2: This schematic diagram that illustrates the process of conversion of biomass material into electricity [11].

1.3 **Geothermal energy**

Geothermal energy is heat stored in the earth crust. It is the thermal energy stored in rocks, and fluid that fills in the fractures and pores in the earth's crust. According to Bahadori *et, al.*[14] geothermal power has a significant benefit because it is environmentally benign [9], it is renewable and the temperatures are being renewed by conduction from adjacent rocks particularly igneous granites rocks, and heat is generated by natural radioactive decay and provide a base-load power and heat for industrial processes[14]. And it is able to provide base-load power and heat from the process. Place of target for the heat energy are: (i) subduction zone, due to place tectonic theory, as earth's plate move towards each other, one with low density subduct (move beneath the other) and the magma (molten material rises), (ii) in faulting area.

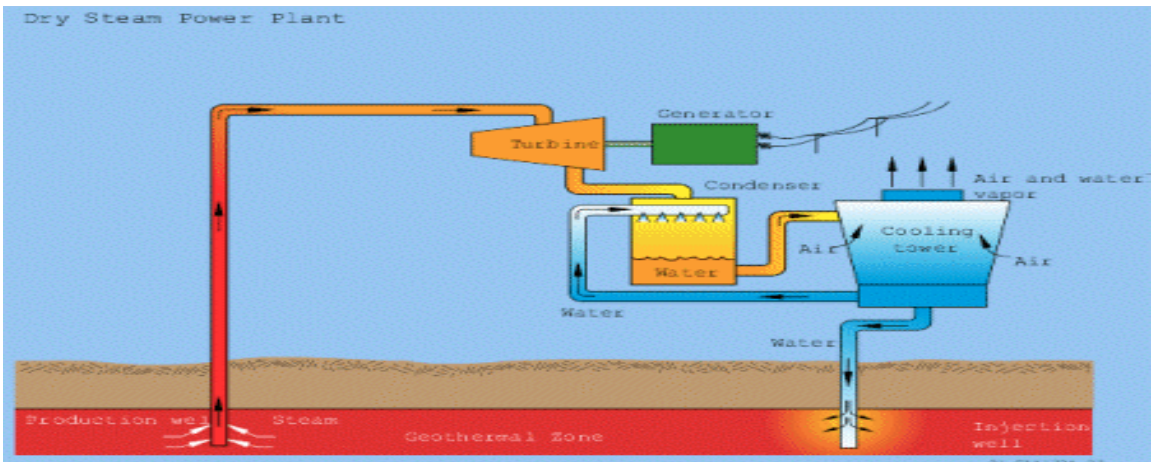

Figure 3: The schematic diagram of a geothermal energy source and the process of electricity generation.

The most compelling feature of the geothermal energy process is that, the production of carbon emission is zero, which is potentially making it one of the cleanest energy sources.

1.4 **Hydrothermal energy**

Hydropower is another type of renewable energy source and in some countries it has been shown that hydropower is the largest source of energy of domestic electricity [15]. According to Darmawi hydro energy can be harnessed from water current by simply utilizing velocity of water stream [16]. The power can be extracted from the ocean and water current by using submerged turbine, capturing energy through as hydrodynamic [6]. The hydropower does not consume or pollute water, instead uses the generated power and it leaves vital resource available for other uses. It has been predicted to take a greater part of electricity generated from renewable energy, but unfortunately it is not widely distributed across the world [15].

Figure 4: The diagram represents the hydropower, generate electricity from the river current [15].

1.5 Solar/ photovoltaic energy source

Photovoltaic energy also known as solar energy, which uses solar cells for the conversion of solar light directly into electricity through photovoltaic effect i.e. movement of electrons into electric field and it create electric current [17]. The most commonly used solar cells are based on first generation conventional crystalline silicon among the second generation amorphous silicon made up of polycrystalline silicon including cadmium telluride (CdTe), and copper indium gallium copper indium gallium diselenide (CIGS) [1,11] which is in the 3rd generation, (ii) dye sensitized solar cells [1,4,11], (iii) quantum dot solar cells [2, 17] which is the derivative of DSSCs. These solar cells have found to have high efficiency in converting light (photon) directly into electricity [18].

1.5.1 Silicon-based solar cells

The operational principle of crystalline (c-Si) based photovoltaic solar cells is quite simple, and it does not mimic the photosynthetic system as DSSC. Silicon based solar cells are classified into three layers:

- The n-type
- The p-type
- P-n-junction type

Silicon based solar cell has high solar energy conversion efficiency [12,13], but its manufacturing process is very costly, for that matter it has limited its popularity [12]. It has a complex preparation process, it needs dopants to create the hole and mobile electron to create the electric current [19]. The major disadvantage of using silicon based semiconductor are, it is not found free in nature, but found as an oxide, for example in quartz, and silicates (clays and phyllosilicates).

i. The n-type semiconductor

This is formed by doping with group V elements, such as phosphorus and arsenic, because silicon has an extra electron to these elements and it works as donor anode

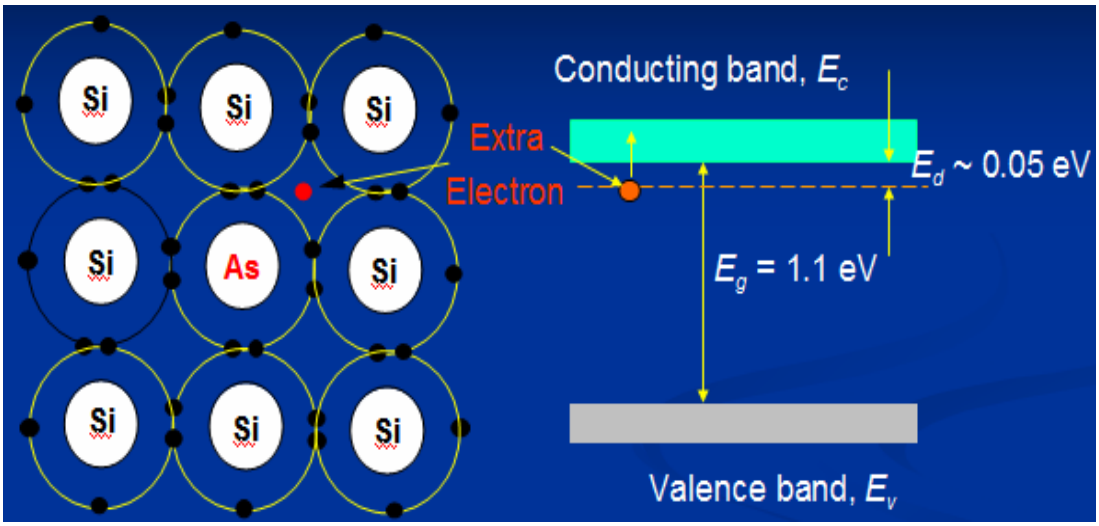

Figure 5. This schematic diagram of the n-type semiconductor layer of crystalline silicon, and its band gap [19].

ii The p-type semiconductor layer

The p-type is formed when the silicon is doped with group(III) elements, e.g. boron, which leave silicon electron deficient, and create a hole and the semiconductor become as cathode ‘acceptor’.

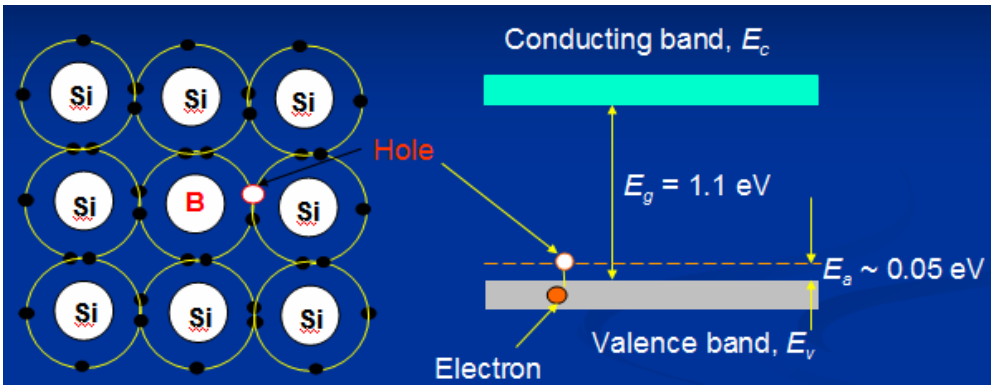

Figure 6: The schematic diagram of the p-type semiconductor layer, and its band gap. Showing how the hole is created and electron trying to fill the hole.

(iii) The p-n-junction

In p-n-junction it is the combination of the p-type semiconductor layer and n-type semiconductor layer. In this semiconductor layer both hole and extra electron is created, and this is known as an electron - hole pair. This mechanism leads to different potential in the anode and cathode, and brings about electron flow, and generates an electric current.

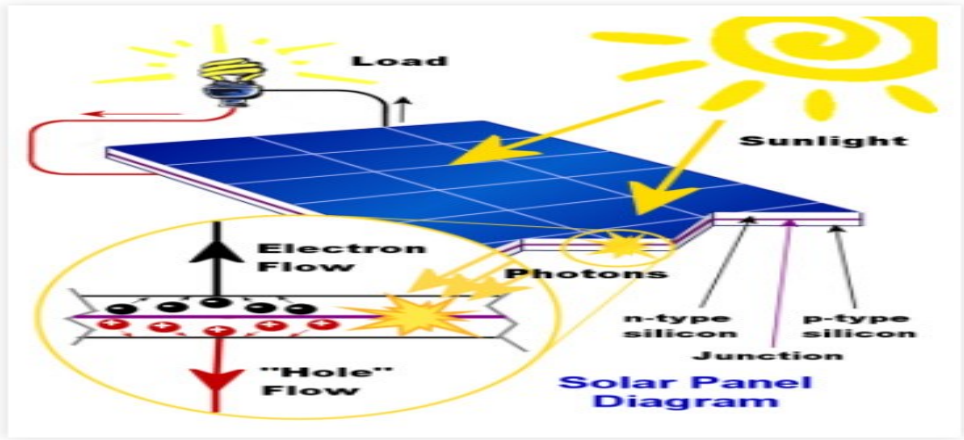

Figure 7: Schematic diagram of the pn-junction. Electrons are driven to the negative layer while leaving the hole behind [19].

1.5.2 **Dye- sensitized solar cells**

As a result of high cost of the current commercial silicon based solar cells, dye-sensitized solar cells appeared to be promising alternative, due to its cost effectiveness [19]. The operational principle of dye sensitized solar cell (DSSCs) is analogous to that of natural photosynthesis by harvesting sunlight and directly convert it to solar energy, and it is known as artificial photosynthesis [20]. Photovoltaic conversion in dye-sensitized solar cells, is solar energy conversion where dye sensitizer absorbs light, and mimics the the process of photosynthesis, which chemical energy produced when plant leaves uses chlorophyll to absorb a photon [20].

The types dyes used in dye-sensitized solar cells (DSSCs) have attracted a considerable attention in the conversion of sunlight directly to electricity [21]. DSSCs are the device for the conversion of visible light into electricity, based on sensitization of metal oxide semiconductor with mono layer of a dye. [22]. This is done by means of photosensitization, and it could be achieved by using the following dyes;

- Ruthenium-based polypyridine family complexes [4].
- Non-ruthenium metal centre complexes
- Metal free organic dyes [23]
- Natural dye (Anthocyanis) [20, 22, 24]]
- Porphyrines and metallo porphyrines

The types of dye used in DSSCs are categorized as third generation of photovoltaic cells and have been used as alternative to traditional silicon-based solar panels (semiconductor), due to its high photon- current conversion efficiency and reduced costs.

The dye-sensitized solar cells based on ruthenium-based pyridine complexes seem like to become a better choice over fossil fuel and silicon, due to following parameters:

(i) Light harvesting enhancement efficiency [4, 23],

(ii) Low cost manufacturing and low cost fabrication [25] ,

(iii) Ease of preparation [12], and

(iv) Its decorative nature.

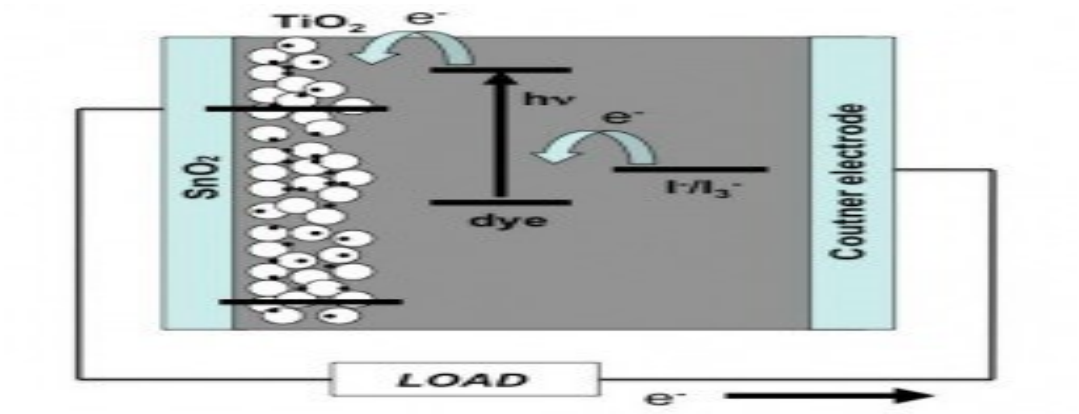

Figure 8: The diagram of dye –sensitized solar cell (DSSC).

Ever since the first discovery by Gratzel and O'Regan in 1991, researches based on DSSCs have attracted tremendous interest. These dyes were to be used as a sensitizer of nanocrystalline TiO_2 thin film based semiconductor.

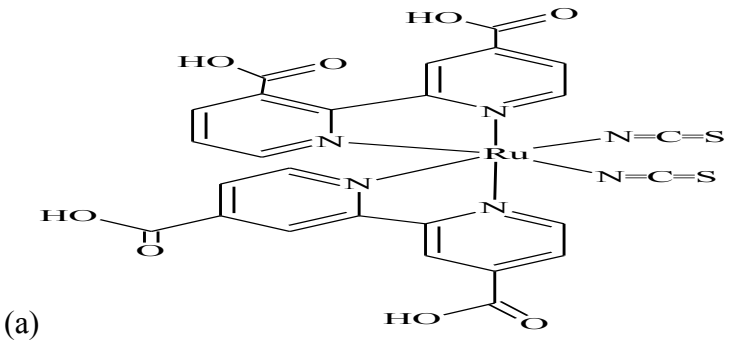

(a)

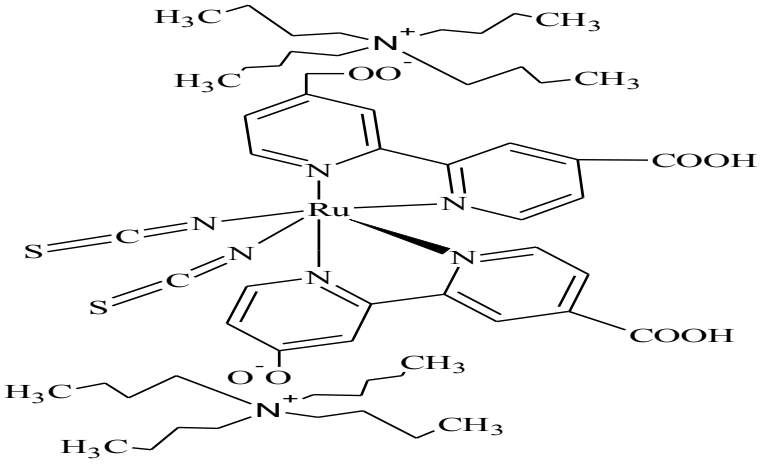

(b)

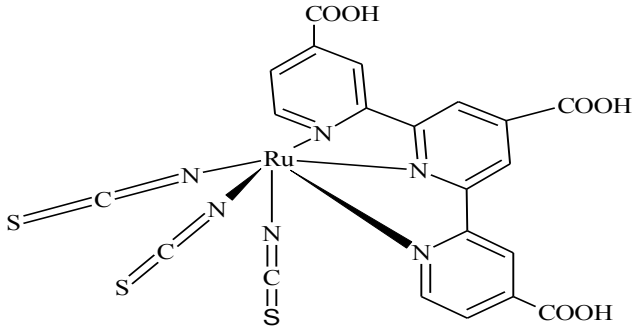

(c)

Figure 9: Molecular structure of (a) N3, (b) the N3 analogous (N719) and (c) the 'black dye"

Later N709 known as 'black dye' was reported. It is therefore these dyes being used as a prototype in the field of development of DSSCs. The purpose behind was to harvest the visible light and convert it to electricity. These complexes used carboxyl group –COOH, -SO_3H, -PO_3H as binding/anchoring to be grafted on the surface of TiO_2 thin film based semiconductor and to transfer an electron to the conduction band of metal oxide semiconductor. TiO_2 has a wide band gap, in its essence made up of the valence band and the conduction band. According to Nazeeruddin *et al the* purpose of introducing –COOH and other anchoring groups, was to:

(i) To increase the molar extinction coefficient of the complex [26], [27],

(ii) To facilitate the grafting of the dye on the semiconductor surface [19],

(iii) To ensure intimate electron coupling between its excited state wave functioning and conduction band manifold of the semiconductor and lowering the energy of ancillary ligand [28].

1.5.3 **Background**

The concept of dye sensitized solar cells was first reported by Gratzel and O'Regan in 1988, and was presented in 1991 which is the sensitization of TiO_2 thin film using ruthenium complex that is N3, N719 as sensitizers [21]. This was the breakthrough, adapting the 19^{th} century study of photography by Moser who enhanced the photoelectric effect of silver halide plates using a dye erythrosine. Their first Ru-complex to be used as sensitizer was N3 dye followed by its derivative N719. The difference between these two, N719 has two tetrabutyl ammonium ions and N3 has four H^+ protons [26]. These dyes were being used to harvest sunlight for the conversion of photon-to-electricity. This conversion mimics that of photosynthesis, it is known as artificial photosynthesis.

Ever since then, researchers have shown an attracted interest on ruthenium-based polypyridine, due to superb photophysical and electrochemical properties observe on archetype $[Ru(bpy)_3]^{2+}$. Gratzel and co-workers modified this early complex to enhance the spectral response, and to fulfil the dye-sensitized solar cell's requirements.

Figure 10: The modules or panels of solar cells built from three different types of dye-sensitized solar cell**.**

1.5.4 **The requirements for dye-sensitized solar cells**

According to Hagfeldt and Gratzel [28] , the most suitable dye for dye-sensitized solar cells, should at least have the following requirements;

(i) It should absorb all light below threshold wavelength of about 900 nm. That is the dye should absorb across the entire electromagnetic spectrum.

(ii) It should have a carboxylate (-COOH) or phosphate group ($-PO_3H$) to firmly attach, anchored on the semiconductor oxide a surface and inject electron to the conduction band of semiconductor at equal quantum yield, and their lowest unoccupied molecular π^* orbital of photosensitizer should localized near anchoring and it should be above the conduction band of oxide semiconductor [29].

(iii) It should have appropriate redox potential, meaning the energy level of HOMO and LUMO should match or suit the conduction band of metal oxide and redox potential of electrolyte system, to allow the efficient injection of electron to semiconductor and dye regeneration by electrolyte [30].

(iv) It should be stable enough to sustain at least 10^8 turnovers under 1.5 AM illumination corresponding to 20 years.

The ruthenium(II) polypyridine based compounds, meet these requirement, and it remains the choice compound for DSSCs application at present.

1.5.4.1 The components of dye-sensitized solar cells

The structure of dye-sensitized solar cells (DSSCs) consist of nano crystalline titanium dioxide (TiO_2) thin film as oxide semiconductor, transparent conducting oxide glass which is photo anode [31], the dye as photo sensitizer, electrolyte containing redox mediator system and platinum metal (PT.) As counter electrode coated on a glass sheet act as catalyst to facilitate the electronic collection from the external circuit [7-8]. The nano crystalline TiO_2 film of anatase phase is found to be most useful in DSSCs, due to its large surface area and its transparency, nontoxic, widely available, and biocompatible [31]. Titanium dioxide in DSSCs is deposited on the conducting glass to help the dye to anchor/ sink in and to enhance electronic conduction due to its wide band gap.

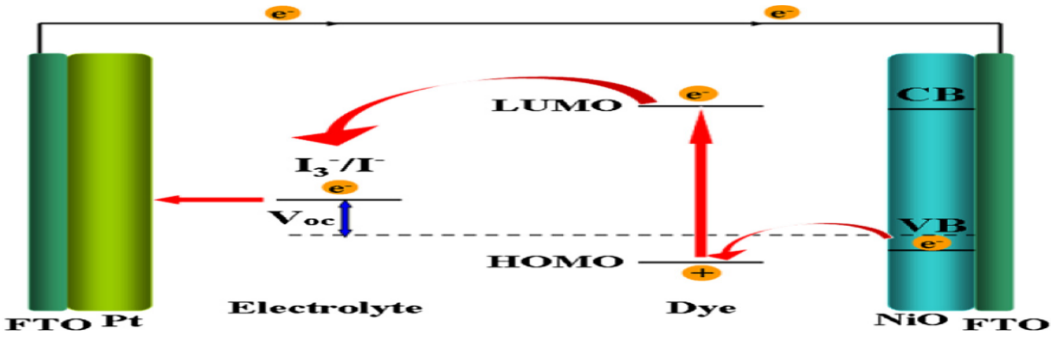

Figure 11: Schematic diagram of the components of dye sensitized solar cells.

In DSSCs, there are two facing electrode: a transparent photoanode, also known as working electrode, comprised of nanocrystalline thin film of titanium dioxide (7-20 um) of which the dye is being adsorbed for photosensitization. Among the most use metal oxides are ZnO, SnO_2, Nb_2O_5, Fe_2O_3, WO_3 etc. But titanium dioxide became a material of choice among the investigated semiconductors. It was recognized as semiconductor due to its greatest and appreciated properties in photochemistry and photo electrochemistry, it is low cost widely available and it showed a good experimental results [6].

1.5.4.2 The basic mechanism for DSSC

The photo excited dye inject an electron to the conduction band of oxide semiconductor, because HOMO and LUMO of a dye has been tuned in such a way that the excitation of electron is injected into the conduction band of the TiO_2 thin film semiconductor and the regenerating oxidized dye by electrolyte electron [7], and the dye undergoes oxidation, the original state of a

dye is regenerated by electron donation from the electrolyte, usually organic solvent (acetonitrile) containing redox system iodide and triiodide [6]. The generation of the sensitizer (dye) by iodide, intercept with the recapture of the valence band by an electron from oxidized dye, then the photo injected electron filter through a nanocrystalline structure of semiconductor and move randomly to get collected at substance known as load (external circuit) performing electrical work, until it encountered by counter electrode (PT.). The oxidized dye is being regenerated by an electron from redox system. And iodine in redox system is in turn regenerated by reduction of triiodide at the counter electrode, and then the circuit is completed via electron migration at external circuit [32]. Electrode, both deposited in a conducting substrate [32]. The redox system as electrolyte which is iodine/tri-iodide as redox mediator is placed between these two electrodes to transfer the charges [2]. The DSSCs are being depended on the visible light [27] of which they directly convert incident photon to electric current, for the efficiency of DSSCs.

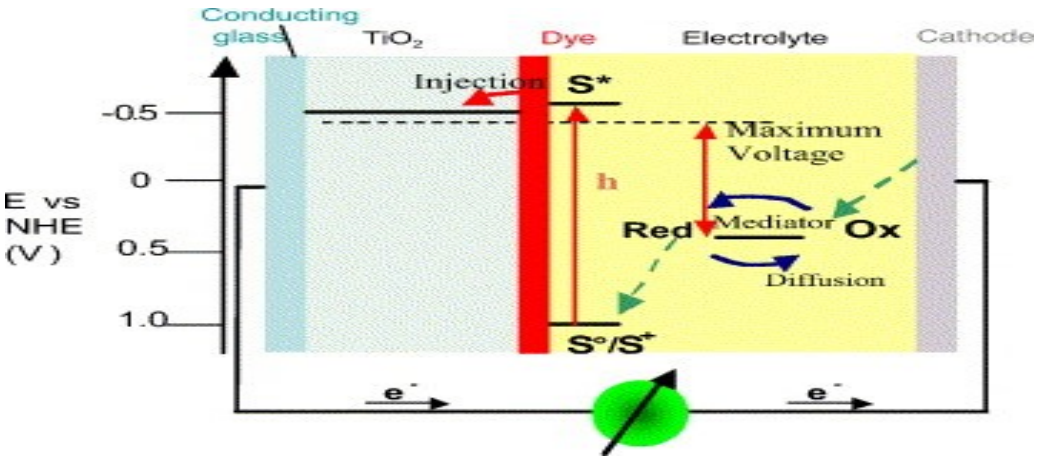

Figure 12: Represents the operational principle of dye sensitized solar cells [26]

According to Nazeerudin et al 2011 there are limitations, that the electron from oxidized dye recombine with crystalline network of titanium dioxide, inhibiting the flow to the load, and the photoexcited dye go for relaxation just before the injection to the conduction band.

1.6 **Literature review**

Bipyridyls has a very remarkable photophysical and, electrocatalytic properties because it has ability to form a very stable complexes with many cations, and therefore they continued to attract attention as important ligands of great interest for chelation of transition metal [34]. Ruthenium(II) polypyridine complexes includes bidentate based ligands such as bipyridine, phenonthroline and terpyridyl ligand that have favourable photophysical properties and are mostly utilized in charge separation particularly in dye sensitized solar cells.

In the last two decades, ruthenium polypyridine complexes have been widely investigated because of their remarkable photochemical and photophysical properties. In particular, in ruthenium(II) complexes containing polypyridine ligands with carboxylate groups substituted at 4,4' positions as anchoring group on semiconductor surface have received considerable attention due to their great ability to adsorb onto nanocrystalline TiO_2, which provide a charge separation and make them suitable photo anode for high performance solar cells [33,34]. Ruthenium-polypyridine also play a key role in the development of multicomponent that is supramolecular system [36] which is capable of performing photo-redox triggered functions for example charge separation devices for photochemical solar energy conversion.

1.6.1 **Some structures of ligands**

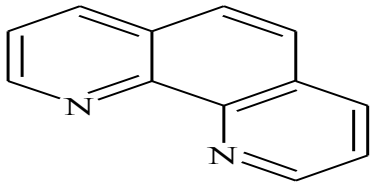

Figure 13: Structure for 1, 10-phenanthroline

1,10-phenanthroline has a rigid frame work and exhibit an excellent ability to chelate many metal ions via two nitrogen donors, and they show potential for technological application, due to their high charge transfer mobility, a good electro and photo-active and bright high emissions[37]. Bipyridines was first synthesized 110 years ago by Fritz Blau [38, 39] and have been known as highly interesting organic ligand for transition metal for more than 100 years. Bipyridines were used in investigation particularly in analytical chemistry, energy conversion and catalysis. These types of ligands in last ten years were used in another area of interest such as polymer [40], and novel architectures in supramolecular chemistry [41]. It was synthesized by two pyridines connected together through α-nitrogen [39].

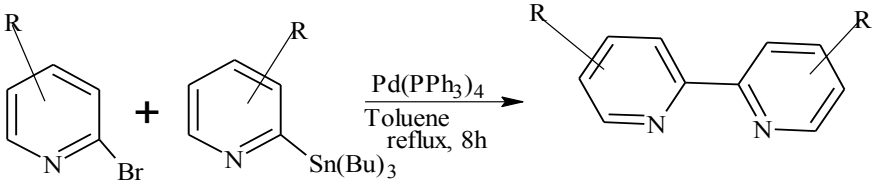

Figure 14: Synthesis of bipyridine by stille coupling, Sn(Bu)3 is tertbutylstannyl, Pd(PPh)3, is tetrakis(triphenylphosphine)Palladium(0) and R is any substituted group.

Since its discovery the bipyridine ligands has been used extensively in chelation of metal ions. Their isomer forms are 2,2'-bipyridine, 2,3-bipyridine, 2,4'bipyridine, 3,3'-bipyridine, 3,4'-bipyridine. Out of these 2,'3 and 3,3'-bipyridine can be found naturally abundant in certain variety of tobacco. According to Newkome *et al.* the 2,2'-bipyridine has been extensively used in

metal chelation due to its redox stability [38]. The 2,2'-bipyridine derivative ligands can form complexes with a lot of different metal more especially those with d^3, d^6, d^8/d^{10} electron configurations [42].

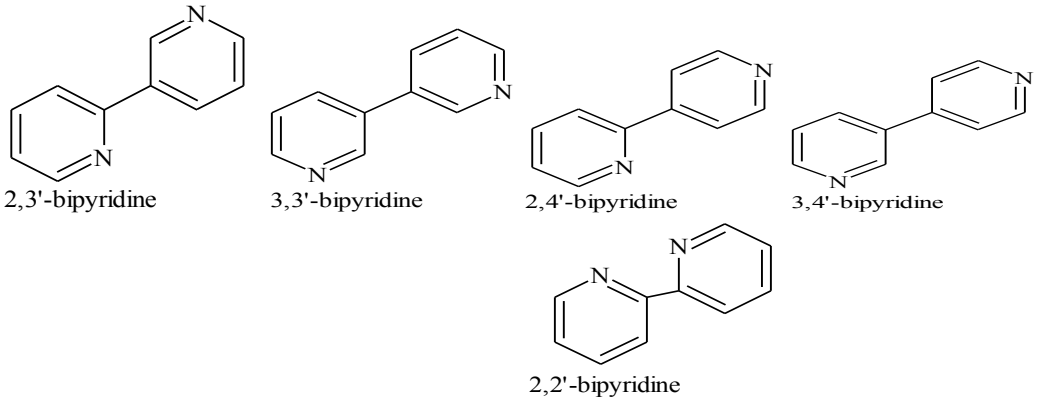

Figure 15: Isomeric form of bipyridine, and their symmetry.

The 2,2':6',2''-terpyridine is a molecule with three pyridine rings connected together through α-nitrogen. Morgan was the first scientist to synthesise and report 2,2',6,2''-terpyridine in 1932. It react with M^{n+} octahedral metal ion to give $[M(trpy)_2]^{2+}$. The substituent being incorporated react at 4'position to avoid the formation of isomers used to be formed in bidentate ligand such as bipyridine.

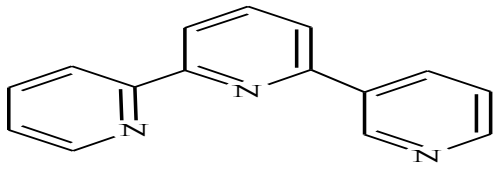

Figure 16 Molecular structure of 2,2':6',2''-terpyridine.

1.6.2 **Ruthenium complexes(II) polypyridyl complexes**

'Ruthenium(II) tris-2.2'-bipyridine $[Ru(bpy)_3]^{2+}$ has been used extensively in several investigation as photosensitizer for over 30 years due to its photoelectrochemical properties [36]. $Ru(bpy)_3^{2+}$ is the d^6 transition metal complex with octahedral geometry. It is widely used because it display a long list of properties that satisfy most of kinetic dynamic, spectroscopic and excited state requirement needed for a photosensitizer, thermodynamic, spectroscopic [43].

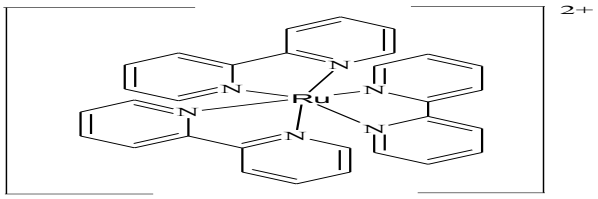

Figure 17: Molecular structure of trisbipyridine Ruthenium(II)

1.6.3 **Dye-based Ru(II) complexes, their details and structure**

Tris(2,2'-bipyridine) ruthenium(II) complex has been the most extensively studied in the field of electrochemical cell and photocatalysis [43]. Ruthenium based complex are being used in a wide variety of field such as part of photovoltaic in dye-sensitized solar cell, redox agent in electron transfer reactions and light emitting diodes because of their unique chemical and photochemical properties such as good luminescence, reactive long-lived excited states and redox activity both in ground and excited states [41-43]. Most Ruthenium(II) complexes based 2,2-bipyridine and 1,10-phenanthroline family emit at 600nm [45], and they have long live excited states.

Evans *et al* reported the starting material or precursor molecule for synthesis of ruthenium(II) polypyridine. This was synthesized by converting ruthenium(III)trichloro hydrate ($RuCl._XH_2O$) to tetrakis (dimethylsulphoxide) ruthenium(II) dichloride [44,45].

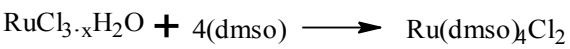

Scheme 1: Synthesis of precursor ruthenium(II) from ruthenium(III), as it also adopted from literature [44, 45].

Ruthenium(II)-based polypyridine family were the most successfully family in dye-sensitized (DSSCs). N3, N719 were reported as first high-performance Ruthenium (II) -based polypyridine by O'Regan, Gratzel and co-workers in 1993 [8].

These complexes seem like to have the same structure but the difference is N719 has TBA (tetra butyl ammonium) instead of H^+ in N3 of the two anchoring carboxyl group (-COOH) [50].

Since the discovery of N3 in 1993, the dye has become a paradigm of the efficient charge transfer sensitizer for nanocrystalline TiO_2 thin film semiconductor with an electric conversion efficiency of 10 %. The evolution continued until 'black dye' was discovered in the field of study for dye-sensitized solar cells [51].

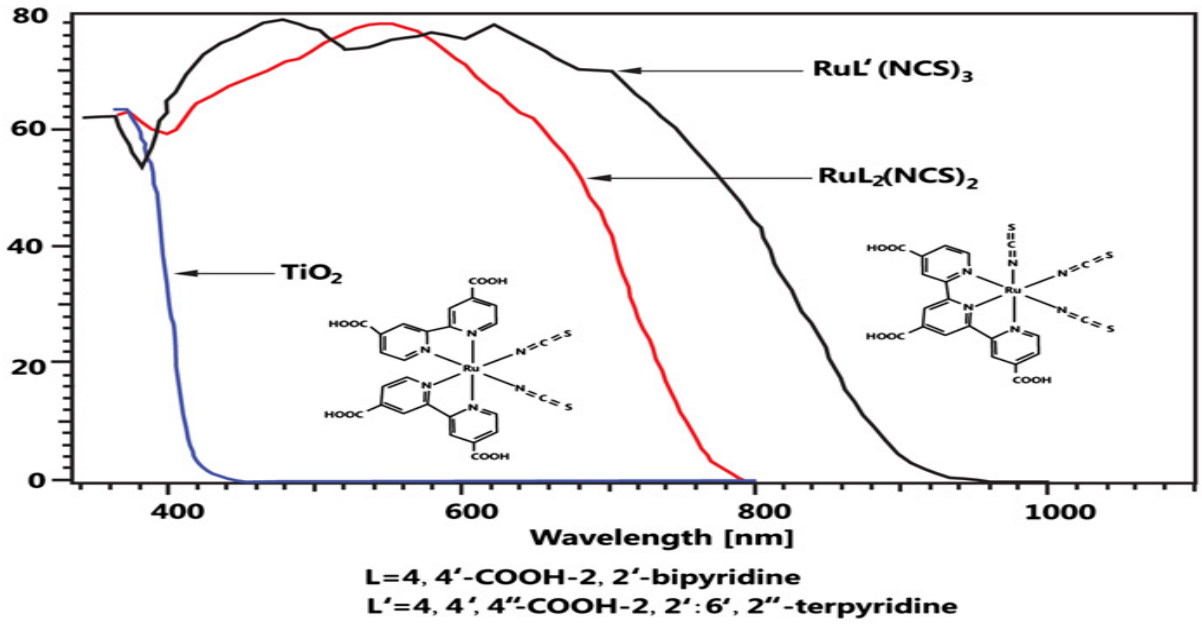

Figure 18: Spectral response curve of N3 with red line and terpyridine-based complex the "black dye" [49]

These Ru(II) complexes 'dyes' become ongoing development by modifying the ancillary ligand [52]. The following reported researchers were trying to introduce π-extending ligand for conjugation, achieve a high molar extinction coefficient, MLCT of complex to absorb in broadband of the solar spectrum to achieve large light harvesting capacity**.** N3 has an absorption band of 800 nm covering visible to the near infrared region, N3 dye uses the carboxylate group as anchoring group to bind to surface of TiO_2 thin film [15] as and it also injects electron that has photo excited from the valence band into the conduction band of TiO_2 as electron transfer channel and other hand links to the bipyridyl moiety to the lower energy of the ligand [53]. In 1997 another dye (photosensitizer) a terpyridyl analogue known as 'black dye' with panchromatic properties, the same research group published its synthesis and evaluation [4]. In these early Ru(II) complexes, a series of modification have made, due to lack efficiency, among

others, led to sensitizer with π-extended conjugation, achieving a photon conversion efficiencies up to 12.2 % [52].

Nazeeruddin, *et. al***.** were first to report the synthesis of 'black dye', which displays the panchromatic sensitization character over the whole visible region extending the near infrared region up to 920 nm [52-54]. In 2009, Funaki *et al* [54], synthesized and characterized Ru(II) complex with phenylene-ethylene moiety, they believed that black dye is more efficient than N3, and they also decided to modify Ru(II) (tctpy) $(NCS)_3$ complex 'black dye'. Phenylene-ethylene subunit was introduced into tpy ligand , to increase conjugation and to improve molar extinction coefficient [57]. Based on Ru(II) complex as photo sensitizer, were characterized by enhanced molar extinction coefficients, by using π-extended conjugation, and directionality in the excited state, by tuning the lowest occupied molecular orbital (LUMO) of a ligand [23].

Nezeeruddin *et al.* also reported the synthesis and photo electrochemical characterization of Ru(II)-dye (N945) .The N945 dye analogue of N719 dye has more π-conjugated ligand (4,4'-di-(2,(3,6-dimethoxy phenyl) ethyl)-2,2'-bipyridine, with this ligand N945 exhibited an improved molar extinction coefficient at λ_{max} 400 nm was 34,500 M^{-1} cm^{-1} and at 550 nm was 18,900 M^{-1} cm^{-1} and was compared to that of N719 [53]. In 2005 Nazeeruddin *et, al* synthesized a novel ligand, 4, 4'-bis (carboxyl vinyl) -2, 2' bipyridine to increase the optical extinction coefficient of dye (photo sensitizer) to make complex coded as k9 [57].The main drawback of modifying the early Ru(II) complexes was really to increase the molar extinction coefficient, by introducing

more π-conjugated ligand. For example in 2006, Wu and co-workers reported the synthesis of Ru(II) dye named as CYC-B1, with the aim of achieving a high absorption coefficient of the main metal to ligand charge transfer (MLCT) band [59].

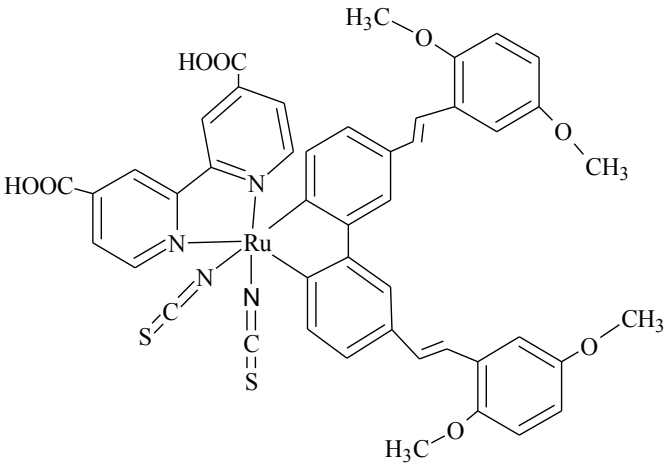

(A)

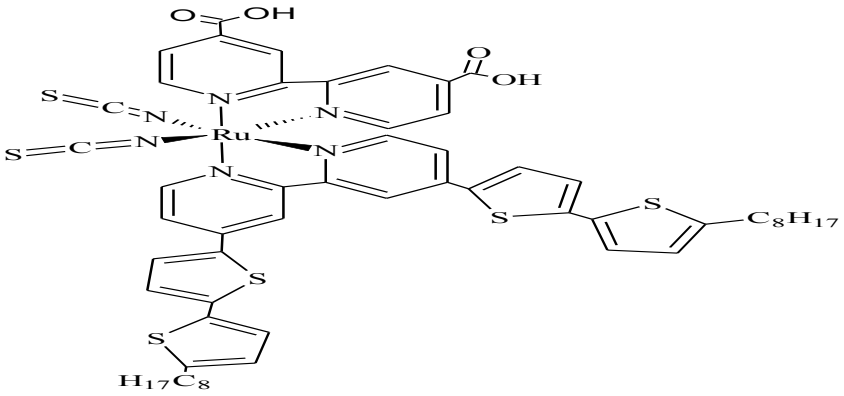

(B)

Figure 19: Molecular structures of N945(A) and CYC-B1 (B)

In the amphiphilic ruthenium complex, the electron rich bithiophen was incorporated to develop CYC-B1, with $2{,}12x10^{4}M^{-1}cm^{-1}$ [60]. The CYC-B1 was also having high power conversion efficiency than N719 dye, because CYC-B1, bearing a highly conjugated ligand substituted with

alkyl bithiosphene groups. The new ruthenium sensitizer was synthesized and reported in which one of the dcbpy ligand in N3 was replaced with abtpy, a bipyridyl ligand substituted with alkyl biothiophene group. Their approach was the replacement dcbpy in N3 with extended conjugation such as [59-60]. According Chen et al. dcbpy ligands cannot bind simultaneously to TiO_2 particle and excited electron in the moieties that is directly connected to TiO_2 provides a very small contribution to the conversion efficiency of dye-sensitized solar cells [63].

Li *et, al.* synthesized CYC-B7 and compared with CYC-B1 for the performance in dye-sensitize solar cells. CYC-B7 exhibited molar absorption coefficient coefficient (ε) $2.19x10^4M^{-1}cm^{-1}$ which is attributed to MLCT associated intensively with IPCE. Li and co-workers enhanced the lowest energy MLCT by incorporating the carbazole unit of the ancillary ligand in CYC-B1 complex, and MLCT achieved red-shift absorption. Ligand7 for CYC-B7 complex showed 12nm bathochromic shift compared to that of ligand1 for CYC-B1 which is showed that incorporation of carbozale unit enhanced a spectral response. This complex exhibited an overall efficiency of $\dot{\eta} = 8.96\%$ [59].

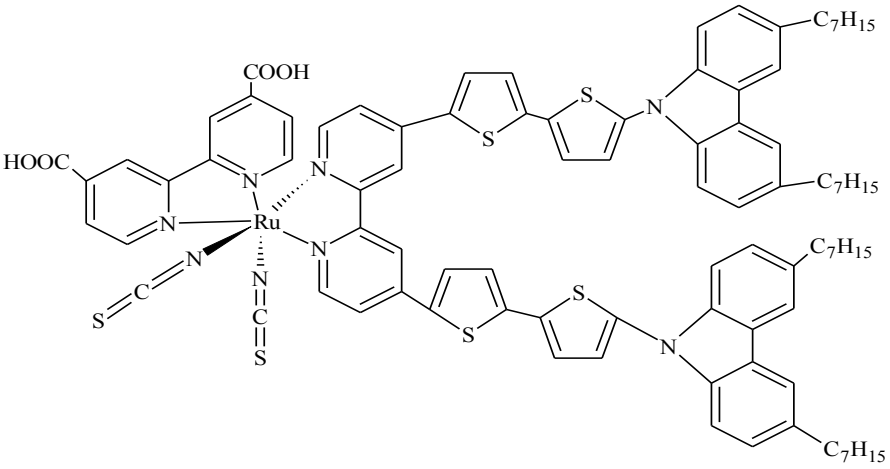

Figure 20: Molecular structure of CYC-B7 complex

In 2001 Islam *et al.* introduced a low-lying π-molecular orbital of a ligand , 4,4'-dicarboxyl-2,2'-bisquinoline (H_2dcbiq) to synthesize the R(II) complex [63-64] the main drawback was to increase the molar extinction of metal to ligand charge transfer (MLCT) band [64], but this complex was unfortunate to be used to its strong reduction injection yield into the conduction band of TiO_2 thin film of the semiconductor. They believed that using this complex, the MLCT will be tuned up to 600nm, by introducing a ligand with low-lying π*-molecule or by destabilizing t_2g orbital of a complex with strong donor ligand [63-64]. Then the synthesis and photo electrochemical properties of cis-Ru-L_2-X_2, where L is one the diimine, with low-lying π*-molecular orbital , and where X is CN, NCS, this ligand knows as 5,8-dicarboxy-6,7-dihydro-dibenzo-1,10- phenanthroline.

The main focus of these researchers was the modification the molar extinction of a complex [64], tuning of the highest occupied molecular orbital (HOMO) and lowest occupied molecular orbital of a complex to make a more efficient dye (photosensitizer) to harvest more sunlight for the

conversion of photon to photocurrent. The following is the 4,4'-dicarboxyl-2,2'-bisquinoline structure [53]. This ligand known to have low-lying π*-orbital.

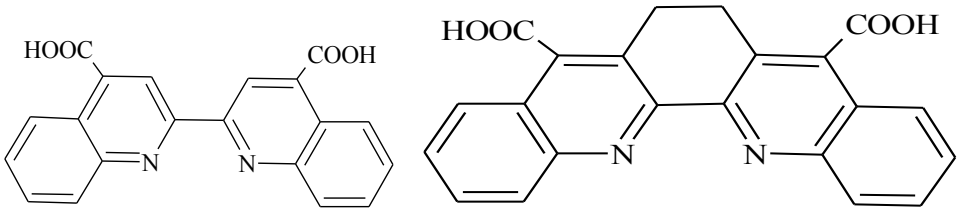

(a) (b)

Figure 21: Molecular structure of (a) H_2dcbiq and of (b) H_2dcdbphen.

The absorption and emission spectra of these ligands was dominated by strong ligand centred π-π^* transition at 268 nm and 350 nm.The charge transfer of Metal-to- ligand(H_2dcbiq) charge transfer transition exhibited an molar extinction coefficient of 1200 $mol^{-1}cm^{-1}$ and Metal-to-ligand (H_2dcdbph) charge transfer transition a molar extinction coefficient of 6000 $mol^{-1}cm^{-1}$. For this interest, another more conjugated amphililic complex was synthesized using a ligand known as k9 in 2005 by Nazeeruddin *et al* to actually increase the molar extinction coefficient of dye (sensitizer) [22].

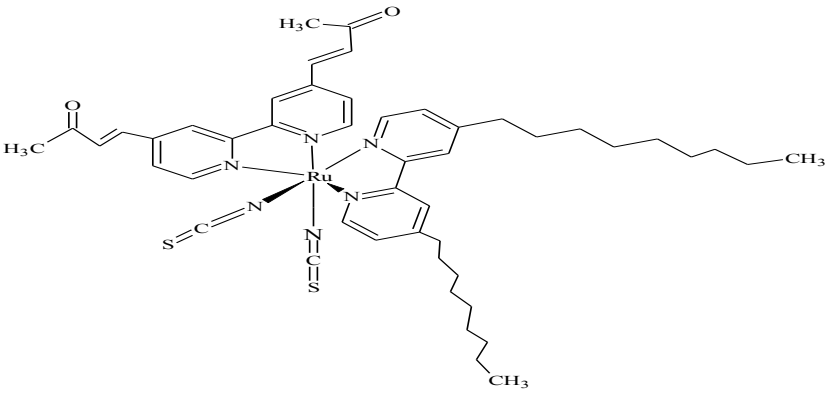

(a)

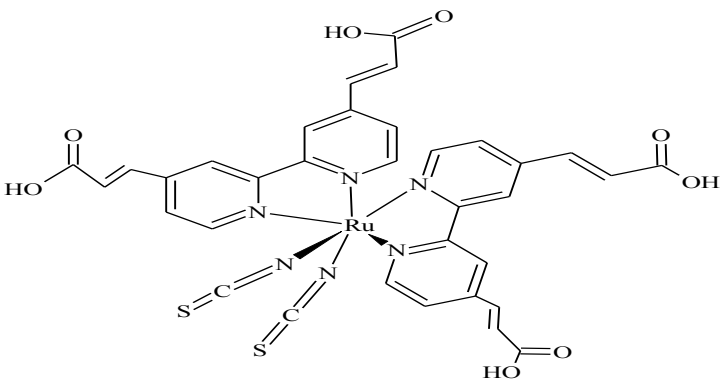

(b)

Figure 22: Molecular structures (a) the heteroleptic ruthenium(II) complex K9, and (b) the homoleptic ruthenium(II) complex K8.

The long term stability found to be the key limitation for dye-sensitized solar cells for outdoor application. Then the amphiphilic ruthenium(II) complexes (cis-$RuL_1L_2(NCS)_2$ where L1 is 2,2'-bipyridyl-4,4'-dicarboxylic acid and L_2 is 4,4'-dinonyl-2,2'-bipyridine, known as Z709 have been synthesized to overcome this short coming. The main factor that was hindering the widespread application of the dye-sensitized solar cells was thermo stability. This complex was in conjugation with quasi-solid state polymer gel electrolyte, and conversion efficiency of over 6% was achieved [67]. The complexes known as k9, k77 and Z709 have alkyl chain and they found to have long term stability [30]. However high conversion efficiency with long term stability found to have more challenges. The complex HRD1 and HRD2 have been synthesized and compared to K77 [57], and were found to have a good efficiency and good durability [68-69].

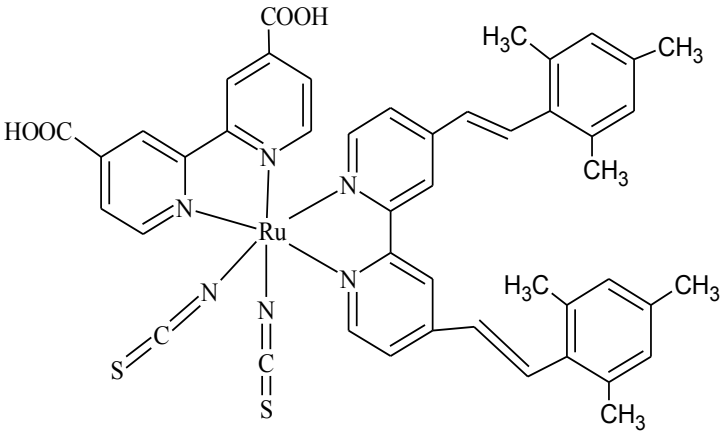

(a)

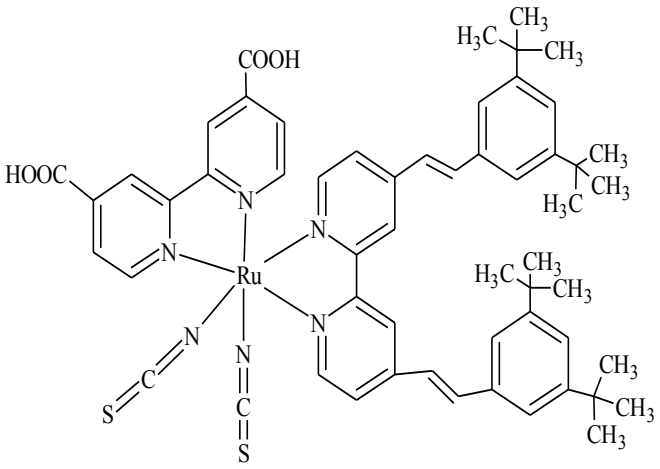

(b)

Figure 22: Molecular structure of the ruthenium complexes; (a) HRD-2 and (b) HRD1.

The aryl substituted aryl moieties connected to bipyridine as ancillary ligand have shown a superb improvement in solar light-to-electricity conversion efficiency [3-4]. It was then seemed like is an idea to explore further these ring-like structure to increase conjugation for achieving good overall performance in photovoltaic device. Chandrasecharam *et, al.* reported and

published the polypridyl complex H101 (cis-Ru (L1) (4,4'-dicarboxylic acid-2,2'bipyridine $(NCS)_2$, the main drawback was complex with long term durability with moderate efficiency of Z709. The L_1 was synthesized for the above complex, where L1 4,4'-bi's [2-(3.5-di-tertbutyl-phenyl)-vinyl]-[2.2']-bipyridyl[67,69].

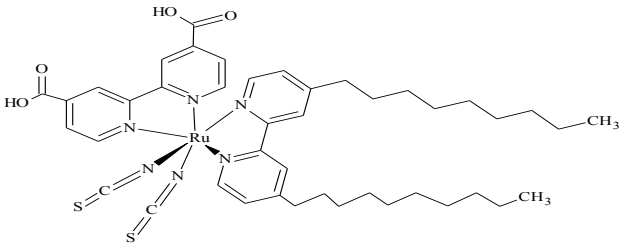

(a)

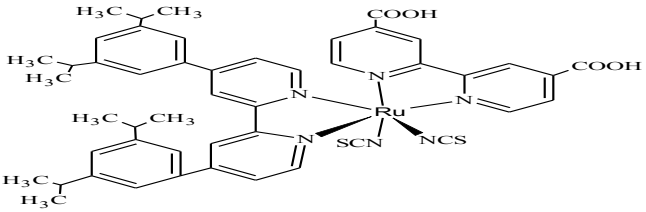

(b)

Figure 23: Molecular structure of Z709 complex (a) and H101 complex (b).

In 2010 Adeloye *et al* , synthesized and characterized a heteroleptic phenanthroline complex $[Ru(L_1)(L_2)(NCS)_2]$ where L_1=4-(9-dianthracenyl-10-(2,3-dimethylacrylic acid)-7-(9-anthracenyl-10-(2.3-dimethylacrylic acid)-1,10-phenanthrolline, L2= 4,7-bis(1-methoxyl-1-but-3-yne)-1,10-phenanthroline). This polyaromatic modified bipyridine and phenanthroline was for the lifetime enhancement from the excited state manifold [72]. Of which the π-conjugation length was increased by introducing anthracene derivative and 1, 3-enyl moiety as substituent for the phenanthroline, the target was to enhance photo physical properties, because the attena units

have a role of absorbing incident light and the electronic transfer [30-32, 48,73] The diagram below show this heteroleptic complex.

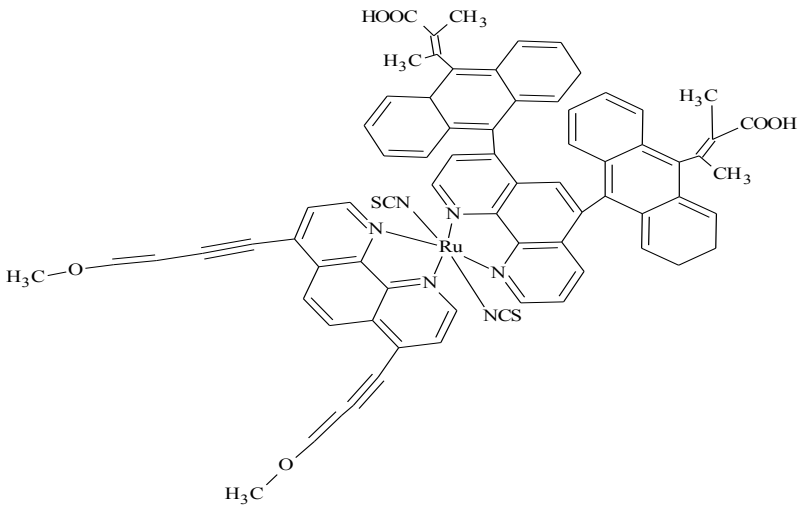

Figure 24: Molecular structure of Ru(II) complex with functionalised phenanthroline ligands having single-double linked anthracenyl and 1-methoxy-but-3yne moieties

In 2011, Adeloye *et al*, synthesized mono-anthracenyl bipyridine heterotopic Ru(II) complexes from the early complexes, the main goal was to increase the conjugation length of the ancillary ligand, by introducing anthracene substituted dimethyl acrylic acid [48]. With this complex their strategy was to tune the excited state properties of Ru(II) complexes, by extending the π-system using alkylene (dimethyl acrylic acid) ligand and polacryaromatic (anthracene) ligand) [48,74]. The ligands uses –COOH for complex to bind on metal oxide for the sensitization of semiconductor [31].

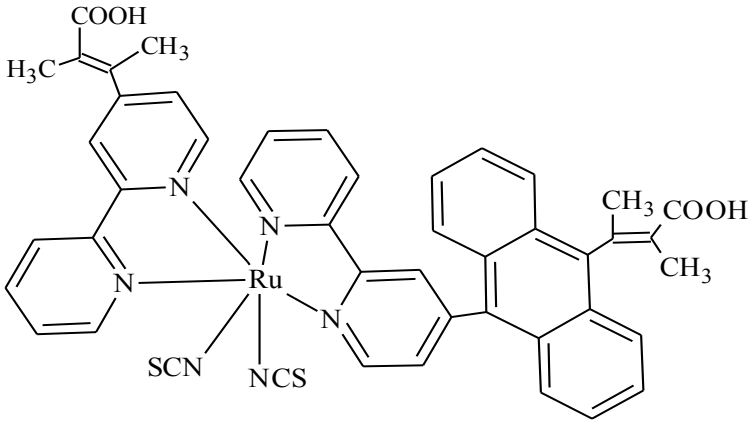

Figure 26: Mono-anthracenyl bipyridyl heteroleptic Ru(II) complex

Adeloye *et.al* the same research group synthesized and characterized heteroleptic Ru(II) complex based on phenanthroline ligand. Their ultimate goal was to improve photophysical property that is to shift MLCT in the red-shift absorption and to enhance molar extinction coefficient [57, 75–77]. The following diagram shows this heteroleptic ruthenium complex, the conjugation has been increased which phenanthroline with trianthracene, and the carboxyl group of dimethyl acrylic acid used to graft on the semiconductor

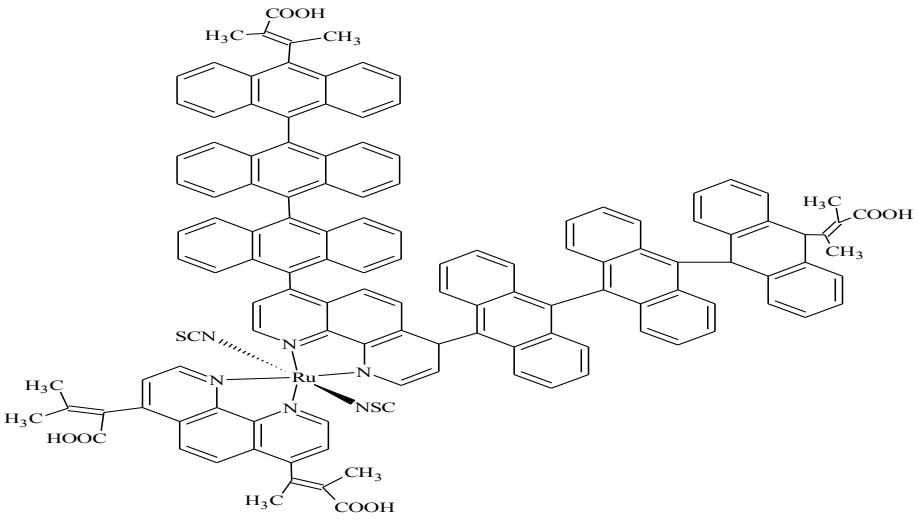

Figure 27: Molecular structure of heteroleptic Ru(II) complex of phenanthroline containing oligo-anthracenyl carboxylic moieties**.**

1.6.4 **Organic dyes**

The large number of organic dyes, such as coumarine, phthalocyanine, indole and polyene-triphenylamine have been synthesized, and test as sensitizer in dsscs with solar cell efficiency between 6-9 % [78].

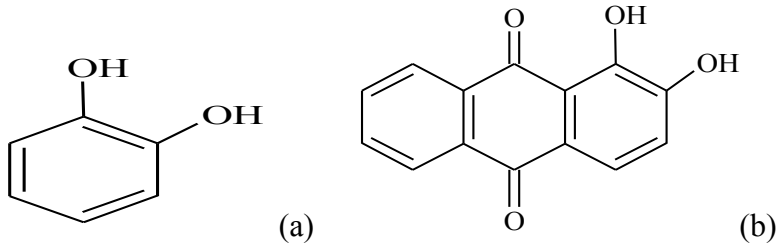

Figure 28: Molecular structure of catechol (a) and alizarin structures (b)

These compounds use hydroxyl groups to bind on the metal oxide semiconductor [79]

1.6.4.1 **Dye extracted from Natural plants and pthalocyanines as dyes in solar cell**

The colours gave by anthocyanins in the flower (pthalocyanin) presumable only attract insect and other pollinators to feed on. Now anthocyanin can absorb visible as well as UV-irradiation. The natural dye has been used in earlier research to harvest sunlight and to convert sunlight-to-electricity by means of photosynthesis. In 2007, Wongchare *et al* reported the dye-sensitized solar cells prepared from natural dyes extracted from rosella isolates that is rich in anthocyanin [80]. Anthocyanin is principal pigments responsible for the red, blue and purple colour of terrestrial plants [79].

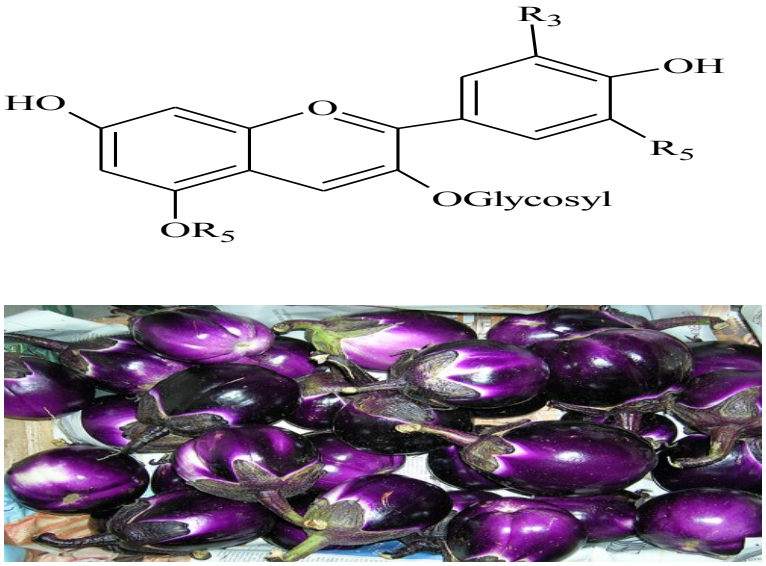

Figure 39: Molecular structure of anthocyanin . and the image of phtalocyanin, where natural anthocyanin is extracted .

They use carbonyl and hydroxyl to anchored and grafted on mesoporous TiO_2 thin film, and to make electron transfer from anthocyanin to the conduction band of TiO_2 [32, 33].

Depending on the plant/ extract and the solvent used, most of anthocyanin have an maximum absorption between 510 and 548 nm.

1.6.5 **Porphyrins**

Porphyrins is a group of highly conjugated heterocyclic macrocycle, many of these porphyrine occur in nature, they act both as electron donors and as acceptor groups and they have large and stable π-molecule [82]. Porphyrins dyes became an alternative, due to which concerns raised about ruthenium. The interest of using porphyrin dye started from their vital role in efficient energy and electron transfer in light harvesting efficiency antenna of biological system [78]. The

consideration of rare ruthenium metal and unlimited resources, the novel dye based on porphyrins uses cheap metals such as copper and zinc based porphyrins. Organic dye, specifically porphyrines with high efficiency composed of donor-π-conjugation unit acceptor (D-π-A) structure [83].

The donor- π conjugation unit structure acceptor (D-π-A based) zinc porphyrins dye known as YD2-o-C8 was reported by Gratzel [84].The dye-sensitized solar cells using YD2-o-C8 to sensitize TiO_2 achieved efficiency of 12.3 % [85]. This porphyrin dye achieved a long wave length of between 500-600nm, but it is still considered to have a low wavelength, hence no appreciated increase in light harvesting ability [68, 77,81, 86]. Porphyrins dye possess an intense soret band at 440-450 nm and moderate Q band at 500-650nm which arises from π-π*-transition [85, 87]. The metal porphyrin with those properties are regarded as potential photosensitizer in DSSC is known as Zn-1 (5-(-4-carboxyphenyl)-10,15,20-tetrakis(2,4,6-trimethylphenyl) porphyrin to zinc(II) with overall efficiency of 4.6 % under AM 1.5 solar light [88].

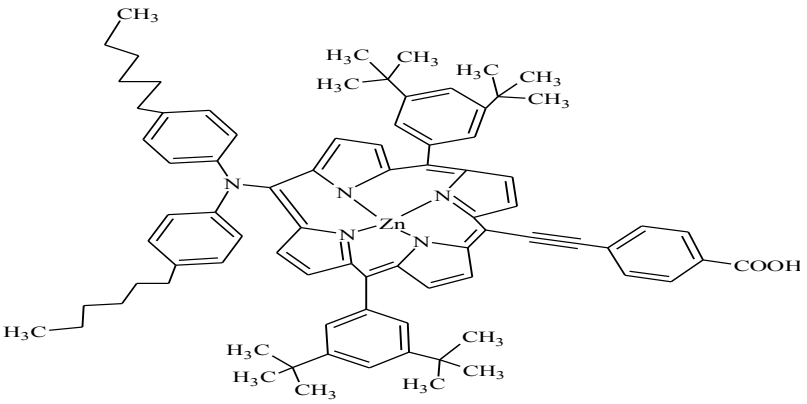

Figure 30: Molecular structure of Zn –porphyrin (YD2).

The porphyrin dye known as YD2 was found to have donor-π conjugation unit acceptor (D-π-A) structure, DSC made up of push-pull porphyrine has reached a standard (11%) comparable to that ruthenium(II) complexes[85, 87].

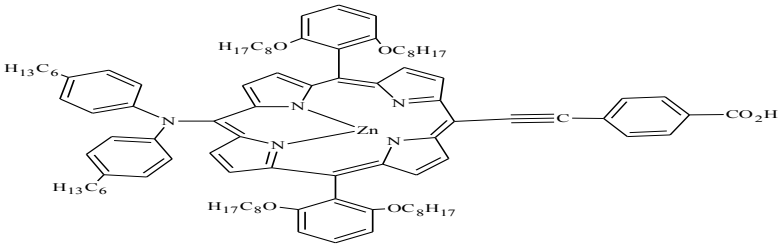

Figure 31:The molecular structure of Zinc porphyrin

1.6.6 **Metal free organic complexes**

Metal-free organic dyes are dyes that are being synthesized without metal centre unlike those of ruthenium-based polypyridine complexes. Metal-free dyes in dye-sensitized solar cells are regarded as the promising alternative over traditional silicon based solar cells, due to their low-cost and acceptable conversion efficiencies [23].

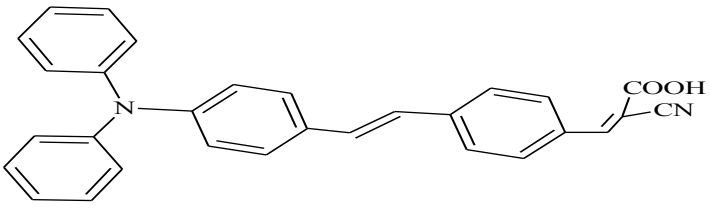

Figure 32: Molecular structure of organic dye know as TA-St-CA dye [49]

An average of 9.1 % solar energy conversion efficiency has been obtained using TA-St-CA. This dye contain p-conjugated oligo-phenylelene unit as electron donor acceptor and acceptor transfer

and carboxyl grafting unit [89, 92]. Metal-free organic dyes such as C2, C3, P2 and P3 were reported by Chen. C. *et al* [23, 92]. The cell obtained with these dyes had the following conversion efficiency (ή) ; C2= 5.51%, C3= 2.14%, P2= 2.69% and P3= 6.55%. The following structures shows the above named metal-free organic dyes [23].

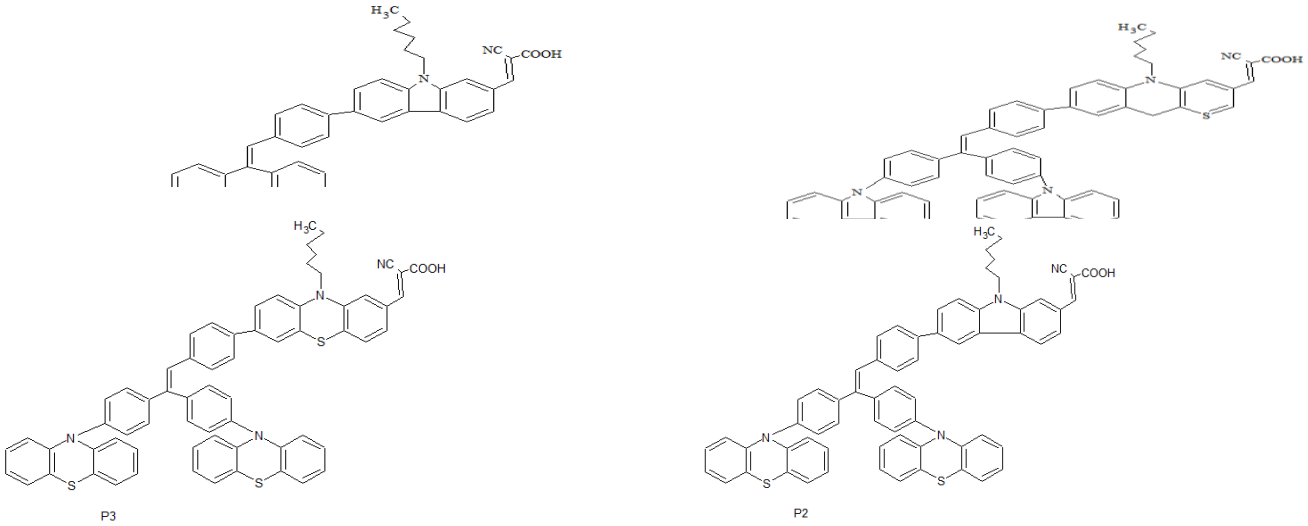

Figure 34: Molecular structure of some metal free organic dyes C2, P2 and P3

1.6.7 **Coumarin dye in dye sensitized solar cells**

Coumarin is a natural substance found in many plant species, with sweet odour and is used in perfumes since 1888 [89]. The novel coumarin-dye photosensitizers were developed by Hara *et, al*. the absorption spectrum of these dyes showed remarkable bathochromic shifts relative to the spectrum of traditional coumarin dye knows as C343 [89, 91]. Hara and co-workers introduced the methine unit as bridge between the cyano group and carboxyl group to increase the π-conjugation in the dye, and thus resulted to wide absorption in a visible region [89–91]. The

novel dye known as NKX-2311 was found as an efficient photosensitizer for dye-sensitized solar cells with 6% solar energy-to-conversion efficiency under A.M 1.5G conditions, which is the highest efficiency obtained in organic dye photosensitizer [92].

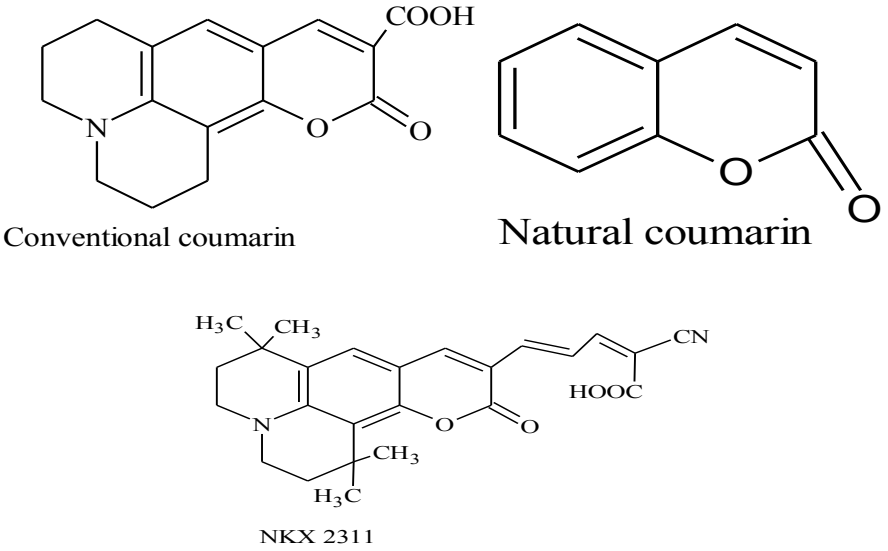

Figure 33: Molecular structure of a natural coumarin from plants , conventional coumarin-dyes C343 and (NKX-2311)

In these compounds, the methane (-CH=CH-) connecting the cyano(-CN) and carboxyl(-COOH) into the traditional coumarin. And were NKX-2311 is 2cyano-5-(1,1,1,6,6-tetramethyl-10-oxo-2,3,5,6-tetrahydro-1H, 4H, 10H- 11-oxa-3a-aza-benzo[de]anthracen-9-yl-penta-2,4-dienoic acid [92].

Hara research group synthesized and reported other novel coumarin-dye derivatives, and suggested various possible ways to increasing dssc efficiency is to extend the conjugation of methine (-CH=CH-) unit in NKX-2311 [89, 93]. Consequently Ko et, al and other co-workers reported class of organic dye sensitizer based on triphenyl amine electron donor where all three phenyl were bridged by a methane (-CH=CH-) unit and dye-sensitized solar cells based on these dyes achieved 9% electric power conversion efficiency.

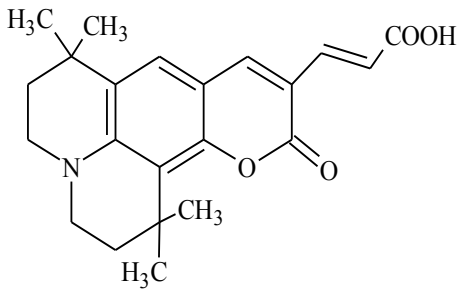

NKX 2398

(a)

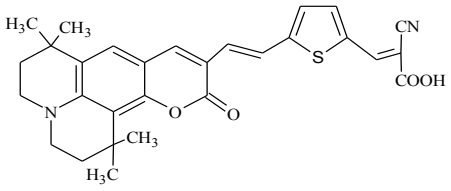

(b) NKX 2593

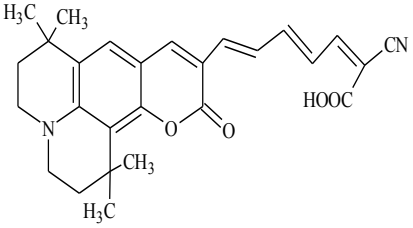

(c)

(d)

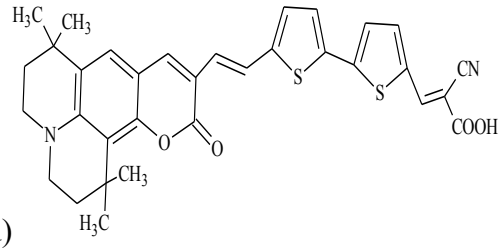

(e)

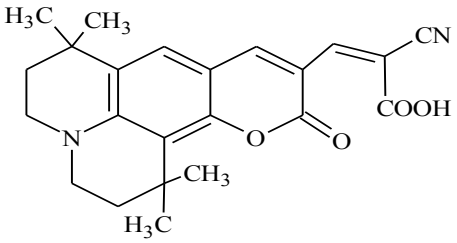

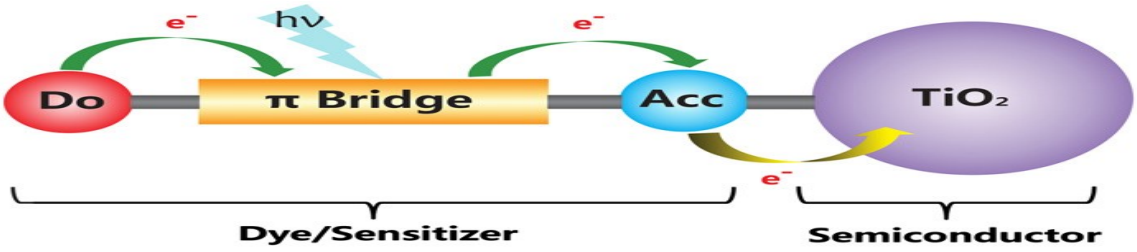

Figure 34: Coumarin dyes coded as (a) NKX-2398, (b) NKX-2593, (c) NKX-2586, (d) NKX-2677, (e) NKX-2388 and (f) The schematic diagram shows the design structure of donor π-conjugation unit acceptor (D-π-A) of metal-free organic dye sensitizing the TiO_2 nanocryatlline [49].

Among D-π-A metal free complex dyes that have been reported is TC4. It possessed a large moler extinction coefficient due to extended π-π^* transition. TC4 dye is based on triphynylamine (TPA) and they contained donor unit as TPA or its derivative and is connected to cyano acrylic

acid acceptor, via bridge methine fragments. The function of methine unit as photon to sink in and that is where a charge separation occurs, while the migration in opposite direction fascinated by donor and acceptor unit [92, 94].

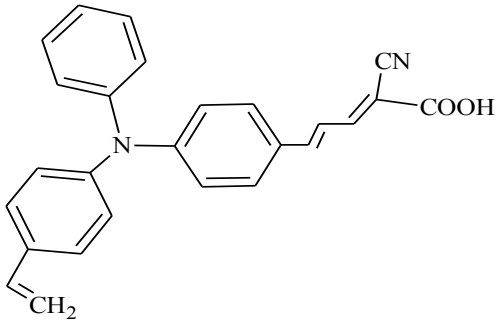

Figure 35: Molecular structure of TC4 dye [92].

1.6.8 **Non-ruthenium metal centre dye sensitizers**

Some non-ruthenium metal centre complexes have been synthesized and used as sensitizers for dye synthesized solar cells (DSSCs) [95]. Promising efficiency was obtained from with iron bipyridine complexes as sensitizer and it had a possibility of replacing an expensive metal ruthenium [96]. Iron is cheaper, abundant and a replaceable metal. The synthesized iron based bipyridine was $[Fe(bpy)_2(CN)_2]^{2+}$, were bpy is bipyridine, and CN is cyanate. But the use of iron(II) complexes are doubted, because their ligand field states have unfavourable electronic overlap with conduction band of semiconductor TiO_2 thin film [97]. The photo excited electron is promoted from MLCT state followed by ultrafast relaxation into lower lying field states, therefore it is questionable for efficient injection of electron to the conduction band of TiO_2 [98]. Whereas Ru(II) complexes are low lying excited states, but lie above the conduction band of the semiconductor and they have long lived excited states, and injection can occur.

1.6.9 **The cyclometallated and thiocyanate free dyes**

The cyclometalated complex known as YEO5 was reported and reached the prototype cyclometalleted ruthenium complexes without thiocyanate, it was compared to N719 complex, and the two thiocyanate was replaced with 2,4-diflouro phenylpyridine. It was believed that the monodentate can bond with S or N, and it is moderate ligand and can discoordinate. The MLCT of this complex YEO5 had a 25 nm bathochromic shift with a remarkable molar extinction coefficient compared to N719. The two fluorine was believed to fine tune the redox potential of the complex [97,99].

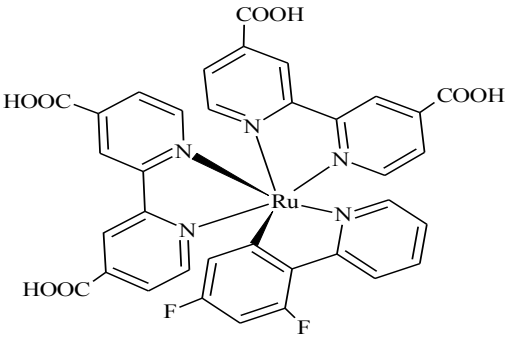

Figure 36: Molecular structure for cyclometallated dye YE05

1.6.10 **Osmium complexes**

Although ruthenium(II) polypyridine has been studied extensively as sensitizer for nanocrystlline TiO_2, osmium has been considered as a possible replacement because it possesses similar photophysical and photochemical properties [98,100,101]. Despite the high efficiency of ruthenium polypyridine as reported in the early study by Gtrazel with N719 complex, and dominated by photoinduced electron and energy transfer assemblies [101], ruthenium is a rare

element. According to Bram, *et. al*, the ruthenium polypyridine complexes is in the green region, as result the recent work is also on osmium(II) polypyridine, and their incident-to- current conversion efficiency extended well to near IR [101, 102, 103,]. It was therefore suggested that a suitable designed Osmium-polypyridyl based complexes as sensitizer that display a broader absorption suppressing ruthenium complexes should lead a better photoelctrochemical energy conversion [102].

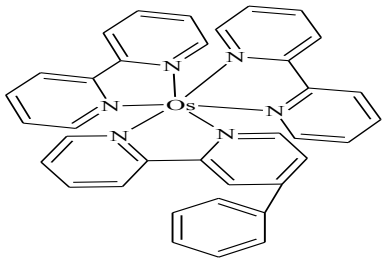

(a) Os-2

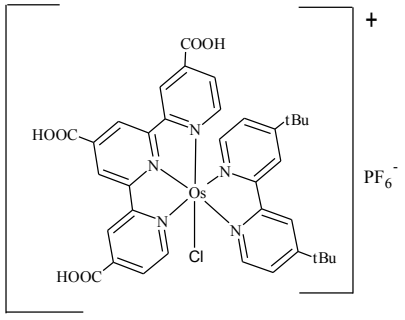

(b) Os-stbpy

Figure 37: Molecular structure for (a) Osmium(II) complex coded as Os-2 $[Os(bpy)_2(dpp)]$ where dpp is dipyridyl pyrazine, (b) [Os(tcterpy)-(4,4'-bis(p-butoxystyryl)-2.2'-bipyridine)Cl]PF_6 coded as Os-stbpy

In order to improve the energy conversion efficiency, it is necessary to extend the absorption threshold of the dye sensitizer to a longer wave length, to near infrared region (NIR). The osmium terpyridine complex on the above Fig 37 (b) was synthesized and reported with extended photoelectric conversion up 900 nm this absorption was attributed to spin-forbidden singlet- triplet metal-to ligand charge transfer transition (MLCT) and spectral response of about 1100 nm, and with this Osmium complex the overall conversion efficiency of 6.1 % was achieved. [101,104].

1.6.11 **Electronic transition and charge transfer transition of ruthenium(II) complexes**

When a transition metal like ruthenium coordinates with polypyridine to form a complex, the molecular orbital created are both located on either metal or in the ligand [103, 105-106]. There are four possible charge transfer transitions for transition metal complexes: (i) The metal-to-ligand charge transfer (MLCT) transition, which is the promotion of an electron from metal-to-ligand. (ii) Ligand-to-metal charge transfer (LMCT) transition, which is the promotion of an electron from ligand to metal. (iii) Metal centred (MC) transition, electron is in between the orbital localize on metal. (iv) Ligand centred (LC) transition; electron is in between orbital localized on the ligand.

Transition that will be low in energy depends on the oxidation state of the metal and on the nature of the ligand. The charge transfer (MLCT, MC, LC) states have a lower energy than ligand field state, that is why ruthenium(II) chromophores is a better choice in DSSC than those

of iron(II) chromophores in the first row, which they have a highest energy level than the ligand field. The electron often go for relaxation before it is injected into the conduction band of metal oxide TiO_2 [107]. Ruthenium(II) polypyridine, the transition of the lowest in energy is the singlet excited state ^{1}MLCT transition, which corresponds to the lowest excited states are ^{3}MLCT.

1.6.12 **Electrochemical study of ruthenium complexes**

The electrochemistry of transition metal complexes such as ruthenium, osmium, and iron based on polypyridine (phenanthroline, bipyridine) as ligands have been investigated. These complexes oxidized and reduced reversibly [106]. Ege et al, tested the oxidation and reduction potential where cyclic voltamogram were recorded for $[Ru(bpy)_3]^{2+}$, the complex was in 1mM solution of tetrabutylammonium hexaflourophosphate as supporting electrolyte and a saturated sodium chloride as reference electrode was used [105, 107]. Funaki, *et al*, suggested that there is a threshold of≈0,5 V vs supporting electrode that is standard calomel electrode (SCE) for efficient dye regeneration [107]. It is therefore important to know the redox potential of the electrolyte, to know the energy difference between ruthenium dye sensitizer and redox couple system(electrolyte) [108, 110].

In complex of the type $[Ru(L1)_2(PF_6)_2]$, the voltamograms, that is square wave and cyclic voltammograms determined and they displayed the metal centre Ru(III)/Ru(II) couple at positive potential, where $E_{1/2}$ = 1.42 V was assigned to the reversible one-electron oxidation process V. And ligand at negative potential (reduction) where three reversible wave at -1.31 **I**, -1.07 **II**, -0.75 **III**. The Ag/AgCl in N,N dimethyl formamide solvent was used as electrode with

0.1M tetrabutylammonium hexafluorophosphate as supporting electrolyte [77]. Ocakoglu *et al,* reported the electrochemical measurement of ruthenium complexes K27 (dcbpy and 1.10-phenanthroline-5.6-dione as ligands), K28(dcbpy and 4,7-diphenyl-1,10phenanthroline-disulphonic acid disodium salt as ligands) and K313 (two of 4.7-diphenyl-1.10-phenanthroline-disulphonic acid disodium salt as ligand) in DMF and standard calomel electrode (0.55V vs SCE) was used and the respective voltammograms, oxidation potential of Ru(II)-Ru(III) couple of 1.39V K27, 0.84 V K28, and 1.50 V for K313 was observed together with the reduction potential of ligands -0.75 of K27, -0.84V of K28 and -1.54V of K313 [115].

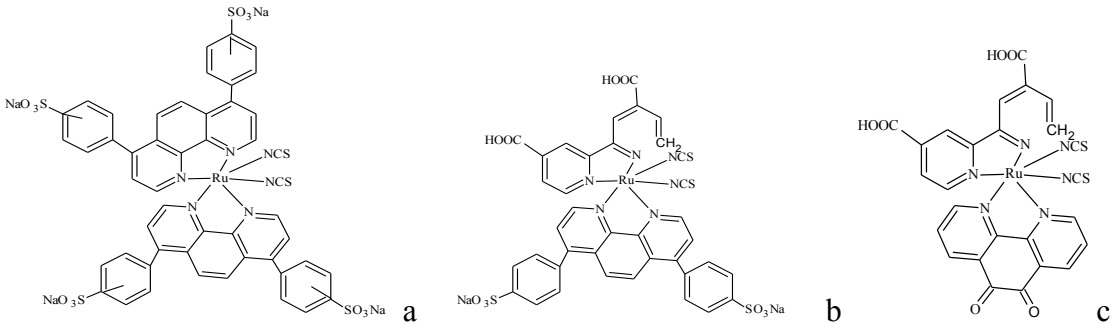

Figure 38: Molecular structures of (a) K313, (b) K28 and (c) K27

1.6.13 **The photo anodes (semiconductor)**

In dye sensitized solar cells, Nb_2O_5, SnO_2 and TiO_2 [6] are used for dye to sink in and it acts as transport for photogene rated electron from the dye [6-5]. The moist and usable is TiO_2 due to its wide band gap of 3.2ev, TiO_2 exists as three crystalline phases: anatase, rutile and brookite phase, but anatine has proven to be superior in solar energy conversion [7].According to Inomata *et al* [109]DSSCs fabricated with rutile and anatase with similar thickness show no difference in open circuit (V_{OC}) value subjected in 1.5 AM illumination, but in short circuit photocurrent (J_{SC})

of the anatase based semiconductor higher by 30 % than rutile based which is attributed to the lower amount of dye absorbed by the retail thin film, which shows the smaller specific surface area [110, 111]. According to Mange. *et al* [110] rutile gives less efficiency in solar cells than anatase due to its low loading and slower electron transport [112]. Although ZnO has also wide band gap as TiO_2 (3,2 ev), according to Gratzel it was then alternative use, but its popularity was limited because it showed low efficiency upon dissolution in the acidic N3 dye solution. And SnO_2 has a large band gap (3.8 ev) compared to TiO_2, it would create a fewer oxidation hole in the valence band under ultraviolet illumination, thereby improving stability, however according to Alhmed *et. al*, [22] the more positive band edge position facilitates electron injection from photoexcited dye, however the performance of SnO_2 is less than that of TiO_2. Also the isoelectric point of SnO_2 pH 4-5 is smaller/lower than that of TiO_2 (pH 6-7), which inhibit the adsorption of dye molecules with acidic –COOH, as anchoring group.

1.6.14 **Evaluation of photovoltaic (dye sensitized solar) cells performance**

Evaluation of photovoltaic performance can be done by measuring the incident photo (wavelength) to conversion efficiency and current-voltage characteristics. The efficiency of solar cell is determined by its current-voltage characteristics under standard air mass illumination conditions [111]. The IPCE depends on the light harvesting efficiency of photon that is the incoming light of wavelength of photon [112]; the quantum yield of electron injection from the excited state of the sensitizer to the conduction band of semiconductor oxide, and the electron transportation or collection. The light harvesting efficiency (LHE) depends on absorption properties of the dye, quantum yield injection depends on excited state oxidation potential of the

dye and its lifetime, while electron transportation or collection depends on structure that crystalline network and morphology of mesoscopic film and also on the effectiveness of regeneration of the sensitizer process from intercept charge recombination from electrolyte.

In the case of current-voltage characteristic can be achieved by three different methods that is diodes forward; p-n junction; and photovoltaic output method. In diode forward method the test of solar cells is done by applying DC power from an external source that is without applying any illumination. The current going into the terminals of solar cells and the voltage across the terminals is measured [113]. The p-n junction method measures the solar cells, in which illumination is done with variable light intensity; the short circuit current and open circuit voltage are determined for every light intensity setting, with which the desired current-voltage curve is plotted.

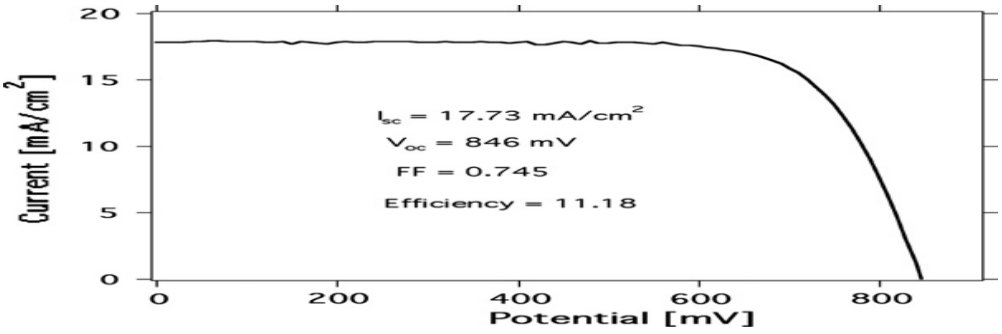

Figure 39: Photocurrent-voltage curve for ruthenium-polypyridine based dye-sensitized solar cells (DSSCs) [97].

According to reports in the literature [112-116] are following parameters to evaluate the performance of DSSCs.

The short-circuit photocurrent (J_{SC} = $mAcm^{-2}$), which is the photocurrent density per square centimetre obtained when solar cell is short circuited, Jsc= e ∫ IPCE (λ)Φ_0 (λ) (1-r)(λ)dλ, where 'e' is the elementary charge and r (λ) the incident light loss. (iii) open-circuit voltage (V_{OC}),corresponding to the cell potential when no current flows, $V_{OC} = \frac{kT}{q}$ In(γ $\phi_0/n_o k_{et}[I_3^-]$, where ϕ_0 is the incident photoflux; n_0 represents the electron density on the conduction band of TiO_2 in the dark, while k_{et} reflects the recombination reaction rate for the given triiodide concentration $[I_3^-]$. (iv) the fill factor (FF), which is defined as the ratio of the maximum electric power produced by the solar cell divided by the open circuit potential and short-circuit current, $FF = \frac{V_{MAX} \times J_{MAX}}{V_{OC} \times J_{SC}}$, where V_{MAX} and J_{MAX} correspond to maximum voltage and maximum current respectively. (v) And the overall power conversion efficiency $\eta(\%)$,representing the ratio to the output electric power of the cell and flux of the incident light, $\eta = \frac{J_{SC} \times V_{OC} \times FF}{P_i} \times 100\%$, where P_i is the intensity of incident light (photon) at 100 $mWcm^{-2}$ [119-120].

1.7 **Problem statement**

Recently the world is facing increasing demands for energy followed by depletion of fossil fuel and increase global warming because of emission of unwanted greenhouse gases like carbon dioxide in the atmosphere. In this study, attempts were made in order to answer the following research questions:

1. Can clean and cost effective solar energy be deployed for direct light conversion into electricity?

Silicon based photovoltaic cells are very expensive. Silicon based photovoltaic cells are not easy to produce, because they need dopants/impurities to create p/n semiconductor for direct conversion of visible light/sunlight (photon) to electricity.

2. Can ruthenium complexes be developed as light harvesting material as alternative to silicon based solar cells?

Although silicon based solar cells have efficient incident photon to current conversion efficiency compared to DSSCs (dye sensitized solar cells), its high costs and difficulties in fabrication limited its popularity.

3. Can the new development of dye-sensitized solar cells pioneered by Gratzel in 1991 be sustainable and economically viable?

Ruthenium complexes do not have absorption in near IR of the solar spectrum.

4. Can a new novel ruthenium polypyridyl complex be designed to absorb all light in the visible region up to 920 nm of the solar spectrum?

1.8 **Motivation and rationale**

Dye-sensitized solar cells is a clean and renewable source of energy, that can address the world's about pollution and global warming caused by consumption of fossil fuels. Fossil fuels are non-renewable source of energy and their use can increase carbon dioxide and unwanted gases in the atmosphere. The use of solar cell can produce clean and renewable energy source. A dye-sensitize solar cell (DSSCs) is also the best alternative use of light (photon) -to-electricity conversion, over traditional-silicon-based solar cells.

Development of DSSCs had attracted attention since the development of N3, N719 dyes and they show a conversion efficiency of 7.4 -11,1%.Ruthenium-based polypyridine complex of earlier reported by Gratzel and O'Regan showed a promising efficiency.

The absorption of metal-to-ligand charge transfer (MLCT) band of ru(II) polypyridyl complexes can extend from the visible region to near-IR region of the electromagnetic spectrum, due to ease of introducing more conjugated ligands.

The introduction of new-ancillary ligand can tune the photophysical and electrochemical properties of ruthenium(II) polypyridyl complexes. DSSCs has a long lifetime, it has no photo degradation in the sunlight (up to 50 °C) exposure, and has no toxic leakage. This research focuses on the photovoltaic type of solar cells, which are good/cheap cells, harvesting sunlight, and are also effective in indoor and outdoor usage.

1.9 **Aims and objectives**

- The aim of this project is to synthesize, characterize and evaluate the potentials of Ru(II) complexes as sensitizer for dye sensitized cell.

To achieve this aim, this project has the following objective:

i. To synthesize 2,2'-bipyridine and 1,0-phenanthroline based ligands
ii. To synthesize the ruthenium-based polypyridine family complexes
iii. To characterize the Ru(II) complexes and their ligands, using FTIR, ^{1}H-NMR, ^{13}C-NMR, the elemental analysis, UV-Vis spectroscopy and the photoluminescence.
iv. To fabricate the dye-sensitized solar cell and evaluate their performance

1.10 **Hypothesis**

The synthesis of ruthenium-polypyridine, increasing conjugation, replacing one bipyridine from $[Ru(bpy)_3]^{2+}$ with two thiocyanate groups could improve and tune the photophysical and electrochemical properties and that could have good advantage into harvesting more sunlight. The substitution could enhance metal-to-ligand charge transfer (MLCT) absorption in the solar spectrum. Introduction/incorporating of different functional group, ancillary ligands into arche type could red shift MLCT absorption to higher wavelength, which is good advantage into harvesting the solar light. Ruthenium(II) complexes based dye-sensitized solar cell could give a better and promising efficiency than metal free dyes and be best alternative over silicon based solar cells.

1.11 **References**

1. Yuksel, I. Renewable energy status of electricity generation and future prospect hydropower in Turkey. *Renew. Energy.* **2013***, 50,* 1037–1043.

2. Grätzel, M. Solar energy conversion by dye-sensitized photovoltaic cells. *Inorg. Chem.* **2005***, 44,* 6841–6851.

3. Nazeeruddin, M. K.; Kay, A.; Miiller, E.; Liska, P.; N. Vlachopoulos, N.; M. Gratzel, M.; Lausanne, -C.; April, R.; Conversion of light to electricity by cis-X_2Bis(2,2'-bipyridyl-4,4'-dicarboxylate)ruthenium(II) charge-transfer sensitizers (X = Cl^-, Br^-, I^-, CN^- and SCN^-) on nanocrystalline TiO_2 electrodes. *J. Am. Chem. Soc.* **1993***, 115,* 6382–6390.

4. Numata, Y.; Singh, S. P.; Islam, A.; Iwamura, M.; Imai, A.; Nozaki, K.; Han, L. Enhanced light-harvesting capability of a panchromatic Ru(II) sensitizer based on π-extended terpyridine with a 4-methylstylryl Group for dye-sensitized solar cells. *Adv. Funct. Mater.* **2013***, 23,* 1817–1823.

5. Hepbasli, A. Development of geothermal energy utilization in Turkey: Areview. *Renew. Sustain. Energy Rev.* **2004***, 8, .* 433–460.

6. Shi. L.; Chew, M.Y.L. A review on sustainable design of renewable energy systems. *Renew. Sustain. Energy Rev.* **2012**, *16*, 192–207.

7. Reynal, A.; Forneli, A.; Martinez-Ferrero, E.; Sánchez-Díaz, A.; Vidal-Ferran, A.; O'Regan, B. C.; Palomares, E. Interfacial charge recombination between E(-)-TiO_2 and the I(-)/I3(-)

electrolyte in ruthenium heteroleptic complexes: Dye molecular structure-open circuit voltage relationship. *J. Am. Chem. Soc.* **2008,** *130,* 13558–13567.

8. Sun, Y.; Collins, S. N.; Joyce, L. E.; Turro, C. Unusual photophysical properties of a ruthenium(II) complex related to $[Ru(bpy)_2(dppz)]^{2+}$. *Inorg. Chem.* **2010***, 49,* 4257–4262.

9. Herzog, A.V.; Lipman, T.E.; Kammen, D.M.; Renewable energy sources: A variable choice. *Environ.Sci. Policy Sustain. Dev.* **2001***, 43*, 8–20.

10. El Chaar, L.; Lamont, L. A.; El Zein, N. Review of photovoltaic technologies. *Renew. Sustain. Energy. Rev.* **2011***, 15,* 2165–2175.

11. Mat, B. S. Biomass energy utilization and environment protection - commercial reality and outlook. Power-Gen. **2003**, 1–21.

12. Nwokolo, N.; Mamphweli, S.; Meyer, E.; Tangwe, S. Electrical performance evaluation of Johansson biomass gasifier system coupled to a 150 KVA generator. *Renew. Energy*. **2014**, *71*, 695–700.

13. Malatji, P.; Mamphweli, N. S.; Meincken, M. The technical pre-feasibility to use briquettes made from wood and agricultural waste for gasification in a downdraft gasifier for electricity generation. *J. Energy South Africa.* **2011**, *22*, 2–7.

14. Bahadori, A.; Zendehboudi, S.; Zahedi, G. A review of geothermal energy resources in Australia: current status and prospects. *Renew. Sustain. Energy. Rev.* **2013***, 21,* 29–34.

15. Sovacool, B. K.; Bulan, L. C. Energy security and hydropower development in Malaysia: The drivers and challenges facing the sarawak corridor of renewable energy (SCORE). *Renew. Energy*. **2012**, *40,* 113–129.

16. Sipahutar, R.; Bernas, S. M.; Imanuddin, M. S. Renewable energy and hydropower utilization tendency worldwide. Renew. *Sustain. Energy*. *Rev.* **2013***, 17,* 213–215.

17. Tian, J.; Gao, R.; Zhang, Q.; Zhang, S.; Li, Y.; Lan, J.; Qu, X.; Cao, G. Enhanced performance of CdS/CdSe quantum dot cosensitized solar cells via homogeneous distribution of quantum dots in TiO_2 film. *J. Phys. Chem. C.* **2012***, 116,* 18655–18662.

18. Üstüntaş, T.; Şahin, A. D. Wind turbine power curve estimation based on cluster center fuzzy logic modeling. *J. Wind Eng. Ind. Aerodyn.* **2008***, 96,* 611–620.

19. Yuasa, T.; Kawakami, R.; Sato, Y.; Mori, Y.; Adachi, M.; Yoshikado, S. Dye adsorption for dye-sensitized solar cell. *Sol. Energy Mater. Sol. Cells.* **2012***, 102,* 2–7.

20. Iain McConnell, Gonghu Li, and G. B. Energy conversion in natural and artificial photosynthesis. *Chem . Biol.* **2010***, 17,* 434–447

21. Wang, P.; Zakeeruddin, S. M.; Moser, J. E.; Nazeeruddin, M. K.; Sekiguchi, T.; Grätzel, M. A stable quasi-solid-state dye-sensitized solar cell with an amphiphilic ruthenium sensitizer and polymer gel electrolyte. *Nat. Mater.* **2003***, 2,* 402–407.

22. Alhamed, M.; Issa, A. S.; Doubal, A. W. Studying of natural dyes properties as photo-sensitizer for dye sensitized solar cells (dssc). *J. Electron Devices.* **2012**, *16*, 1370–1383.

23. Chen, C.-Y.; Wu, S.-J.; Li, J.-Y.; Wu, C.-G.; Chen, J.-G.; Ho, K.-C. A new route to enhance the light-harvesting capability of ruthenium complexes for dye-sensitized solar cells. *Adv. Mater.* **2007** *, 19,* 3888–3891.

24.Chen.; C.; Ting, C. Photoelectrode fabrication of dye-sensitized nano solar cells using multiple spray coating technique. *Int. J. Photoenergy.* **2013***, 2013,* 1–8.

25. Tobin, L. L.; O'Reilly, T.; Zerulla, D.; Sheridan, J. T. Characterising dye-sensitised solar cells. *Opt. Int. J. Light Electron Opt.* **2011**, *122*, 1225–1230.

26. Grätzel, M. Solar energy conversional by dye-sensitized solar cell. *Inorg.Chem.* **2005**, *44* , 6841-6851.

27. Bansal, R. .; Bhatti, T. .; Kothari, D. On some of the design aspects of wind energy conversion systems. *Energy Convers. Manag.* **2002**, *43*, 2175–2187.

28. Hagfelt, A.; Gratzel, M. Molecular photovoltaics. *Acc. Chem. Res.* **2000***, 33,* 269-277.

29. Zhu, W.; Wu, Y.; Wang, S.; Li, W.; Li, X.; Chen, J.; Wang, Z.; Tian, H. Organic D-A-π-A solar cell sensitizers with improved stability and spectral response. *Adv. Funct. Mater.* **2011***, 21,* 756–763.

30. Bari, D.; Wrachien, N.; Tagliaferro, R.; Penna, S.; Brown, T. M.; Reale, A.; Di Carlo, A.; Meneghesso, G.; Cester, A. Thermal stress effects on dye-sensitized solar cells (DSSCs). *Microelectron. Reliab.* **2011***, 51,* 1762–1766.

31. Kim, J.-J.; Yoon, J. A new ruthenium sensitizer containing dipyridylamine ligand for effective nanocrystalline dye-sensitized solar cells. *Inorg Chim. Acta.* **2013***, 394,* 506–511.

32. Chang, W.-C.; Chen, H.-S.; Li, T.-Y.; Hsu, N.-M.; Tingare, Y. S.; Li, C.-Y.; Liu, Y.-C.; Su, C.; Li, W. -R. Highly efficient n-heterocyclic carbene/pyridine-based ruthenium sensitizers: Complexes for dye-sensitized solar cells. *Angew. Chem. Int. Ed. Engl.* **2010***, 49,* 8161–8164.

33. Winnischofer, H.; Araki, K.; Ribeiro, P. E. A.; Donnici, C. L. Photophysical and photoelectrochemical properties of the bis (2,2'-bipyridine)(4, 4'-dimethylthio-2,2'-bipyridine) ruthenium(II) complex. *J. Photochem. Photobiol. A Chem.* **2000***, 135,* 185–191.

34.Baudin, H. B. Electron and energy transfer in supramolecular complexes designed forArtificial photosynthesis. PhD thesis. Uppsala University. **2001**.

35. Kumar, S.; Sharma, T. R. Synthesis, structure and luminescent properties of Ti(III),V(III) transition metal polymeric macrocyclic complexes derived from phenanthroline and biphenyl groups. *Orient. J. Chem.* **2012***, 28,* 963–967.

36. Newkome, G. R.; Patri, A. K.; Holder, E.; Schubert, U. S. Synthesis of 2,2'-bipyridines : versatile building blocks for sexy architectures and functional nanomaterials. *J. Eur. Org. Chem.* **2004***,* 235–254.

37. Wang, J.-L.; Li, X.; Shreiner, C. D.; Lu, X.; Moorefield, C. N.; Tummalapalli, S. R.; Medvetz, D. a.; Panzner, M. J.; Fronczek, F. R.; Wesdemiotis, C. Shape-persistent, ruthenium(II)- and iron(II)-bisterpyridine metallodendrimers: Synthesis, traveling-wave ion-mobility mass spectrometry, and photophysical properties. *New J. Chem.* **2012***, 36,* 484-491.

38. Li, X. Synthesis of bipyridine-derived ligands for DNA binding and shape switching. Masters dissertation. Queen's Univertsity. Canada. September 2009.

39. Schubert, U. S.; Eschbaumer, C.; Heller, M. Stille-type cross-coupling an efficient way to various symmetrically and unsymmetrically substituted methyl-bipyridines : Toward new ATRP catalysts. *Org. Lett.* **2000***, 3–6.*

40. Rosenthal, J.; Nepomnyashchii, A.B.; Kozhukh, J.; Bard, A.J.; Stephen, J.L. Synthesis, photophysics, electrochemistry and electrogenerated chemiluminescence of homologues set of BODIPY-appended bipyridine derivatives. *J. Phys. Chem C. Nano mater. Interface.* **2011**. *115.* 17993-18001.

41. Abrahamsson, M. L. A. Electron transfer in ruthenium-manganese complexes for artificial photosynthesis. PhD Thesis. Uppsala University. **2001**.

42. Polo, A. S.; Itokazu, M. K.; Murakami Iha, N. Y. Metal complex sensitizers in dye-sensitized solar cells. *Coord. Chem. Rev.* **2004**, *248*, 1343–1361.

43. Shen, Y.; Maliwal, B. P.; Lakowicz, J. R. Red-emitting ru(II) metal – ligand complexes. *J. Fluoresc.* **2003***, 13,* 8–13.

44. Evans, I, P.; Spencer, A.; Wilkinson, G. Dichlorotetrakis(dimethylsulphoxide)ruthenium(II) and its use as a source material for some new ruthenium(II) complexes. *J. Chem. Soc. Dalt. Trans.* **1973**, 204-209.

45. Harvey, A.; Draganjac, M.; Chui, S.; Snell, R.; Benjamin, E. Microwave synthesis of cis-dichlorotetrakis (dimethylsulfoxide) ruthenium(II). *J. Arkansas Acad. Sci.* **2009**, *63*, 72467.

46. Adeloye, A. O.; Ajibade, P. A. A High molar extinction coefficient mono-anthracenyl bipyridyl heteroleptic ruthenium(II) Complex: Synthesis, photophysical and electrochemical properties. *Molecules.* **2011**, *16*, 4615–4631.

47. Sánchez-de-Armas, R.; . San-Miguel, M. A.; Oviedo, J.; Sanz, J. F. Direct vs. indirect mechanisms for electron injection in DSSC: Catechol and alizarin. *Comput. Theor. Chem.* **2011***, 975,* 1–3.

48. Vougioukalakis, G. C.; Philippopoulos, A. I.; Stergiopoulos, T.; Falaras, P. Contributions to the development of ruthenium-based sensitizers for dye-sensitized solar cells. *Coord. Chem. Rev.* **2011***, 255,* 2602–2621.

49. Gong, J.; Liang, J.; Sumathy, K. Review on dye-sensitized solar cells (DSSCs): F11undamental concepts and novel materials. *Renew. Sustain. Energy Rev.* **2012***, 16,* 5848–5860.

50. Zhan, J.; Que, W.; Jia, Q.; Zhong, P.; Liao, Y.; Ye, X.; Ding, Y. Novel bilayer structure ZnO based photoanode for enhancing conversion efficiency in dye-sensitized solar cells. *J. Alloys Compd.* **2011***, 509,* 7421–7426.

51. Cao, Y.; Bai, Y.; Yu, Q.; Cheng, Y.; Liu, S.; Shi, D.; Gao, F.; Wang, P. Dye-sensitized solar cells with a high absorptivity ruthenium sensitizer featuring a 2-(hexylthio)thiophene conjugated bipyridine. *J. Phys. Chem. C*. ***2009***, *113*, 6290–6297.

52. Nazeeruddin, K.; Klein, C.; Liska, P.; Gr, M. Synthesis of novel ruthenium sensitizers and their application in dye-sensitized solar cells. *Coord. Chem. Rev.* **2005***, 249,* 1460–1467.

53. Funaki, T.; Yanagida, M.; Onozawa-Komatsuzaki, N.; Kasuga, K.; Kawanishi, Y.; Sugihara, H. A 2-quinolinecarboxylate-substituted ruthenium(II) complex as a new type of sensitizer for dye-sensitized solar cells. *Inorg. Chim. Acta*. **2009**, *362*, 2519–2522.

54. Funaki, T.; Yanagida, M.; Onozawa-Komatsuzaki, N.; Kawanishi, Y.; Kasuga, K.; Sugihara, H. Ruthenium(II) complexes with π-expanded ligand having phenylene–ethynylene moiety as sensitizers for dye-sensitized solar cells. *Sol. Energy Mater. Sol. Cells.* **2009** , *93*, 729–732.

55. Giribabu, L.; Vijay Kumar, C.; Rao, C. S.; Reddy, V. G.; Reddy, P. Y.; Chandrasekharam, M.; Soujanya, Y. High molar extinction coefficient amphiphilic ruthenium sensitizers for efficient and stable mesoscopic dye-sensitized solar cells. *Energy Environ. Sci.* **2009**, *2*, 770-773.

56. Chen, C.; Liao, J.-Y.; Chi, Z.; Xu, B.; Zhang, X.; Kuang, D.-B.; Zhang, Y.; Liu, S.; Xu, J. Metal-free organic dyes derived from triphenylethylene for dye-sensitized solar cells: Tuning of the performance by phenothiazine and carbazole. *J. Mater. Chem.* **2012***, 22,* 8994-9005.

57. Nazeeruddin, M. K.; Klein, C.; Liska, P.; Grätzel, M. Synthesis of novel ruthenium sensitizers and their application in dye-sensitized solar cells. *Coord. Chem. Rev.* **2005***, 249,* 1460–1467.

58. Chen, C.-Y.; Lu, H.-C.; Wu, C.-G.; Chen, J.-G.; Ho, K.-C. New ruthenium complexes containing oligoalkylthiophene-substituted 1,10-phenanthroline for nanocrystalline dye-Sensitized Solar Cells. *Adv. Funct. Mater.* **2007**, *17*, 29–36.

59. Li, J.; Chen, C.; Chen, J.; Tan, C.; Lee, K.; Wu, S. Heteroleptic ruthenium antenna-dye for high-voltage dye-sensitized solar cells. *J. Mater. Chem.* **2010***, 20,* 7158–7164.

60. Chen, C.-Y.; Wu, S.-J.; Wu, C.-G.; Chen, J.-G.; Ho, K.-C. A ruthenium complex with superhigh light-harvesting capacity for dye-sensitized solar cells. *Angew. Chem. Int. Ed. Engl.* **2006***, 45,* 5822–5825.

61. Chen, C.; Pootrakulchote, N.; Hung, T.; Tan, C.; Tsai, H.; Zakeeruddin, S. M.; Wu, C.; Gr, M. Ruthenium sensitizer with thienothiophene-linked carbazole antennas in conjunction with liquid electrolytes for dye-sensitized solar cells. *J. Phys. Chem.* **2011***, 115,* 20043–20050.

62. Qin, Y.; Peng, Q. Ruthenium sensitizers and their applications in dye-sensitized solar cells. *Int. J. Photoenergy.* **2012***, 2012,* 1-21

63. Islam, A.; Sugihara, H.; Singh, L. P.; Hara, K.; Katoh, R.; Nagawa, Y.; Yanagida, M.; Takahashi, Y.; Murata, S.; Arakawa, H. Synthesis and photophysical properties of ruthenium(II) charge transfer sensitizer containing 4,4'-dicarboxy-2,2'-biquinoline and 5,8-dicarboxy-6,7-dihydrozo-1,10-phenanthroline. *Inorg. Chim.* **2001***, 322,* 7–16.

64. Chiba, Y.; Islam, A.; Watanabe, Y.; Komiya, R.; Koide, N.; Han, L. Dye-sensitized solar cells with conversion efficiency of 11.1%. *Jpn. J. Appl. Phys.* **2006**, *45*, 638–640.

65. Zakeeruddin, S. M.; Nazeeruddin, M. K.; Pechy, P.; Rotzinger, F. P.; Humphry-Baker, R.; Kalyanasundaram, K.; Grätzel, M.; Shklover, V.; Haibach, T. Molecular engineering of photosensitizers for nanocrystalline solar cells: Synthesis and characterization of Ru dyes based on phosphonated terpyridines. *Inorg. Chem.* **1997**, *36*, 5937–5946

66. Wang, P.; Zakeeruddin, S. M.; Moser, J. E.; Nazeeruddin, M. K.; Sekiguchi, T.; Grätzel, M. A stable quasi-solid-state dye-sensitized solar cell with an amphiphilic ruthenium sensitizer and polymer gel electrolyte. *Nat. Mater.* **2003**, *2*, 402–407.

67. Giribabu, L.; Vijay Kumar, C.; Rao, C. S.; Reddy, V. G.; Reddy, P. Y.; Chandrasekharam, M.; Soujanya, Y. High molar extinction coefficient amphiphilic ruthenium sensitizers for efficient and stable mesoscopic dye-sensitized solar cells. *Energy Environ. Sci.* **2009**, *2*, 770-773.

68. Giribabu, L.; Kanaparthi, R. K. Are porphyrins an alternative to ruthenium(II) sensitizers for dye-sensitized solar cells. *Current. Sci.* **2013***, 104,* 847-855.

69. Chandrasekharam, M.; Rajkumar, G.; Rao, C. H. S.; Suresh, T.; Reddy, P. Y.; Soujanya, Y. Ruthenium(II)- bipyridyl with extended-π-system : Improved thermo-stable sensitizer for efficient and long-term durable dye sensitized solar cells. *J. Chem. Sci.* **2001***, 123,* 555–565.

70. Adeloye, A. O.; Ajibade, P. A; Cummings, F. R.; Roux, L. J.; Mamphweli, S. N.; Meyer, E. L. Synthesis, photophysical and preliminary investigation of the dye-sensitized solar cells properties of functionalized anthracenyl-based bipyridyl and phenanthrolyl ru(II) complexes. *J. Chem. Sci.* **2013**, *125*, 17–27.

71.Adeloye, A. O. Synthesis, photophysical and electrochemical properties of a mixed bipyridyl-phenanthrolyl ligand Ru(II) heteroleptic complex having trans-2-methyl-2-butenoic acid functionalities. *Molecules.* **2011***, 16,* 8353–8367.

72. Adeloye, A. O.; Ajibade, P. A. Synthesis and characterization of a heteroleptic Ru(II) complex of phenanthroline containing oligo-anthracenyl carboxylic acid moieties. *Int. J. Mol. Sci.* ***2010***, *11*, 3158–3176.

73. Sheeba.; D. A. G. R. George, G. R. Luminescence quenching of tris(4,4′-dinonyl-2,2′-bipyridyl) ruthenium(II) cation with phenolate ions in DMSO. *Arab. J. Chem.* **2013**. *14*, 4–10.

74. Adeloye, A. O.; Ajibade, P. A. Synthesis and characterization of a Ru(II) complex with functionalized phenanthroline ligands having single-double linked anthracenyl and 1-methoxy-1-buten-3-yne moieties. *Molecueles.* **2010***, 15,* 7570–7581.

75. Ahmed, M. O.; Pisula, W.; Mhaisalkar, S. G. Synthesis and characterization of new thieno[3,2-b]thiophene derivatives. *Molecules.* **2012***, 17,* 12163–71.

76. Adeloye, A. O.; Olomola, T. O.; Adebayo, A. I.; Ajibade, P. A. A high molar extinction coefficient bisterpyridyl homoleptic Ru(II) complex with trans-2-methyl-2-butenoic acid functionality: potential dye for dye-sensitized solar cells. *Int. J. Mol. Sci.* **2012***, 13,* 3511–3526.

77. Barea, E. M.; Victoria, G.; Ripoll, T.; Wu, H.; Li, L.; Yeh, C.; Diau, E. W.; Bisquert, J. Porphyrin dyes with high injection and low recombination for highly efficient mesoscopic dye-sensitized solar cells. *J. Phys. Chem. C.* **2011***, 115,* 10898–10902.

78. Wongcharee, K.; Meeyoo, V.; Chavadej, S. Dye-sensitized solar cell using natural dyes extracted from rosella and blue pea flowers. *Sol. Energy Mater. Sol. Cells.* **2007**, *91*, 566–571.

79. Quina, F. H.; Moreira, P. F.; Vautier-Giongo, C.; Rettori, D.; Rodrigues, R. F.; Freitas, A. a.; Silva, P. F.; Maçanita, A. L. Photochemistry of anthocyanins and their biological role in plant tissues. *Pure Appl. Chem.* **2009**, *81*, 1687–1694.

80. Imahori, H.; Umeyama, T.; Ito, S. Large pi-aromatic molecules as potential sensitizers for highly efficient dye-sensitized solar cells. *Acc. Chem. Res.* **2009***, 42,* 1809–1818.

81. Hsieh, C.-P.; Lu, H.-P.; Chiu, C.-L.; Lee, C.-W.; Chuang, S.-H.; Mai, C.-L.; Yen, W.-N.; Hsu, S.-J.; Diau, E. W.-G.; Yeh, C.-Y. Synthesis and characterization of porphyrin sensitizers with various electron-donating substituents for highly efficient dye-sensitized solar cells. *J. Mater. Chem.* **2010***, 20,* 1127-1134.

82. Karthikeyan, S.; Lee, J.Y. Zinc-porphyrin based dyes for dye-sensitized solar cells. *J. Phys. Chem. A.* **2013***, 117,* 10973-10979.

83. Umar, A. A.; Rahman, M. Y. A.; Taslim, R.; Salleh, M. M.; Oyama, M. Effect of the thickness of quasi one-dimensional zinc oxide nanorods synthesized via multiple growth process

under ammonia assisted hydrolysis technique on the performance of dye-sensitized solar sell. *Int. J. Electrochem. Sci.* **2012***, 7,* 8384–8393.

84. Adeloye, A.O.; Ajibade, P.A. Towards the development of functionalized polypyridine ligands for Ru(II) complexes as photosensitizers in dye-sensitized solar cells (DSSCs). *Molecules.* **2014***, 19,* 12421–12460.

85. Han, L.-H.; Zhang, C.-R.; Zhe, J.-W.; Jin, N.-Z.; Shen, Y.-L.; Wang, W.; Gong, J.-J.; Chen, Y.-H.; Liu, Z.-J. Understanding the electronic structures and absorption properties of porphyrin sensitizers YD2 and YD2-O-C8 for dye-sensitized solar cells. *Int. J. Mol. Sci.* **2013***, 14,* 20171–20188.

86. Campbell, W. M.; Burrell, A. K.; Officer, D. L.; Jolley, K. W. Porphyrins as light harvesters in the dye-sensitised TiO_2 solar cell. *Coord. Chem. Rev.* **2004***, 248,* 1363–1379.

87. Rokesh, K.; Pandikumar, A.; Jothivenkatachalam, K. Dye sensitized solar cell: A summary. *Mater. Sci. Forum.* **2013**, *771*, 1–24.

88. Hara, K.; Tachibana, Y.; Ohga, Y.; Shinpo, A.; Suga, S.; Sayama, K.; Sugihara, H.; Arakawa. H. Dye-sensitized nanocrystalline TiO_2 solar cells based on novel coumarin dyes. *Sol. Energy Mater. Sol. Cells.* **2003***, 77,* 89–103.

89 Hara, K.; Sato, T.; Katoh, R.; Furube, A.; Ohga, Y.; Shinpo, A.; Suga, S.; Sayama, K.; Sugihara, H.; Arakawa, H. Molecular design of coumarin dyes for efficient dye-sensitized solar cells. *J. Phys. Chem. B.* **2003**, *107*, 597–606.

90. Mishra, A.; Fischer, M, K, R.; Bäuerle. P. Metal-free organic dyes for dye-sensitized solar cells : From structure : property relationships to design rules *Angew. Chem. Int. Ed.* **2009***, 48,* 2474–2499.

91. Zijian, X.C. Characterization of the Dye- Sensitized Solar Cell. BSc. Worcester Polyy Technique Institude. Dec. **2012**.

92. Xu, W.; Peng, B.; Chen, J.; Liang, M.; Cai, F. New triphenylamine-based dyes for dye-sensitized solar cells. *J. Phys. Chem. C.* **2008**, *112*, 874–880.

93. Huang, Y.; Lee, K.; Rochford, J.; Tsai, M. Electronic structure investigation on non-innocent ruthenium quinolate complexes for DSSC application. *Photochem. Photobiol.* ***2009****, 86, 1230-1236.*

94. Kuang, D.; Klein, C.; Snaith, H. J.; Humphry-Baker, R.; Zakeeruddin, S. M.; Grätzel, M. A new ion-coordinating ruthenium sensitizer for mesoscopic dye-sensitized solar cells. *Inorg. Chim. Acta.* **2008**, *361*, 699–706.

95. Xu, W.; Peng, B.; Chen, J.; Liang, M.; Cai, F. New triphenylamine-based dyes for dye-sensitized solar cells. *J. Phys. Chem. C*. **2008**, *112*, 874-880.

96. Chergui, M. Ultrafast studies of the light-induced spin change in Fe(II) -polypyridine complexes. *J. Phys. Chem. C.* **2009***,117, 9–12*.

97. Nazeeruddin, M. K.; Baranoff, E.; Grätzel, M. Dye-Sensitized Solar Cells: A brief overview. *Sol. Energy.* **2011**, *85*, 1172–1178.

98. Onicha, A. C. Heteroleptic osmium(II) polypyridine complexes and carbazole-based chromophores as sensitizers in dyesensitized solar cells. PhD Thesis. Bowling Green StateUniversity. December, **2010**.

99. Qin, Y.; Peng, Q. Ruthenium sensitizers and their applications in dye-sensitized solar cells. *Int. J. Photoenergy.* **2012***, 2012,* 1–21.

100. Treadway, J. A.; Loeb, B.; Lopez, R.; Anderson, P. A.; Keene, F. R.; Meyer, T. J. Effect of delocalization and rigidity in the acceptor ligand on MLCT excited-state decay. *Inorg. Chem.* **1996**, *35*, 2242–2246.

101. Messina, F.; Barano, E.; Cannizzo, A.; Nazeeruddin, M. K.; Chergui, M. Ultrafast relaxation dynamics of osmium− polypyridine complexes in solution. *J. Phsy. Chem. C.* **2013**.*117,* 15958-15966

102. Kinoshita, T.; Fujisawa, J.; Nakazaki, J.; Uchida, S.; Kubo, T.; Segawa, H. Enhancement of near-IR photoelectric conversion in dye-sensitized solar cells using an osmium sensitizer with strong spin-forbidden transition. *J. Phys. Chem. Lett.* **2012***, 3,* 394-398.

103. Balzani, V.; Juris, A.; Venturi, M.; Campagna, S.; Serroni, S. Luminescent and redox-active polynuclear transition metal complexes. *Chem. Rev.* **1996**, *96*, 759–834.

104. Balzani, V.; Juris, A. Photochemistry and photophysics of Ru(II) polypyridine complexes in the Bologna group from early studies to recent developments. *Coord. Chem. Rev.* **2001**. *211,* 97–115.

105. Cannizzo, A.; Milne, C. J.; Consani, C.; Gawelda, W.; C. Bressler, C.; Mourik, F. V.; Chergui, M. Light-induced spin crossover in Fe(II)-based complexes: The full photocycle unraveled by ultrafast optical and X-ray spectroscopies. *Coord. Chem. Rev.* **2010***, 254,* 2677–2686.

106. Morita, M.; Tanaka, Y.; Tanaka, K.; Matsuda,Y. Eletrochemical oxidation of ruthenium and iron complexes at rotating disk electrode in acetonitrile solution. *Bull. Chem. Soc. Japan.* **1998***, 61,*2771- 2774.

107. Ege, D.; Becker, W. G.; Bard, A. J. Electrogenerated chemiluminescent determination of tris(2,2'-bipyridine)ruthenium ion $(Ru(bpy)_3)^{2+}$ at low levels. *Anal. Chem.* **1984**, *56*, 2413–2417.

108. Funaki, T.; Otsuka, H.; Onozawa-Komatsuzaki, N.; Kasuga, K.; Sayama, K.; Sugihara, H. Systematic evaluation of HOMO energy levels for efficient dye regeneration in dye-sensitized solar cells. *J. Mater. Chem. A*. **2014**, 00, 1–7.

109. Inomata, T.; Yamamoto, K.; Funahashi, Y.; Ozawa, T.; Masuda, H. Characterization and application of Ru^{2+} complex with square-planar quadridentate ligand containing arylamines for dye-sensitized solar cells. *Jpn. J. App. Phys.* **2013***, 52,* 1–5.

110. Magne, F. Dufour, F. Labat, G. Lancel, O. Durupthy, S. Cassaignon, and T. Pauporté. Effects of TiO_2 nanoparticle polymorphism on dye-sensitized solar cell photovoltaic properties. *J. Photochem. Photobiol. A Chem.* **2012**, *232*, 22–31.

111. Marinado, T. Photoelectrochemical studies of dye-sensitized solar cells using organic dyes. PhD Thesis. School of chemical science and engineering Kungliga Tekniska Hogskilan. Stockholm December. **2009**.

112. Atiq, A. A. Design and synthsis of novel ruthenium based sensitizer for dye- sensitized solar cells. MSc Desertation, North Carolina State University, March. **2011**

112. Takagi, K.; Magaino, S.; Saito, H.; Aoki, T.; Aoki, D. Measurements and evaluation of dye-sensitized solar cell performance. *J. Photochem. Photobiol. C Photochem. Rev.* **2013**, *14*, 1–12

114. Erten-ela, S. Characterization and performance evaluation of dye sensitized solar cell using nanostructured TiO_2 electrode. *Int. J. Photo. Photoergy.* **2014***, 2014,* 1–6.

115. Ocakoglu, K.; Harputlu, E.; Guloglu, P.; Erten-Ela, S. The photovoltaic performance of new ruthenium complexes in DSSCs based on nanorod ZnO electrode. *Synth. Met.* **2012**, *162*, 2125–2133.

116. Nguyen, H. M.; Nguyen, D. N.; Kim, N. Improved performance of dye-sensitized solar cells by tuning the properties of ruthenium complexes containing conjugated bipyridine ligands. *Adv. Nat. Sci. Nanosci. Nanotechnol.* **2010**, *1*, 1-6.

117. Nazeeruddin, M.K.; Bessho, T,; Cevey, L.; Ito, S.; Klein, C.; Angelis, F. D.; Fantacci, S.; Comte, P.; Liska, P.; Imai, H.; Graetzel, M. A high molar extinction coefficient charge transfer sensitizer and its application in dye-sensitized solar cell. *J. Photochem. Photobiol. A Chem.* **2007***, 185,*331–337.

118. Mishra, A.; Fisher, K, R.; Bauerle, P. Metal free organic dye-sensitized solar cells: From structure: Property relationships to design rules. Angew. *Chem. Int. Ed.* **2009***, 48,* 2774-2499.

119.Giribabu, L.; Singh, V.K.; C. V. Kumar, C. V.; Soujanya, Y.; Reddy, V.G.; P. Y. Reddy, P.Y. Organic-ruthenium(II) polypyridyl Complex Based Sensitizer for Dye-Sensitized Solar Cell Applications. *Adv. Optoelectro.* **2011***, 2011.* 1-8

120. Takagi, K.; Magaino, S.; Saito, H.; Aoki, T.; Aoki, D. Photochemistry reviews measurements and evaluation of dye-sensitized solar cell performance. *J. Photochem. Photobiol. C Photochem. Rev.* **2013***, 14,* 1-12.

CHAPTER 2
EXPERIMENTAL

2.0 **Material**

All chemical were purchased from sigma Aldrich, and were being used as received without any further purification, ruthenium(III) chloro hydrate ($RuCl_3. xH_2O$) purchased from sigma Aldrich 2.2'-bipyridine, 1.10-phenanthroline, 2.9-dimethyl-1.10-phenanthroline, 4.7-dichloro-1,10-phenanthroline, 4.4'-dimethyl-2.2'-bipyridine, dimethyl sulphoxide, N,N dimethyl formamide, Toluene, Methanol, Sulphuric acid conc, Nitric acid (60%), Acetone, Diethyl ether.

2.1 **Physical measurements**

The instrumental techniques for sample characterization are: ultraviolet-visible (UV-Vis), photoluminescence (PL), Fourier transform infra-red (FTIR) and nuclear magnetic resonance spectroscopy (NMR).

2.1.1 **Melting point**

Sample of ligands and complexes in capillary tubes were introduced into a Stuart melting point apparatus model SMP 11 for melting point determination.

2.1.2 **Solubility test**

Solvents such as water, N,N dimethyl formamide, dimethylsulfoxide of different dielectric constant and polarities at hot and cold temperatures were used to determine the solubility of complexes.

2.1.3 **Infrared spectroscopy**

Infrared spectra of polypyridine ligands and ruthenium(II) polypyridine complexes was recorded on Perkin Elmer 2000 FTIR spectrophotometer as KBr discs in the range 4000-370 cm^{-1} region. Attenuated total reflectance (ATR) spectra was recorded on Bruker Tensor 27 attenuated total reflectance (ATR)-FTIR equipped with narrow band MCT detector, dedicated flow-through cell, made from a Teflon piece, a fused silica plate (45 x 35 x 3 mm) with holes for in- and outlet (36 mm apart), and a flat (1mm) viton seal. The cell will be mounted on an attachment for ATR measurements in the region of 4000-600 cm^{-1}.

Figure 2.1The Perkin Elmer 2000 FTIR spectrophotometer

2.1.4 **UV-Vis spectroscopy**

Electronic spectra of ruthenium(II) polypyridine complexes in different solvents were run in the range 200-900 nm on Perkin Elmer λ25 UV-Vis spectrophotometer. The samples were prepared using N,N dimethyl formamide and dimethyl sulphoxide as solvents and placed in glass cuvettes of 1 cm path length. All ruthenium(II) complexes were soluble in dimethyl formamide, DMSO and water as stated in solubility test table.

2.1.5 **Photoluminescence**

The photoluminescence of the ruthenium(II) polypyridine complexes in different solvent were measured using Perkin Elmer LS 45 Fluorimeter. The samples were dissolved in DMF, DMSO were placed in glass cuvettes of 1 cm path length.

Figure 2.2 The Perkin Elmer Photoluminscence

2.1.6 **Elemental analysis**

Elemental analyses for C, H, N and S were carried out on a Fison elemental analyzer.

2.1.7 ^{1}H- NMR spectroscopy

The NMR spectra of ligands and complexes were recorded on a Bruker ultrashield 600 NMR spectrometer operating at frequencies of 600 MHz for ^{1}H and 100.6 MHz. The temperature of the measurements was 303 K. NMR samples was prepared by dissolving the complexes in dmso-d_6 as solvent and placed in a magnetic field. A radiofrequency generator then irradiates the sample with a short pulse of radiation, causing resonance.

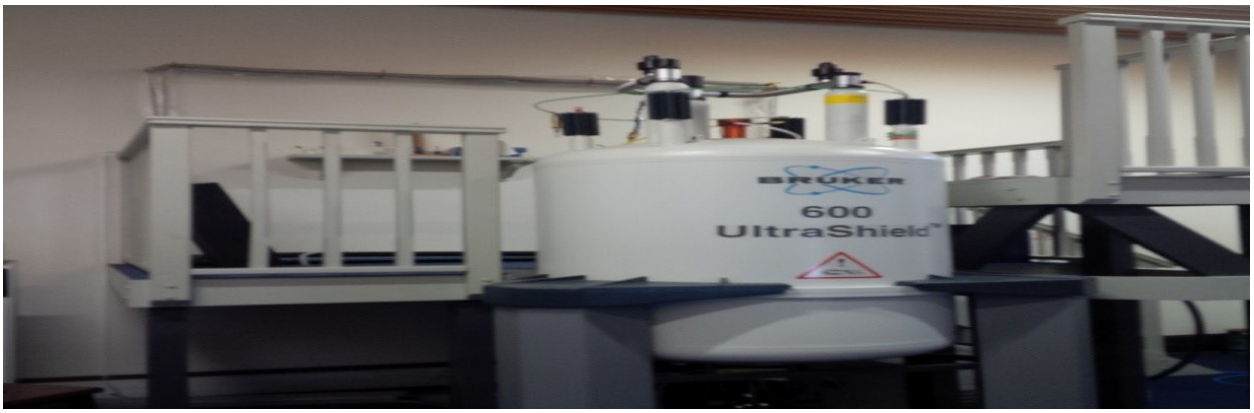

Figure 2.3 The Bruker Ultrashield 600M ^{1}H-NMR spectroscopy.

2.2 Synthesis of ligands

2.2.1 Synthesis of 4.7-disulphinic acid-1.10-phenanthroline (L1) [2]

In 100 mL two neck flask, 4.7-dichloro-1.10-phenanthroline (100 mg, 0.44 mmol), sodium sulphate (566 mg, 10 equivalent) excess was added to ethanol: water (1:1 v/v) (18 mL), the reaction mixture was refluxed at 80 ^{o}C was refluxed for 72 hours. Then the reaction was allowed to cool to room temperature and the solvent was removed using rotatory evaporator, and the pure white precipitate was formed and collected using a G4 crucible sintered glass, and the product

was washed using distilled water. Yield = 1.1126 g; 81%, Mp = 258 ºC; IR(cm^{-1}): 3329, 1675, 1210, 848, 759, 617.(^{1}HNMR, DMSO-d6) σ(ppm): 8.87; 8.86; 8,321; 7.86; 7.84.

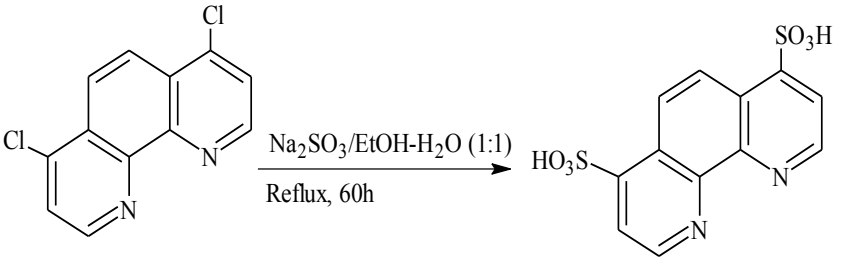

Scheme 1: Synthesis of 4.7-disulphonic acid-1.10-phenanthroline

Synthesis of 1.10-phenanthroline-2.9-dicarboxaldehyde (L2) [2.5]

In 100 mL two neck flask, 2.9-dimethyl-1.10-phenanthroline (neucuproine) (28 mg, 0.29 mmol) was added, and selenium dioxide in 1.4 dioxane : distilled water (95:5 %) (45:2.5 mL) was prepared separately and it was added directly into the flask, the reaction was stirred for 5-10 min, and refluxed at 100 ºC for 4hours. The solution was poured while it is hot using a G4 crucible sintered glass, and the black solids remain were collected on sintered glass, the yellow filtrate was concentrated on rotatory evaporator to remove the solvent and the yellow residue formed was collected and precipitated using the diethyl ether. Pale yellow product was obtained collected using sintered glass and washed with diethyl ether.

Yield = 0.92 g, 52 %, MP = 295 ºC IR (cm^{-1}): 1726; 2012; 2953, 3512; 3550. (^{1}H NMR DMSO-d_6): σ(ppm) 8.31; 8.324, 8,416; 8.77; 8.79; 8. 80; 9.964.

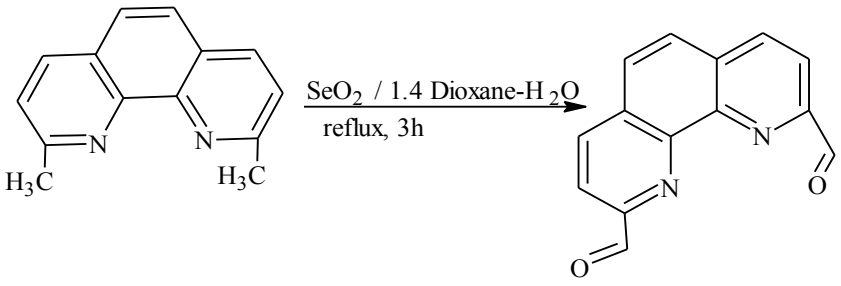

Scheme 2: Synthetic of 1.10-phenanthroline-2.9-dicarboxaldehyde.

2.2.2 **Synthesis of 2.2'-bipyridine-4.4'-dicarboxylic acid (L3)**

4.4'-dimethyl-2.2'-bipyridine (1000 mg-5.43 mmol) will be dissolve in 30mL of sulphuric acid at room temperature, and to this solution sodium dichromate (6100 mg- 23 mmol) will be added in portion for 4 hours, to oxidize methyl groups to carboxylate group. The reaction flask was heated to 80 ^{o}C for 12 hours while stirring. The reaction will be cooled, and thereafter was poured into ice water (200 mL) and kept at 0 ^{o}C for 12 hours. The formed suspension was filtered by suction. The expected green-yellow precipitate separated will be washed with distilled water till it is back to colourless. The solid was suspended in concentrated nitric acid and will be refluxed for 8 h, and then poured to an ice water for 12 h. The white powder was obtained. Yield = 0.12 g, 89 %, Mp: 295 ^{o}C , IR (nujol, cm^{-1}): 3415 ; 3548; 1620; 1721; 1292; 1367. ^{1}HNMR (DMSO-d$_6$): 8. 88; 8.86; 8.87; 8.72; 8.73; 8.09; 8.08.

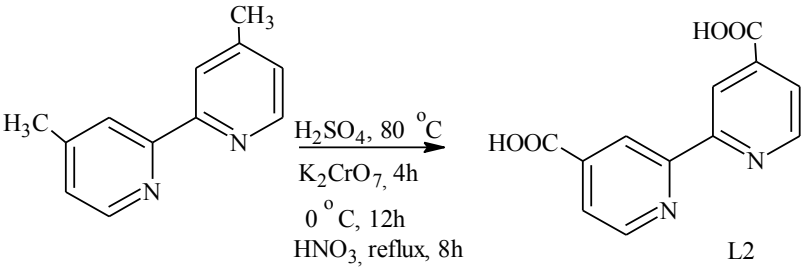

Scheme 3: Synthesis of 2.2'-bipyridine-4.4'-dicarboxylic acid

2.3 Synthesis of ruthenium-polypyridine complexes

2.3.1 Synthesis of tetrakis(dimethylsulfoxide)dichlororuthenium(II) [$Ru(DMSO)_4Cl_2$] [3-4]

In 100 mL two neck flask, well sorted condenser, ruthenium(III) chloro hydrate (100 mg, 4.82 mmol), dimethyl sulphoxide (6 mL) was mixed and stirred and heated to refluxed at 100-110 ^oC for 15 min. The dip orange solution was taken to rotatory evaporator to reduce the solvent to half. Then the deep orange solution was precipitated using acetone, then filtered using a G4 sintered glass, the product was washed using acetone followed by ether, the bright yellow product was formed. Mp = 197 ^oC, Yield = 1.1202 g.

$$RuCl_3\ _xH_2O + (DMSO)_4 \xrightarrow[\text{Acetone, washed}]{\text{Reflux, 100 }^oC\text{, 15min}} [RuCl_2\ (DMSO)_4]$$

Scheme 4: Synthesis of tetrakis (dimethyl sulfoxide) dichoro ruthenium(II) [$Ru(DMSO)_4Cl_2$.

2.3.2 Synthesis of [$Ru(bpy)_2$ (dcbpy)$(NCS)_2$]

In 100 mL two neck round bottom flask, with well sorted condenser, [$Ru(dmso)_4Cl_2$] (100 mg; 0.2 mmole) was dissolved in DMF (30 mL) and the reaction was stirred for 5-10 min, the 2.2'-bipyridine(64.3mg, 0.4119 mmol) was added and the reaction was purged with nitrogen and heated to reflux at 80-100 ^oC for 4 hours . The solution turns to purple brown colour, subsequently 2.2'-bipyridine-4.4'-dicarboxylic acid (100 mg; 0.4199 mmol) was added and the temperatures was adjusted to reflux the solution to 120-140 ^oC for 4 hours the reaction flask covered with alluminum foil to keep it under the dark, to this solution an excess of ammonium thiocyanate (250 mg) was added and the reaction was refluxed at 150 ^oC for another 4 hours. The

solvent was removed completely using rotatory evaporator and the crude product was dissolved in using dichloromethane was evaporated in atmosphere, then n-hexane was used to precipitate, the red-brown solid was collected using crucible sintered glass, and filtered by suction. Yield = 1.05 g , 77 %, Mp = 318 ^{o}C , IR (nujol,cm^{-1}): 3175; 2107.18; 1619; 1461; 1376; 847; 617; 377 UV-Vis (λ_{max} nm): 278, 346, 514)

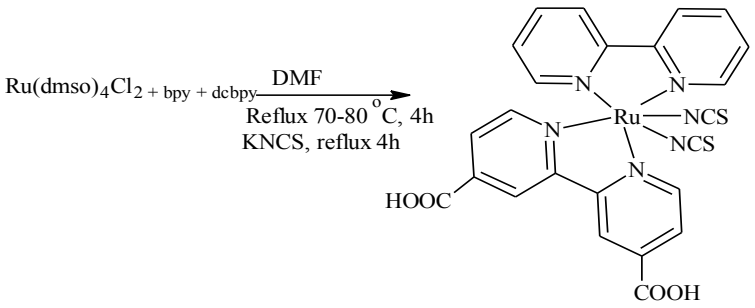

Scheme 5: Synthesis of [Ru(bpy)(dcbpy)(NCS)$_2$].

2.3.3 **Synthesis of [Ru(dsphen) (dcbpy)(NCS)$_2$]**

In 100 mL two neck flask, [Ru(dmso)$_4$Cl$_2$] (100 mg, 0,22 mmole) was dissolved in N,N dimethyl formamide (30 mL) the solution was stirred at room temperature for 5-10 min, then 1.0-phenanthroline-4,7-disulphonic acid(136 mg, 0.44 mmole), the reaction was refluxed at 80-100 ^{o}C under nitrogen gas for 4,5 hours the reaction was covered with aluminium foil to reduce the light. To this deep brown solution, 4.4'-dicarboxylic acid-2.2'-bipyridine (107 mg, 0.44 mmole) was added and the reaction was heated to reflux at 120-140 ^{o}C in the dark for about 4 hour, and then excess potassium thiocyanate (500 mg) was added as solid to this solution, and the temperature was raised to 150 ^{o}C to reflux for another 4 hours then the solution turned to be red-brown after which solvent was removed. Acetone was used to precipitate the brick-red product,

filtered using suction and washed with acetone: ether, the crucible sintered glass was used. Yield = 0.986 g, 58 %, Mp= 324 ^{o}C; Colour = redish-brown, IR (nujol, cm^{-1}) : 3385, 2920; 2093; 1646.69; 1376; 1456; 1238; 1067; 759. UV-Vis (λ_{max} nm): 300; 380; 531.

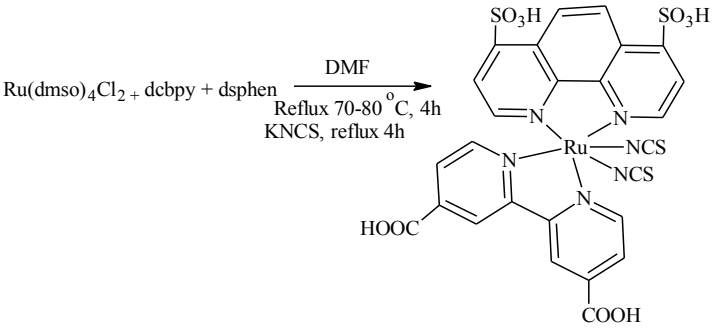

Scheme 6: Synthesis of [Ru(dcbpy)(dsphen)$(NCS)_2$]

2.3.4 **Synthesis of [Ru(dmbpy)(bpy)$(NCS)_2$]**

In a three neck 250 mL round bottom flask, [$Ru(dmso)_4Cl_2$], (100 mg, 0.22 mmole) was dissolved in DMF (30 mL), and the solution was stirred for 4-5 min to completely dissolve. In this solution 2.2'-bipyridine (81.065 mg; 0.44 mmole) was added and the flask was covered with aluminium foil to avoid the light coming through, the reaction was then heated to reflux at 60-75 ^{o}C for 4 hours under nitrogen gas. After that time, 2.2'-bipyridine-4.4'-dimethyl was added and the temperatures were raised to 150 ^{o}C for 4 hours keeping the reaction in the dark. Finally excess of ammonium thiocyanate (350 mg) was added and the reaction was refluxed at 160 ^{o}C for another 4 hours. The reaction was then cooled to room temperature, then was taken to rotatory evaporator to remove the solvent. The product was precipitated using diethyl ether and the precipitate was collected by suction filtration using the G4 sintered glass, the product was washed using the diethyl ether. The shiny dark product was obtained. Yield (%): 87, 1.04 g.

IR(nujol, cm^{-1}): 2858; 3352; 2900; 3166; 3352; 1457; 1373; 2092; 680 UV-Vis(υ_{max} nm): 277; 384; 520

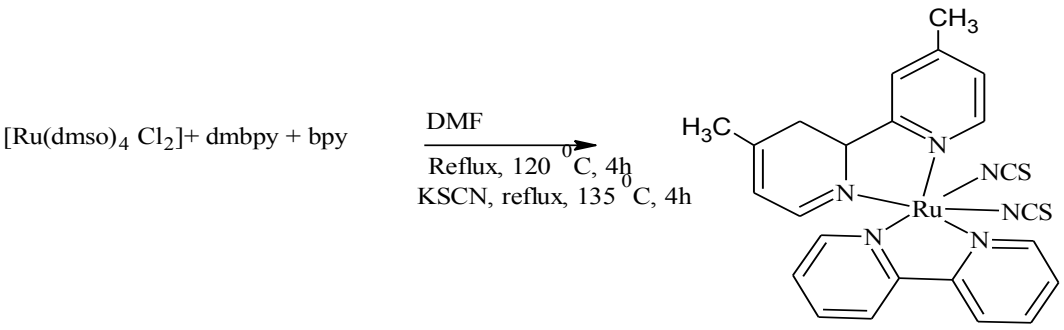

Scheme 7: Synthesis of $[Ru(dmbpy)(bpy)(NCS)_2]$

2.3.5 **Synthesis of $[Ru(bpy)_2(NCS)_2]$**

In two neck 100 mL flask, well sorted condenser, $[Ru(dmso)_4Cl_2]$ (100 mg, 0.22 mmole) was dissolved in DMF (30 mL) the reaction was stirred for 5 min-10 min, the 2.2'bipyridine (64.3 mg, 0.44 mmole) was added and the reaction was covered with aluminium foil, then it was heated to reflux at 80-120 ^oC for 8 hours. To this solution, excess ammonium thiocyanate (500 mg) was added and the reaction was refluxed at 150 ^oC for 4 hours under the dark. Then the brick red solution was taken to rotatory evaporator to reduce the solvent (DMF) and the product was dissolved in dichloro methane and precipitated using n-hexane, and filtered using suction, and filtered using suction , and crucible sintered glass was used to collect the product. Yield= 0.989 g, 84 % , Mp= , IR (nujol, cm^{-1}) ND: Uv-vis (λ_{max} nm): 277, 346, 503.

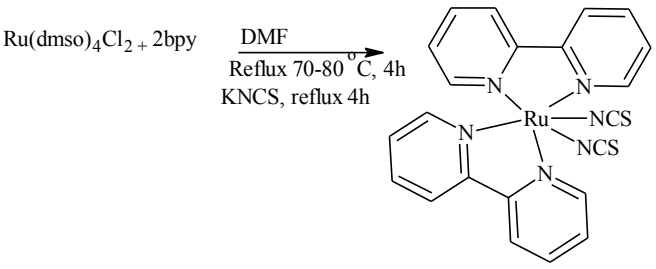

Scheme 8: Synthesis of $[Ru(bpy)_2(NCS)_2]$

2.3.6 **Synthesis of $[Ru(dcbpy)_2(NCS)_2]$**

The tetrakis(dimethyl sulphoxide) dichlororuthenium(II) (100 mg, 0.2 mmol) in a 100 mL round bottom flask was dissolved using N,N dimethyl formamide (40 mL), and the reaction was stirred, then 2,2'-bipyridine-4,4'-dicarboxylic acid (100 mg, 0.44 mmol), the reaction was heated to reflux at 120-140 ^oC for 8 hours, to this red-brown solution the excess of potassium thiocyanate was added and the reaction was heated to reflux at 150 ^oC for 4 hours, the reaction flask covered with aluminium foil to reduce light. The product was taken to rotatory evaporator to remove the solvent completely, acetone was used to precipitate, and the product was filtered using suction, and was washed using ether, the brick red solid was obtained. Yield= 0.88 g, 59 %, Mp= 334 ^oC, IR(nujol, cm^{-1}): 3365 ; 2923; 2092; 1649; 1374.95; 1304; 887: . UV-Vis (λmax, nm): 274; 340; 514.

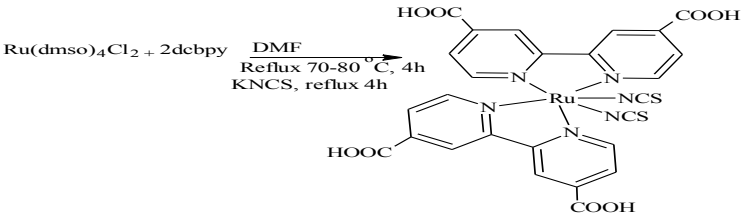

Scheme 9: Synthesis of $[Ru(dcbpy)_2(NCS)_2]$

2.3.7 **The synthesis of [Ru(dcAldphen)(dcbpy)(NCS)$_2$]**

In a two neck 100 mL flask [Ru(dmso)$_4$Cl$_2$] (100 mg, 0.22 mmol) was dissolved in DMF (40 mL), the solution was stirred at room temperature for 5 min, 2.9-dicarboxyaldehyde-1.10-phentanthroline (1.038 mg; 1.03 mmol) was added and the solution was heated to reflux at 80-100 ^{o}C under inert conditions for 4 hours and the reaction was covered with aluminium foil to reduce the light, subsequently 2.2'-bipyridine-4.4'-dicarboxylic acid (100 mg, 0.44 mmole) was added and the temperature was adjusted to reflux at 140-150 ^{o}C for 4 hours, then excess of potassium thiocyanate was added to this solution (300 mg) and the reaction was refluxed for another 4 hours. The dark solution was taken to rotatory evaporator to remove the solvent (DMF). Acetone was used to precipitate the product and filtered using suction and the crucible sintered glass was used to collect the product and was washed using acetone: ether and shiny dark solid was obtained. Yield = 1.02 g, 60 %, Mp= 234 ^{o}C, IR(nujol) υ(cm^{-1}): 3729; 2920; 2856; 2096; 1670; 1254. UV-Vis (λ_{max}, nm): 305; 366; 535.

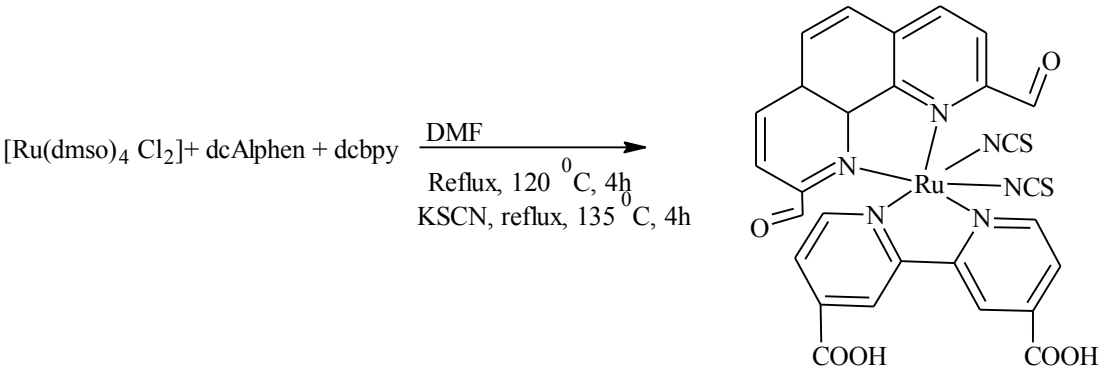

Scheme 10: Synthesis of [Ru(dcAldphen)(dcbpy)(NCS)$_2$]

2.4 **References**

1. Schwarz, O.; Van Loyen, D.; Jockusch, S.; Turro, N.J.; Dürr, H. Preparation and application of new ruthenium (II) polypyridyl complexes as sensitizers for nanocrystalline TiO_2. *J. Photochem. Photobiol. A Chem.* ***2000****, 132. 91-98* .

2. Dean, D.E. Metal ion complexing properties of the highly preorganized 1.10-phenanthroline-2.29-dicarboxylic acid. *Univ. North Carolina Wilmingt.* **2007**.

3. Evans, I.P.; Spencer, A.; Wilkinson, G. Dichlorotetrakis(dimethyl sulphoxide)ruthenium(II) and its use as a source material for some new ruthenium(II) complexes. *J. Chem. Soc. Dalt. Trans.* **1973**, 204.

4. Harvey, A.; M. Draganjac, M.; S. Chui, S.; R. Snell, R.; and E. Benjamin, E. Microwave synthesis of cis -dichlorotetrakis (dimethylsulfoxide) ruthenium(II). *Journal. Arkansas. Acad. Sci.* **2009**, *63*, 72467.

5. Melton, D, L. Metal ion complexing properties of the two-dimension, highly preorganized ligand 1.10-phenthroline-2.9-dicarboxylic acid. Ph.D. Thesis. Univ. North Carolina Wilmington. **2005.**

CHAPTER 3

3.0 SPECTROSCOPIC STUDIES OF THE LIGANDS AND METAL COMPLEXES

3.1 The FT-IR of ruthenium polypyridyl complexes introduction

The FTIR absorption at around 1610 and 1638 cm^{-1} are due to symmetric and asymmetric stretching modes of carboxylate groups $\upsilon(COO^-)$. The most prominent peak at around 2100 cm^{-1} corresponds to stretching mode of thiocyanate υ(NCS) group which indicates that N of NCS^- is coordinated to the ruthenium metal centre through N-atom [1,2]. The less intense absorption around this region to symmetric υ(C=S) vibration stretching [3].The bands which confirms the υ(Ru-N) are being observed at ~520 cm^{-1}, this is confirmation of polypyridyl ligand being attach to ruthenium metal using the N-atom.

3.2 The FT-IR spectra for ruthenium(II) polypyridyl complexes summary

The absorption peaks in these complexes seem to be identical due to similar structural features of the ligands, from 4000-400 cm^{-1}. The absorption peak of Ru-N could not be assigned due to absorption at lower finger print region at ~495 cm^{-1}. There are two peaks at 2920 and 2856 cm^{-1} which due to υ(OH) stretching vibration of carboxylic group. There is a broad peak at 3385.70 cm^{-1} which is due to OH of sulphonic acid but when attached to metal complex, the intensity was decreased. There is medium intense peak at 2093 cm^{-1} which is due to υ(C-N) stretching vibration mode of NCS, which is bonded to ruthenium with N-atom.

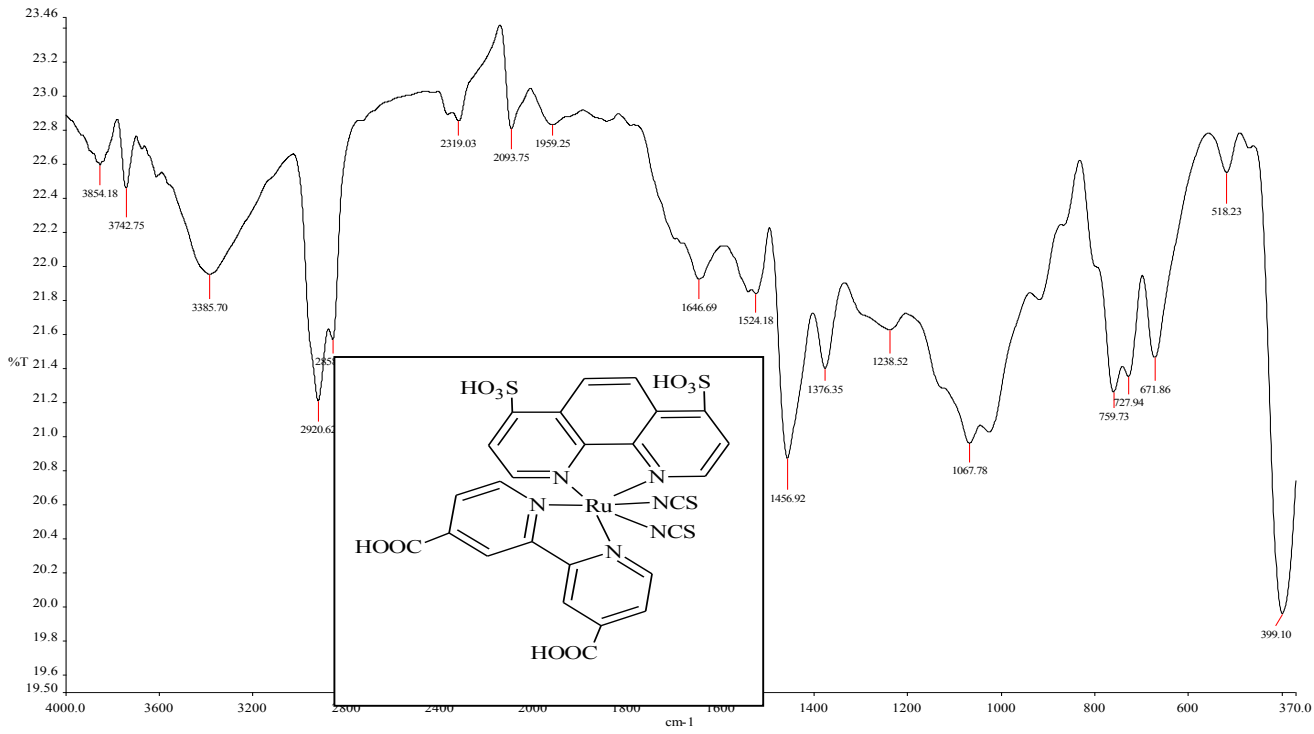

Figure 3.1 **The FT-IR spectrum of [Ru(dsphen)(dcbpy)(NCS)$_2$]**

The fig 3.1 above shows the Fourier Transform Infrared (FT-IR) spectrum of the complex [Ru(dsphen)(dcbpy)(NCS)$_2$]. This complex shows a similar absorption band frequency as that of ligand attached, but the is a unique broad, intense absorption band frequency at 2101.25 cm^{-1} which is due to υ(CN) vibrational stretch mode of thiocyanate group, and is bonded to the metal centre. This band is three to four times more intense compared to band exhibited at 810 cm^{-1}, which is due to υ(CS) of thiocyanate group. The band at observed at 807 show the υ(CS) of sulphonic group bonded to 1.10-phenathroline, this spectra also shows the absence of υ(C-Cl) band from the starting material (1.10-phenanthroline-4,7-dichoro). The absorption peak at around 848 cm-1 is due to υ(S=O) of sulphonic acid and the absorption peak at around 1238 cm^{-1} which is due to υ(C-S-O) stretching vibration mode [4]. The band from 2900-3300 cm^{-1} shows the υ(OH) of the carboxyl group and υ(C-H) of aromatic ring.

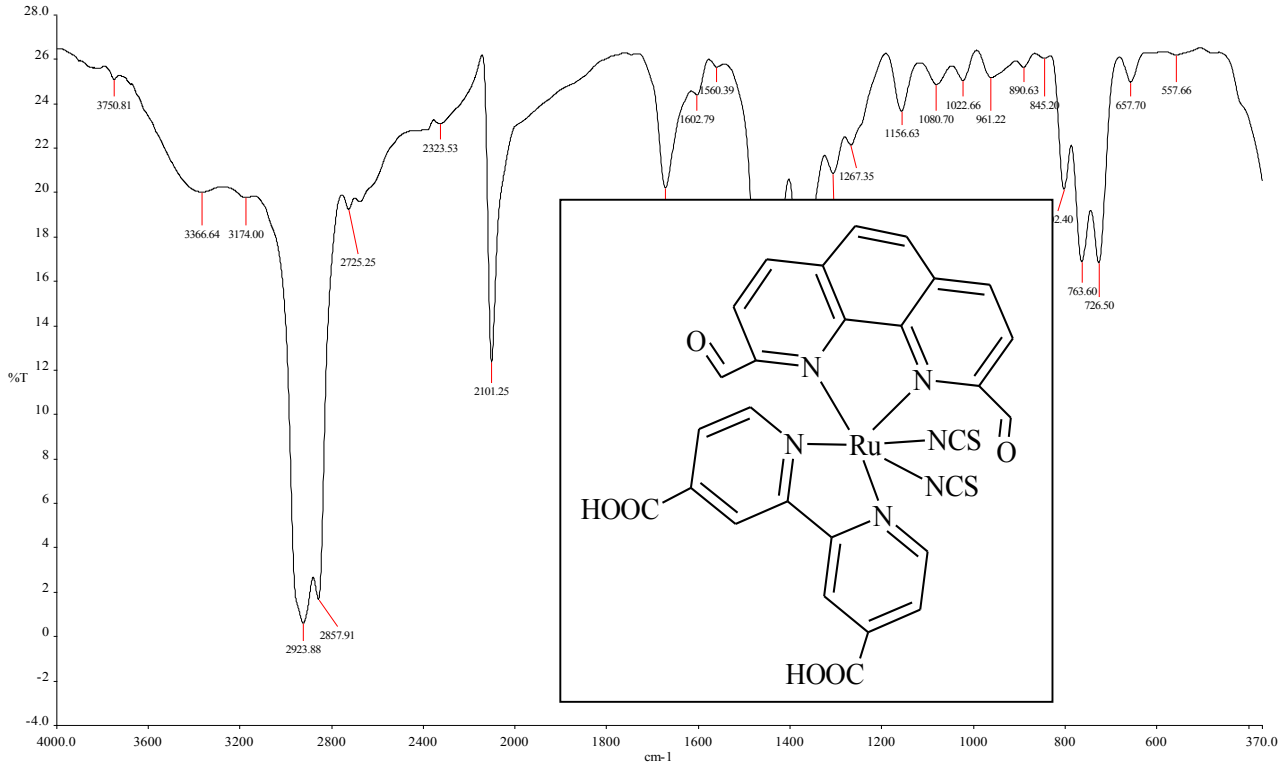

Figure 3.2:The FTIR spectrum of [Ru(dcAld)(dcbpy)$(NCS)_2$].

In Figure 3.2, the spectra shows a similar absorption across from 4000 cm^{-1} to finger print region, There is unique and prominent peak at 2101 cm^{-1}, this peak is assigned to υ(-NCS) stretching vibration the thiocyanate group, this confirms the N-coordination to the metal centre. There is also another confirmation of the thiocyanate group N-coordination to metal centre at 802 cm^{-1} is due to υ(CS) vibration band, because NCS- has two characteristic modes[5]. This peak is four times less intense compared to that of N-coordination [6]. The intense signal at 1671 cm^{-1} can be assigned to υ(C=O) stretching vibration of the carbonyl group of the carboxylic acid. There is also υ(C-O) stretching vibration at 1375 cm^{-1} and 1306 cm^{-1} this is due to υ (C-O) of aldehyde and carboxylic acid respectively. The absorption peaks at 2857-3366 cm^{-1} corresponds to stretching vibration of υ(C-H) of aromatic ring of polypyridyl ligands and O-H of the carboxylic acid.

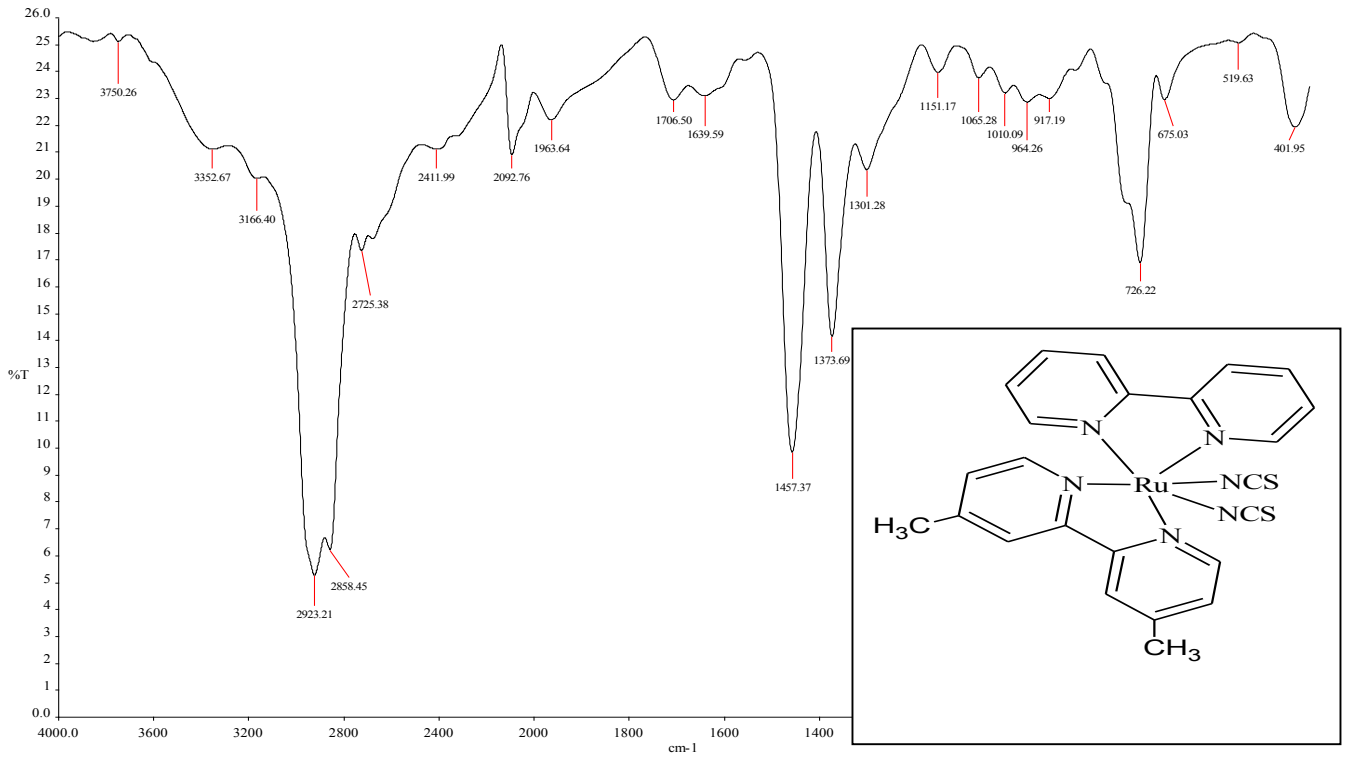

Figure 3.3 The FTIR spectrum of [Ru(II)(dmbpy)(bpy)$(NCS)_2$]

The peaks at 2858.3-3352.67 cm^{-1} indicates the C-H stretching , of which the weak peak at 3166 and 3352 cm^{-1} are C-H for aromatic and the one at around 2900 cm^{-1} is for aliphatic that is the methyl groups. The peak at 1457 cm^{-1} is attributed to aromatic υ(C=C) stretch. The υ(C-N) stretch of aromatic has appeared at around 1373 cm^{-1}. The C-C bond between carbon of the aromatic bipyridine and the carbon of the aliphatic methyl at 4,4'-positions has exhibited at around 680-800 cm^{-1} which can be that peak at 675 cm^{-1}. There is also a peak at 2092 cm^{-1} , this signal is for absorption of υ(NCS^-) which indicates the N-coordination to the ruthenium as metal centre, and this peak could be confirmed by absorption band at 726 cm^{-1} which can be assigned to υ (CS) stretching band.

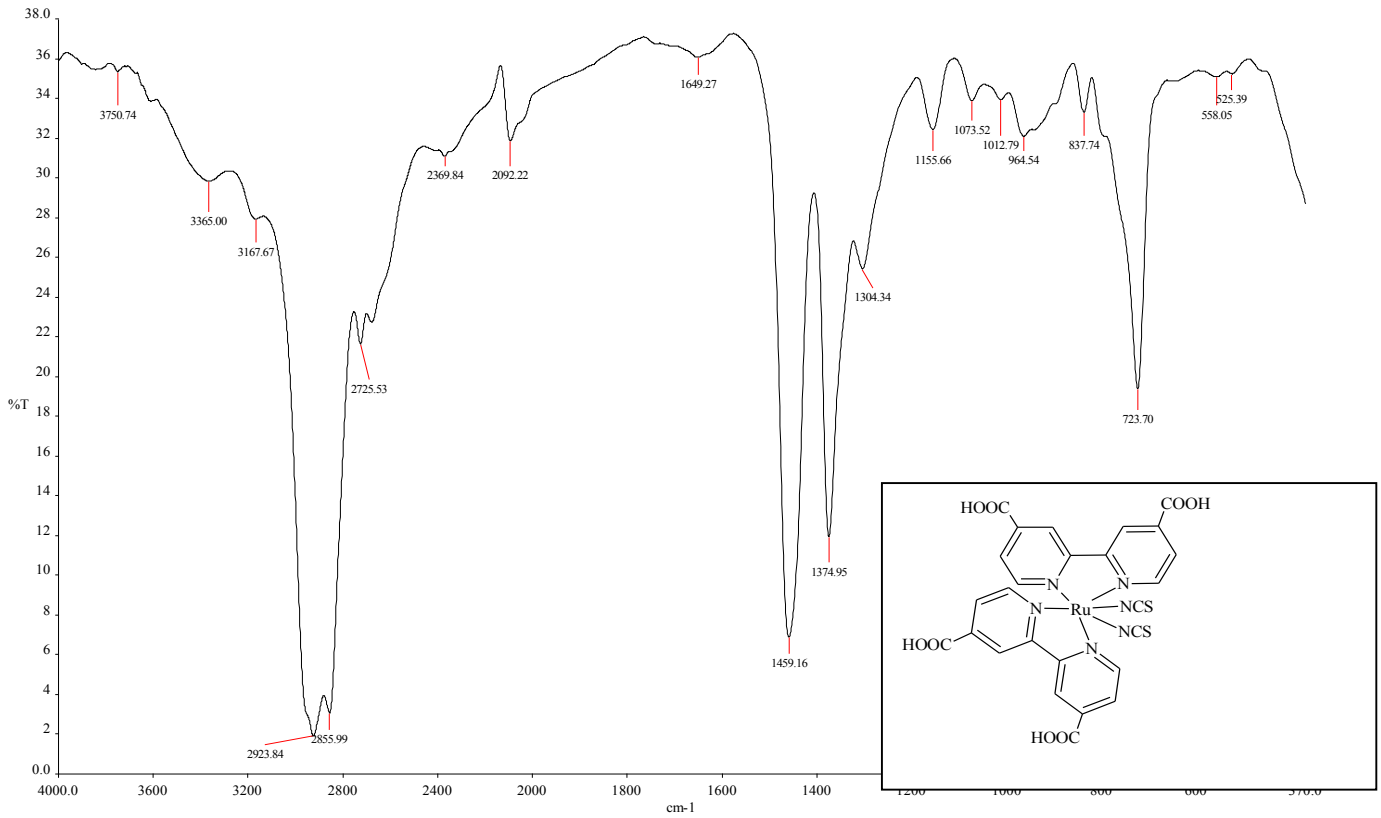

Figure 3.4. The FTIR spectrum of $[Ru(dcbpy)_2(NCS)_2]$

The FTIR absorption peak of the above complex, measured using nujole, shows absorption at 2923-3369 cm^{-1} which can be assigned to the aromatic υ(C-H) stretching band of bipyridine ligand and the hydroxyl group of carboxylic acid attached at 4.4'-position of bipyridine. The peak at 2089 cm^{-1} can be attributed to υ(NCS) which is the N-coordination to the metal centre. This coordination has confirmed by the peak at 807 that is assigned to υ(CS) stretching vibration which has low intensity compare to that of N-coordination.

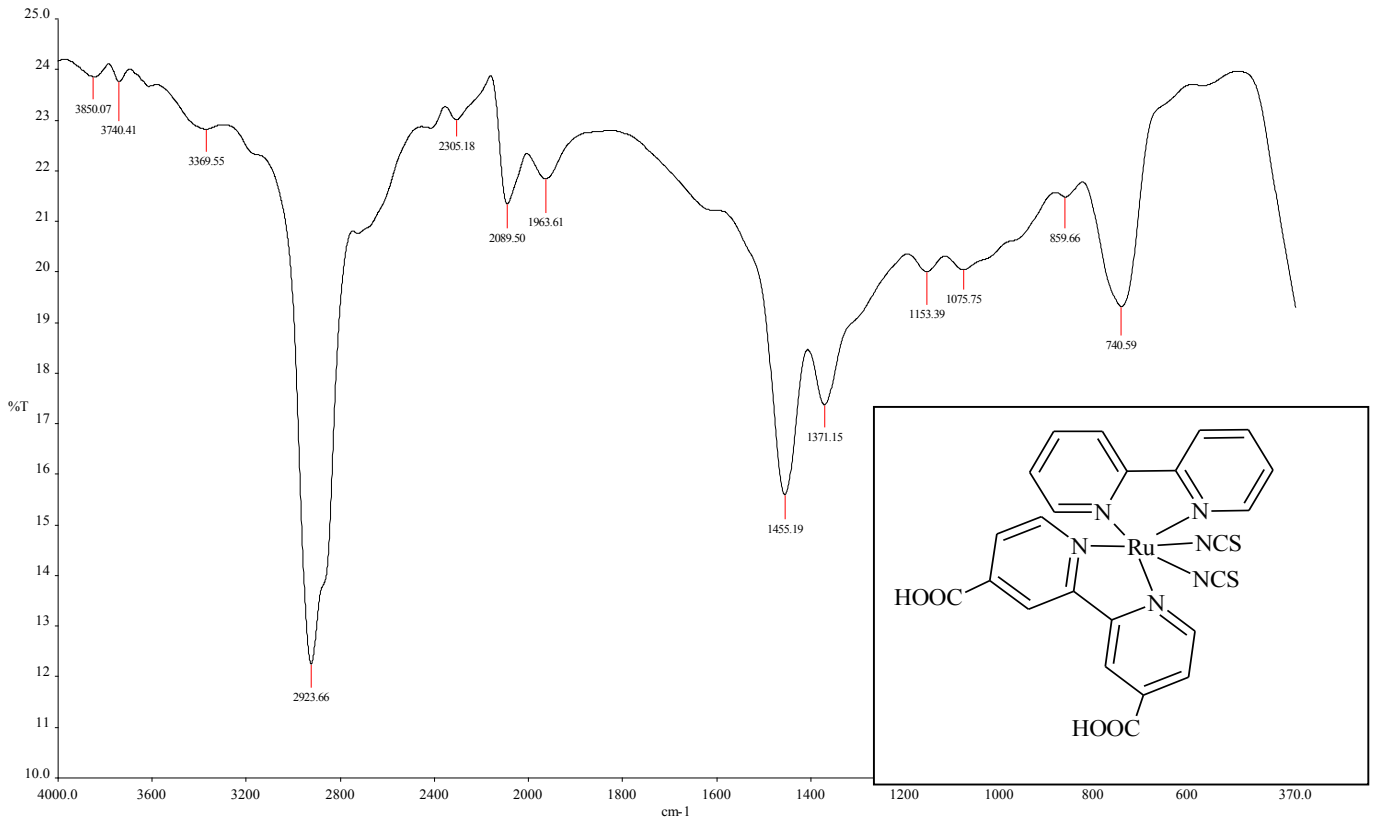

Figure 3.5: FTIR spectrum of $[Ru(bpy)(dcbpy)(NCS)_2]$

The FTIR absorption peak of the above complex, , shows absorption at 2923-3369 cm^{-1} which can be assigned to the aromatic υ(C-H) stretching band of bipyridine ligand and the hydroxyl group of carboxylic acid attached at 4.4'-position of bipyridine. The peak at 2089 cm^{-1} can be attributed to υ(NCS) which is the N-coordination to the metal centre. This coordination has confirmed by the peak at 726 cm^{-1} that is assigned to υ(CS) stretching vibration.

Table 3.1: Physical properties of the synthesized compounds

Compound	Yield(%)	Mp(^{o}C)	Colour
Ru-1 $[Ru(bpy)_2(NCS)_2]$	77	325	Brick-red
Ru-2 $[Ru(dcbpy)_2(NCS)_2]$	58	334	Purple red
Ru-3 $[Ru(dcaldphe)(dcbpy)(NCS)_2]$	84	355	Brown red
Ru-4 $[Ru(dsphen)(dcbp)(NSC)_2]$	59	298	Dark red
Ru-5 $[Ru(dmbpy)(bpy)(NCS)_2]$	60	311	Dark-red
Ru-6 $[Ru(bpy)(dcbpy)NCS)_2]$	72	318	Dark
L1 [dsphen]	81	258	Pure white
L2 [dcAldphen]	52	295	Purple-white
L3 [dcbpy]	89	215	White
L4 [bpy], commercial		240	White

Table 3.2: Vibrational frequencies of the important functional groups

Complex	Wave number/ wave length(cm^{-1})
υ(CN) N-coordinated	~2090-2200
υ(CS)	~800-810
υ(COO-)	~1430
υ(C-O) stretching	~1100-1300 of a carboxylic acid
υ(C=O)	~1600-1700
υ(C-H)	~2900-3300

υ(Ru-N)	~495-500

Table 3.3 Solubility test for ruthenium(II) polypyridyl complexes

	SOLVENTS			
COMPLEX	**DMF**	**DMSO**	**Water**	**Acetonitrile**
Ru-1	Completely dissolved	Soluble	Not soluble	Not soluble
Ru-2	Soluble	Not soluble	~	~
Ru-3	Not soluble	Partially soluble	Completely soluble	Not soluble
Ru-4	Soluble	Not soluble	Not soluble	Not soluble
Ru-5	Not soluble	~	Soluble	Not soluble
Ru-6	Soluble	~	~	~

3.3 The electroscopic spectroscopy of ruthenium(II) polypyridyl complexes

3.3.1 Introduction

The absorption and fluorescence spectra of ruthenium(II) polypyridyl complexes are generally dominated by MLCT/LMCT (dπ-based Ru(II) -to-π*-based phen, bpy) and (π-π*)-based polypyridyl ligands transtisitions [7], adopting from properties of the prototype tris-bipyridine ruthenium(II) $[Ru(bpy)_3]^{2+}$, ruthenium polypyridyl complexes have metal-to-ligand charge transfer (MLCT) transition whereas $[Ru(bpy)_3]^{3+}$ has ligand-to-metal charge transfer (LMCT) transition[8][9]. Ruthenium(II) polypyridyl complexes shows two well distinct absorption shoulder band at shorter wavelength and one at longer wavelength in the UV-visible spectrum [1]. Zakeruuddin *et al* reported a complex with two absorption shoulder band 390-530 nm region which was due to metal to ligand charge transfer (MLCT) transition and high intense absorption at 296-314 nm [3] which was ascribed to (π-π*) of polypyridyl ligand [10-11].

3.3.2 The UV-Visible spectroscopy analysis of the synthesized ruthenium polypyridyl complexes

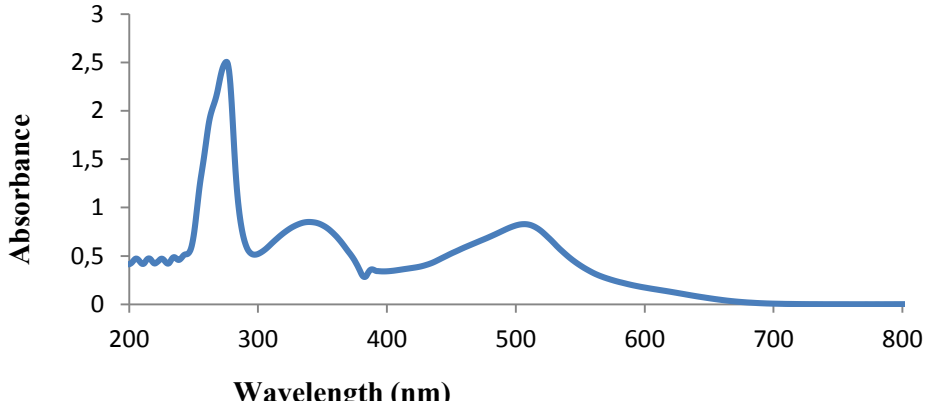

A

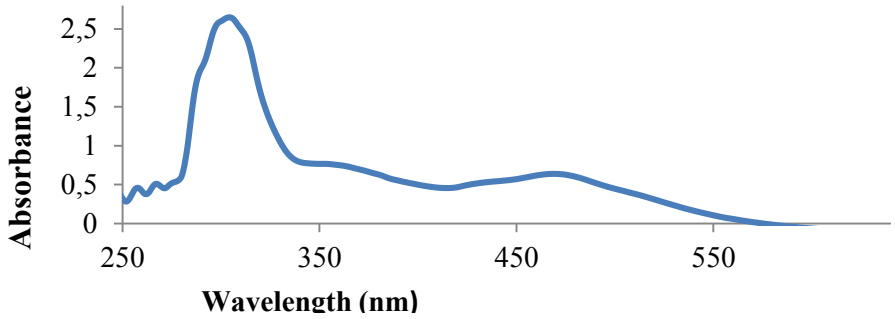

B

Figure 3.6: The UV-Vis spectrum for $[Ru(dcbpy)_2(NCS)_2]$ (A) and (B) $[Ru(bpy)_2(NCS)_2]$

The UV-vis spectra of synthesized of $[Ru(bpy)_2(NCS)_2]$ coded as Ru-1 and $Ru(dcbpy)_2(NCS)_2$ coded as Ru-2 where bpy, dcbpy is 2.2'-bipyridine and 2.2'-bipyridine-4.4'-dicarboxylic acid, these complexes are being compared, these complexes both have a sharp, intense absorption bands at 276-310 nm is based to intraligand (π-π^*) transition. There are two observed absorption shoulder bands at 350-360 and 490-514 nm region which is due to metal-to-ligand charge

transfer (MLCT) transition. In the case of Ru-1 the absorption at 310 nm which have strong intensity is due to ligand-centred (π-π*) transition between the 2.2'-bipyridines, and there are two shoulder band absorption at lower and higher wavelength across the visible region of the spectrum at 373 nm and 490 nm which is due to absorption of MC(d-d) and metal-to-ligand charge transfer (MLCT $d_{M\pi}$-π*) respectively . This is the important transition where there is charge or electron transfer between the t_{2g} (dπ) of a metal to (π_L*) of a polypyridyl ligands. In the case of Ru-2 the intraligand charge transfer transition is observed at 277 nm below the visible region also with a high energy and strong intensity. This is the ligand-centred (π-π*) transition between the 2, 2'-bipyridine and 2.2'-bipyridine-4.4'-dicarboxylic acid. The metal-to-ligand charge transfer (MLCT) transition was observed at longer wavelength at 514 nm region across the visible region than that of Ru-1. There is a bathochromic shift of about 11 nm which may be due to the presence of low lying π-orbital, which might be caused by carboxylic acid at 4.4'-position in bipyridine ligand which is not present in Ru-1. The low-lying π-orbital make energy gap between metal and ligand small, the MLCT band is enhanced to a higher wavelength [12-16].

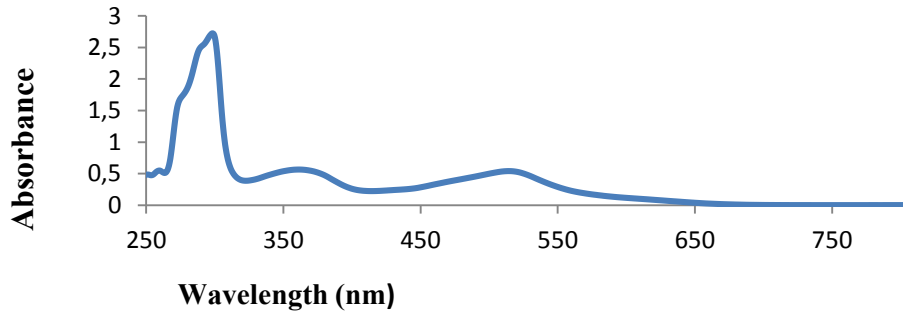

C

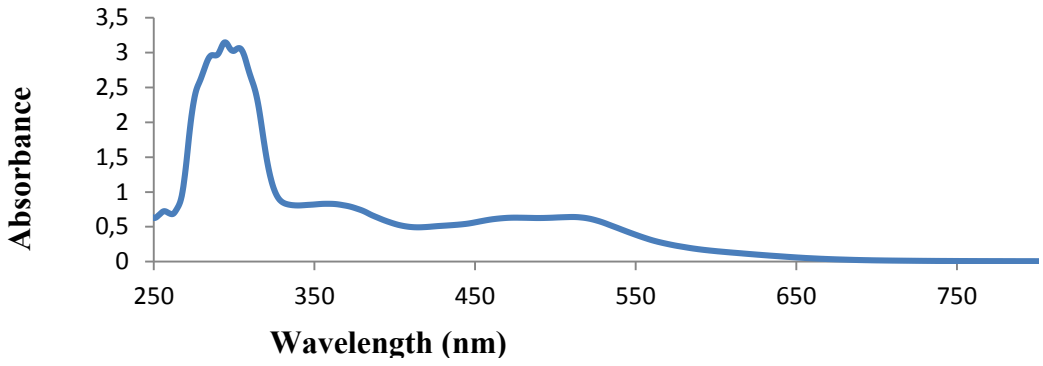

D

Figure 3.7: The UV-Vis spectra for [Ru(dcald)(dcbpy)$(NCS)_2$] (C) and [Ru(dsphen)(dcbpy)$(NCS)_2$] (D)

In the case of [Ru(dcaldphen)(dcbpy)$(NCS)_2$] coded as Ru-3,there is strong and intense absorption band at around 305 nm which is the region attributed to intraligand (π-π*) a transition between 2.9-dicarboxaldehyde-1.10-phenanthroline and 2.2'-bipyridine-4.4'-dicarboxylic acid. There is also two absorption shoulder bands, the one at shorter wavelength 366 nm and the broad one at higher wave length across the visible region at 535 nm , these region being dominated by metal-to- ligand charge transfer which is the transition between metal centre ($d_{\pi Ru(II)}$ to π* of a ligands). And for [Ru(dsphen)(dcbpy)$(NCS)_2$] coded as Ru-4. The intraligand (π-π*) transition was observed at absorption 300 nm which corresponds to 1.10-phenanthroline-4.7-disulphonic acid and 2.2'-bipyridine-4.4'-dicarboxylic acid. The very important two broad absorption bands was observed at 380 nm and 531 nm regions which is the metal-to-ligand charge transfer (MLCT) transition. There is 4-6 nm red shift across the visible spectrum in ruthenium complex containing dicarboxaldehyde substituted on ancillary ligand. For that reason ancillary ligand substituted dicarboxaldehyde have low-lying π*-orbital as compared to the one

substituted with disulphonic acid, which is therefore the absorption has been enhanced to a bit higher absorption region of the UV-Vis spectrum.

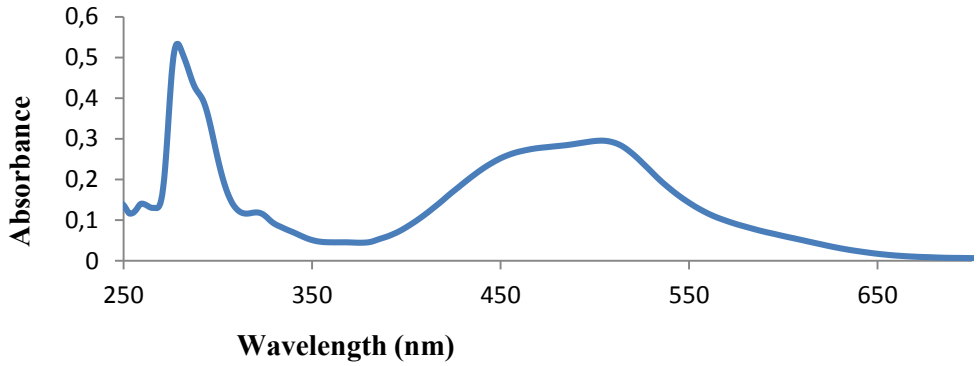

E

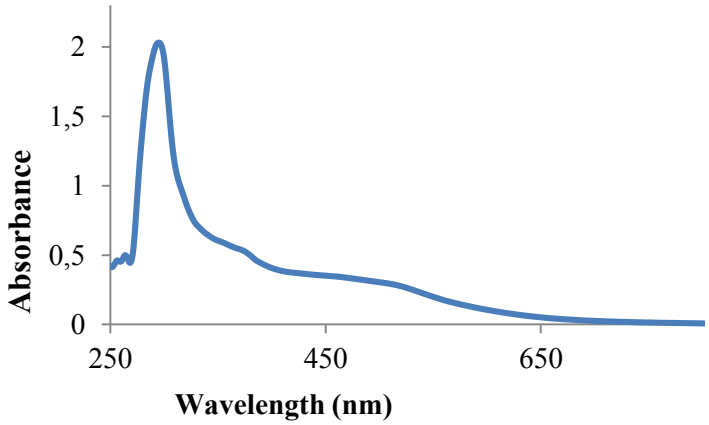

F

Figure 3.7 The UV-Vis spectra for $[Ru(dcbpy)(bpy)(NCS)_2]$ coded as Ru-5 (E) $[Ru(dmbpy)(bpy)(NCS)_2]$ coded as Ru-6 (F).

In the case of the two ruthenium polypyridyl complexes, the one with methylated bipyridyl $[Ru(bpy)(dmbpy)(NCS)_2]$ coded as Ru-5 in the table and the carboxylated

[Ru(bpy)(dcbpy)$(NCS)_2$] one coded as Ru-6, their absorption spectrum are being compared. Ru-5 has a high intense band at 278 nm which the absorption for intraligand (π-π*) or (ligand-centred orbital) transition. This transition could be the charge transfer within 4.4'-dimethyl-2.2'bipyridiyl or 2.2'-bipyridyl. There is also broad absorption band, dominated the visible region of the spectrum, this corresponds to metal-to-ligand charge transfer (MLCT) transition which is the characteristic of Ru(II) complexes. This charge transfer could be the transfer of electron from dπ- orbital of the metal centre, ruthenium in this case to the π* of the bipyidyls ligands. Ru-6 have high intensity band at 277 nm which corresponds to intraligand (π-π*) , which is the charge transfer transition assigned to 2.2'-bipyridyl-4.4'-dicarboxylic acid or bipyridyl ligand.

There is broad absorption band, with lower energy, dominated the visible region at 520 nm; this corresponds to metal-to-ligand charge transfer (MLCT) transition. This is the charge transfer transition from the 4d orbital of ruthenium, the metal centre to the empty π* orbital of the polypyridyl ligand. In comparison [Ru(dmbpy)(dcbpy)$(NCS)_2$] (λ_{max} =520 nm) has red-shifted with 3 nm across the visible region compared to [Ru(dmbpy)(bpy)$(NCS)_2$] (λ_{max} =517 nm). This could be the result of chromophoric group (-COOH) at 4.4'-positions in Ru-6, which is not there in Ru-5, which resulted to MLCT band to absorb at higher region.

3.3.3 The emission of ruthenium(II) polypyridyl complexes

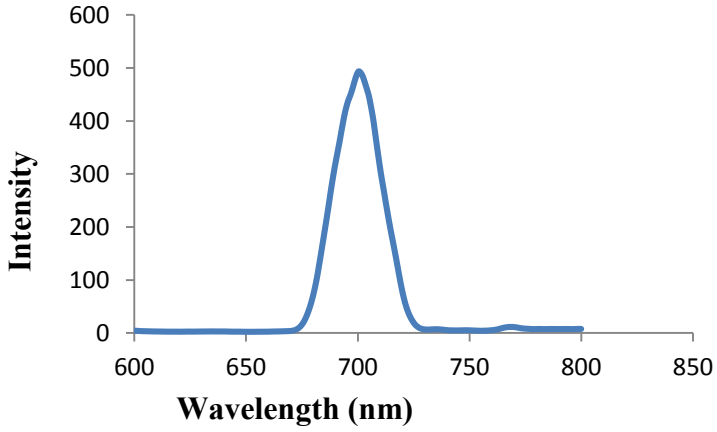

Figure 3.8: Emission spectrum of [Ru(II)(dsphen)(dcbpy)$(NCS)_2$] at 293K

The emission spectrum of complex [Ru(dcald)(dcbpy)$(NCS)_2$] measured in DMF, has been selected among other synthesized complexes and is displayed in Fig. 3.8 Upon the excitation into ^{1}LC and ^{1}MLCT band (λ_{exc} =535 nm), the complex exhibited a luminescence at 293K. Its emission wavelength (λ_{max}) was found at 700 nm. of which luminescence properties of ruthenium complexes as well as its ability to play role of excited state reactant or product are related to the energy ordering of its low energy excited state and, to the orbital nature of its lowest excited state (^{1}MLCT) [16].

It has been shown that the properties of moiety or functional group attached to the ancillary ligand, bipypyridine especially carboxylate group enhance the luminescence of the ruthenium(II) polypyridine complexes. The carboxylate group assists to lower the LUMO energy. This influence the position of metal centred orbital, ligand centred orbital and metal-to- ligand charge transfer (MLCT) of ruthenium(II) polypyridyl complexes. The high intensity of this ruthenium

complex shown in the spectra, indicates that could have longer excited lifetime, which is the desirable property for sensitizer in dye sensitized solar cells, enhancing the injection of electron to the conduction band of semiconductor before the relaxation.

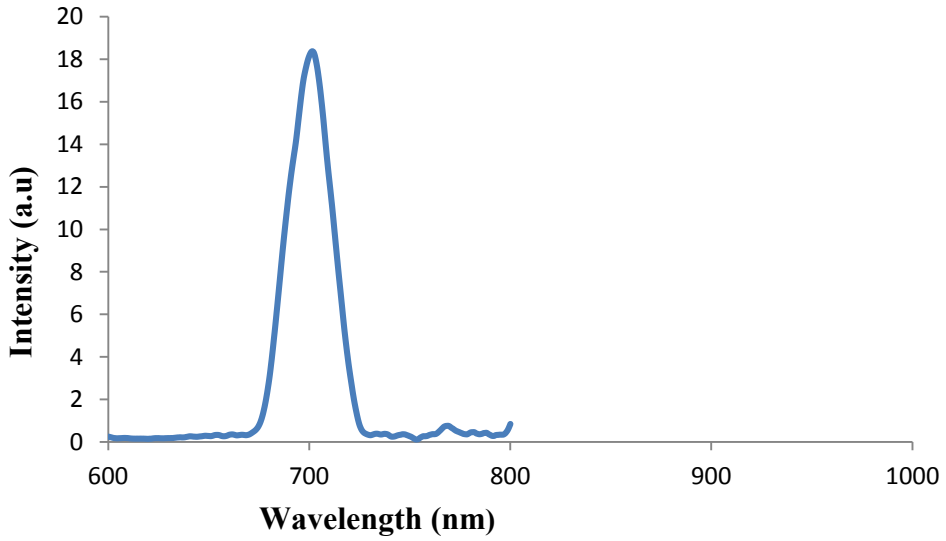

Figure 3.9: The emission spectrum of [Ru(dsphen)(dcbpy)$(NCS)_2$] at 293 K

The Table below shows UV-Vis absorption an emission of ruthenium(II) polypyridyl complexes, which measured in different solvent , DMF, DMSO, water depending to their solubility in these solvents.

Table 3.4: The UV-Vis absorption and emission properties

Complexes	λ_{max}- transition (nm)	λ_{max}(nm)	λ_{max}(nm)
	LC(π-π^*)	^{1}MLCT(d-π^*)	MLCT
Ru-1	278	345	503
Ru-2	277	346	514
Ru-3	305	366	535
Ru-4	300	380	531
Ru-5	278	~	517
Ru-6	277	373	520

3.4 **Results for ^{1}H NMR ligands**

Table 3.5: Relevant: ^{1}H NMR for polypyridyl ligands

Compound	Multiplicity	Chemical shift, ^{1}HNMR, σ(ppm)
1,10phenanthroline-2.9-dicarboxaldehyde	(s, 2H) (m, 7H)	9.964 8.31, 8.32; 8.34, 8.77; 8.80
1.10-phenathroline-4.7-disulphonic acid	(s, 2H) (d, 2H) (d, 2H)	8.87; 8.86; 8.32; 7.86; 7.84
2,2-bipyridine-4.4'-dicarboxylic acid	(d, 2H) (s, 2H) (d, 2H)	8.88; 8.86; 8.87 8.72; 8.73 8.09; 808

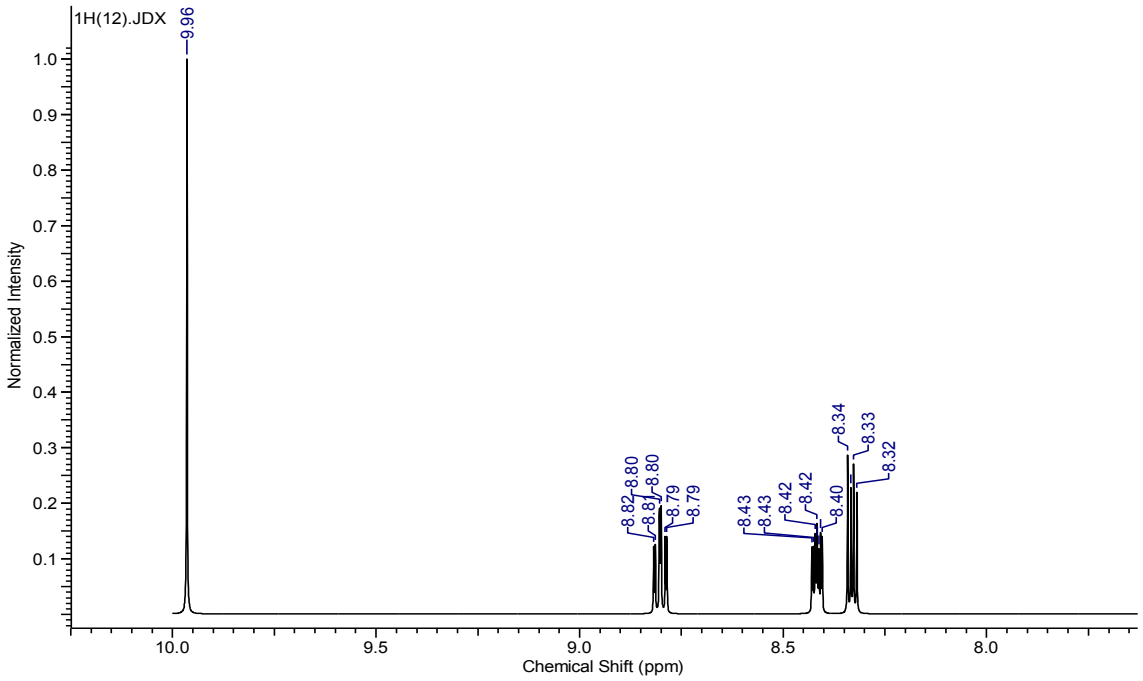

Figure 3.9: The ^{1}H NMR spectrum of 1.10-phenanthroline-2.9-carboxaldehyde in DMSO-d_6

There is a resonance at σ 8.80 ppm which could be assigned to the proton on 1.10-phenanthroline, this resonance could be assigned to the proton at the para postion with high electronegativity nitrogen of the 1.10-phenanthroline which is doublet (2d, 2H) at 4.7-position. There is also a prominent peak (2H, singlet) of the aldehyde downfield at 9.96 ppm adopting from literature [19], this proton was deshielded by the electron rich of carboxyl. There is also a resonance at around 8.79 ppm and 8.80 ppm which could be assigned to (d, 2H) at 4.7- position of 1.10-phenathroline and at bit upfield that is also doublet (d, 2H) at 8.42 ppm which could be assigned to protons at 3.8 position on the 1.10-phenanthroline ring. Another doublet found (2d, 2H) at 8.33 pm which is due to protons at 5.6 position of 1.0-phenanthroline.

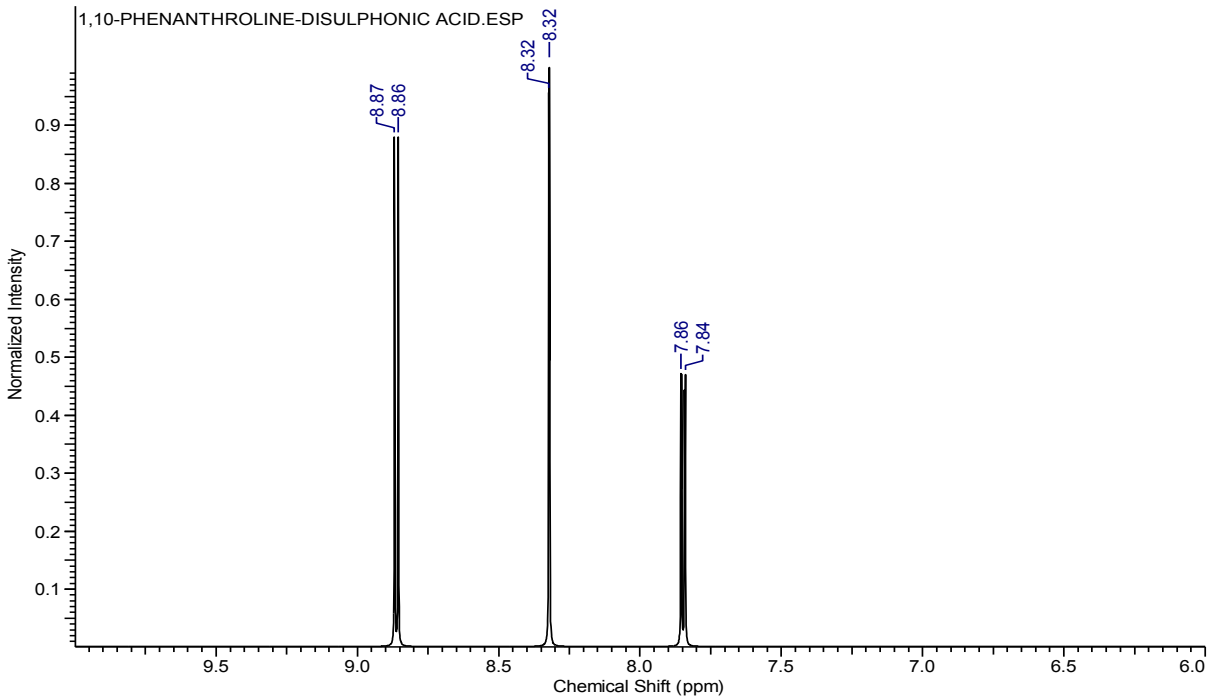

Figure 3.10: The ^{1}H NMR spectrum of 1.10-phenanthroline-4.7-disulphonic acid in DMSO-d_6

The ^{1}H NMR spectrum of 1.10-phenanthroline-4.7-disulphonic acid showed an area of interest doublet at (2H, d) 8.87 and 8.86 ppm, this is due to proton at 2.9-position of 1.10-phenanthroline (d, 2H). These protons are deshielded to a lower field because the are protons of carbon that is adjacent to nitrogen of 1.10-phenanthroline. This spectrum also exhibited a doublet(2H, d) at 8.32 ppm which could be assigned to protons at 3.8 positions, this could be result of adjacent to the electron rich carbon that is bonded to sulfur. There is another doublet (d, 2H) a bit upfieled in the spectrum, this could be assigned to protons at 5.6 position of the phenanthroline.

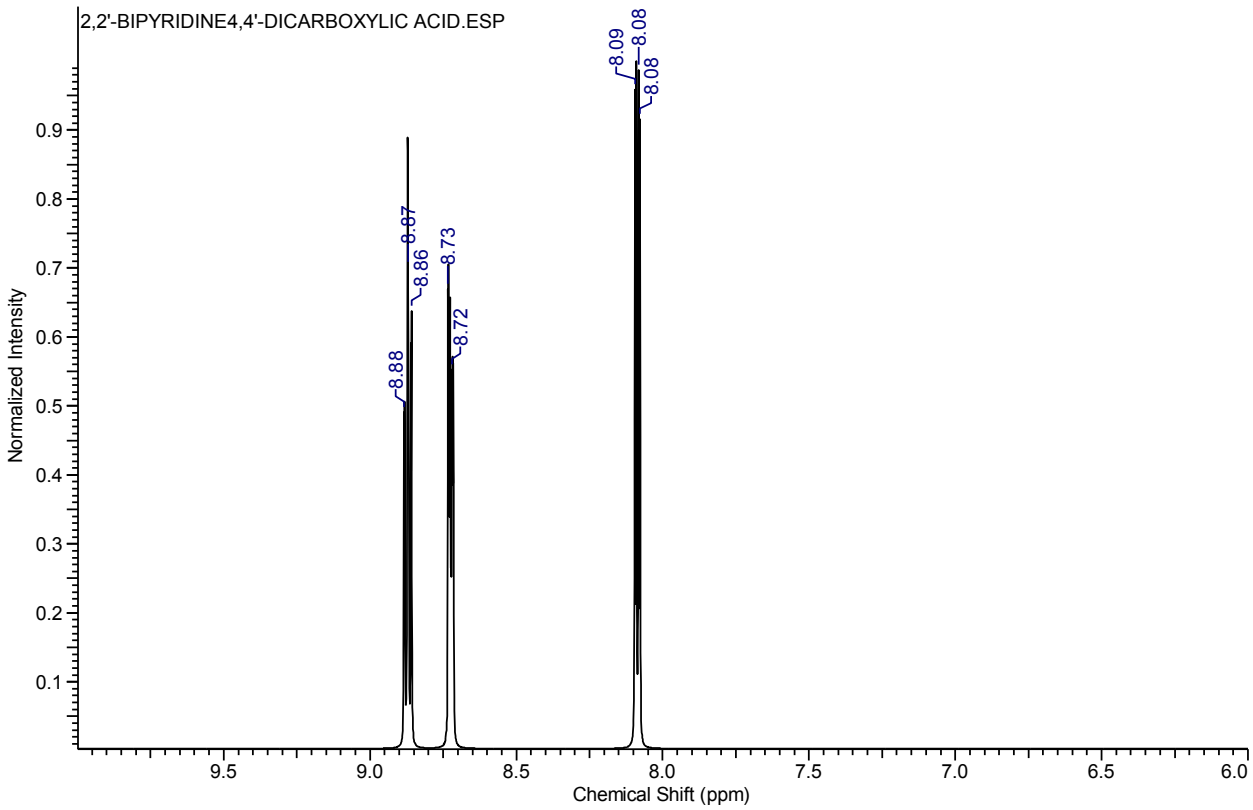

Figure 3.11: The ^{1}H NMR spectrum of synthesised 2.2'-bipyrydyl-4.4-dicarboxylic acid in DMSO-d_6.

The ^{1}H-NMR spectrum of 2.2'-bipyridine-4.4s'-dicarboxylic acid, showed three doublets at (d, 3.3' H); (d, 5.5'H) and (d, 6.6'H) positions of bipyridine [17]. The resonance at around 8.88 ppm, 8.87 ppm can be assigned to the proton at 6.6'-ortho position to the nitrogen of bipyridine which is at downfield deshielded by high electronegative nitrogen (d, 2H). There is also a doublet (d, 2H) at 8.73, 8.72 ppm which is assigned to proton at 3.3' and is found in downfield which could be the results of being ortho position to electron rich carbon of carboxyl group. This spectrum also shows another resonance with doublet (d, 2H) at upfield that can be assigned to proton at 5.5' position of bipyridine.

3.5 **References**

1. Chandrasekharam, M.; Rajkumar, G.; Rao, C. H. S.; Suresh, T.; Reddy, P. Y.; Soujanya, Y. Ruthenium(II)-bipyridyl with extended π -system : Improved thermo-stable sensitizer for efficient and long-term durable dye sensitized solar cells. *J. Chem. Sci.* **2011***, 123,* 555–565.

2. Adeloye, A. O.; Ajibade, P.A. Synthesis and characterization of a heteroleptic Ru(II) complex of phenanthroline containing oligo-anthracenyl carboxylic acid moieties. *Int. J. Mol. Sci.* **2010***, 11,* 3158–3176.

3. Philippopoulos, A. I.; Terzis, A.; Raptopoulou, C.P.; Catalano, V.J.; Falaras, P. Synthesis, characterization, and sensitizing properties of heteroleptic Ru(II) complexes based on 2,6-bis(1-pyrazolyl)pyridine and 2,2′-Bipyridine-4,4′-dicarboxylic acid ligands. *Eur. J. Inorg. Chem.* **2007**, *2007*, 5633–5644.

4. Fourest, E.; Volesky, B. Contribution of sulfonate groups and alginate to heavy metal biosorption by the dry biomass of Sargassum fluitans. *Enviro. Sci. Technol.* **1996***, 30,* 277–282.

5. Ocakoglu, K.; Harputlu, E.; Guloglu, P.; Erten-Ela, S. The photovoltaic performance of new ruthenium complexes in DSSCs based on nanorod ZnO electrode. *Synth. Met.***2012***, 162,* 2125–2133.

6. Mitsopoulou, C.; Veroni, I.; Philippopoulos, A.I.; Falaras, P. Synthesis, characterization and sensitization properties of two novel mono and bis-carboxyl-dipyrido-phenazine ruthenium(II) charge transfer complexes. *J. Photochem. Photobiol. A Chem.* ***2007****, 191,* 6–12

7. Verma, S.; Kar, P.; Das, A.; Ghosh, H. N. Photophysical properties of ligand localized excited state in ruthenium(II) polypyridyl complexes: A combined effect of electron donor-acceptor ligand. *Dalton Trans.* **2011**, *40,* 9765–73.

8. Balzani, A.; Juris, M.; Venturi, M.; Campagna, S.; Serroni, S. Luminescent and redox-active polynuclear transition metal complexes. *Chem. Rev.* **1996**, *96,* 759–834.

9. Domain, M. S. Ru(II) polypridyl complexes investigated from the pico to the micro second domain. Ph.D. thesis, School of chemical science. Dublin city University.

10. Adeloye, A.O.; Ajibade, P.A. Synthesis and characterization of a heteroleptic Ru(II) complex of phenanthroline containing oligo-anthracenyl carboxylic acid moieties. *Int. J. Mol. Sci.ol.* **2010**, *11,* 3158–76.

11. Ryan, J. H. The study of ruthenium polypyridyl complexes for dye sensitized solar cell application. Ph.D Thesis . Univ. Minnesota. June **2013**.

12. Badaeva, E.; Albert, V.V.; Kilina, S.; Koposov, A.; Sykora, M.; Tretiak, S. Effect of deprotonation on absorption and emission spectra of Ru(II)-bpy complexes functionalized with carboxyl groups. *Phys. Chem. Chem. Phys.***2010**, *12,* 8902–8913.

13. Adeloye, A. O.; Ajibade, P. A. A high molar extinction coefficient Ru(II) complex functionalized with cis-dithiocyanato-bis-(9-anthracenyl-10-(2-methyl-2-butenoic acid)-1.10-phenanthroline: Potential sensitizer for stable dye-sensitized solar cells. *J. Spectrosc.* **2014**, *2014,* 1–10.

14. Anthonysamy, A.; Balasubramanian, S.; Muthuraaman, B.; Maruthamuthu, P. 4′-functionalized 2.2′:6′.2″ terpyridine ruthenium (II) complex: A nanocrystalline TiO_2 based solar cell sensitizer. *Nanotechnology*. **2007**, *18*, 1–5.

15. Adeloye, A. O.; Ajibade, P. A.; Towards the development of functionalized polypyridine ligands for Ru(II) complexes as photosensitizers in dye-sensitized solar cells (DSSCs). *Molecules*. **2014**, 12421–12460.

16. Adeloye, A. O.; Olomola, T. O.; Adebayo, A.I.; Ajibade, P.A.; A high molar extinction coefficient bisterpyridyl homoleptic Ru(II) complex with trans-2-methyl-2-butenoic acid functionality: potential dye for dye-sensitized solar cells. *Int. J. Mol. Sci.* **2012**, *13,* , vol. 13, 3511–3526.

17. Mogale, D. M. Synthesis of ruthenium dye (N3) from recycled ruthenium trichloride for application in dye sensitized solar cells. Ph.D. Thesis. Tswane University of Technology. South Africa. October. **2009**. http://libserv5.tut.ac.za:7780/pls/eres/wpg_docload.download_file?p_filename=F1331644051/Mogale,%20D.M.pdf.

18. Melton, D. L. Metal ion complexing properties of the two- dimension, highly preorginised ligand 1,10-phenanthroline-2,9-dicarboxylic acid. Ph.D. Thesis. University of North Carolina Wilmington. **2005**.

CHAPTER 4

4.0 SOLAR CELL FABRICATION, EFFICIENCY TEST AND CHARACTERIZATION

4.1 Methodology : Fabrication of dye-sensitized solar cells (DSCCs)

4.2 Material

All material were purchased and used without modification. The fluorine-doped Tin Oxide (F-SnO_2) as glass substrate, colloidal suspension TiO_2, Surly (Solar nix), scotch tape , copper conductive tape from Solaronix, Furnace Lenton thermal design model.

4.3 Substrate and Cleaning

One type of substrate has been used throughout this project, these substrates were coated with conductive material that is fluorine doped tin oxide of which those glasses were purchased from Solaronix. Substrates were carefully cuts into 0.6 cm^{-2}, after cuts then washed with paraffin, followed by isopropanol then acetone, since cleaning is the crucial factor for homogeneity and adherence for future coating.,

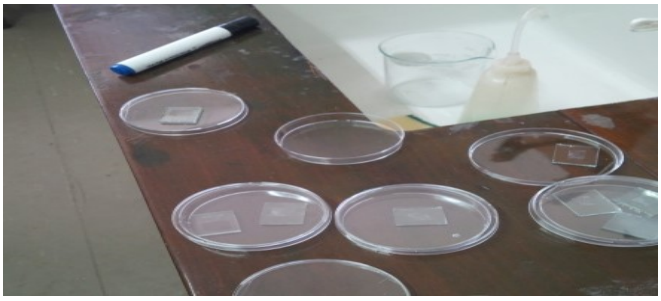

Figure 4.1: The cleaned and cut glasses

After drying in air the glass substrate were fixed on abench with scotch tape to maintain the common area for TiO_2 paste, and doctor blade technique was applied using a glass rod .

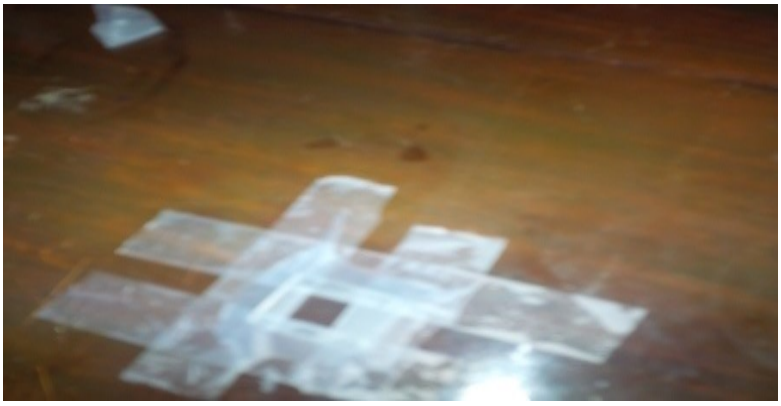

Figure 4.2: Shows the doctor blade technique, on a bench**.**

The glass substrates with colloidal TiO_2 were sintered at 450 ^oC in the furnace for 4 hours to obtain the TiO_2 thin film [1].

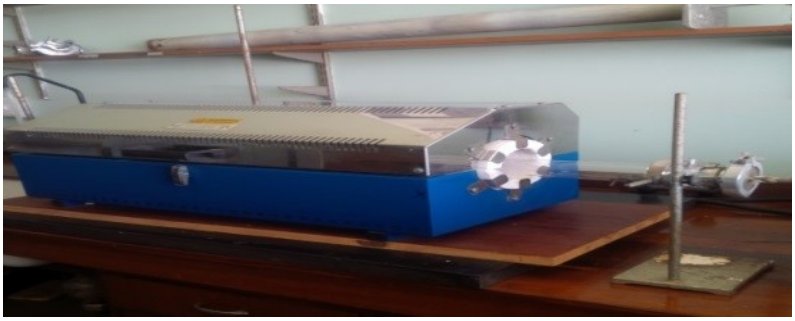

Figure 4.3: Shows the sintering of TiO_2 thin films

This TiO_2 thin film was soaked into solution of ruthenium complexes (Ru-1, Ru-2 and Ru-3 at a conc. of $3x10^{-3}$ M in DMF for 4-8 hours. The two substrate the one coated with TiO_2 and one with platinum were held together using polyethylene and soldering iron. The syringe was used to inject the liquid electrolyte (iodide in acetonitrile).

Figure 4.4: Sensitization of thin film

4.4 **Solar cell characterization and evaluation**

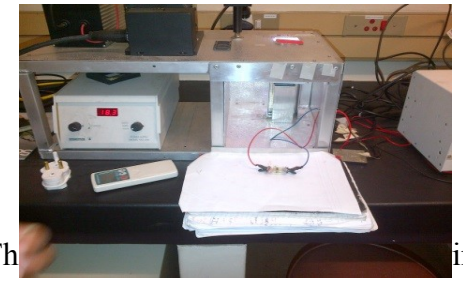

Figure 4.5: Th ing photo current- voltage characterization at CSIR

4.5 **Material characterization**

All measurements were done under 100 $mWcm^{-2}$ intensity with solar simulator sciencetech power supply 550- 200 model. Voltmeter used is NI PXI-1033 model.

The solar cell was being evaluated through overall efficiency. The solar cell efficiency of a cell was determined by the measurement of the photo current density versus photo voltage [1]. This technique composed of the measurement of current density generated by a solar cell under light illumination. The cell is illuminated by a light source (solar simulator) and capable to reproduce the solar spectrum. The calibrated light source were used to achieve global air mass (1.5 AM) illumination.

4.6 **Results and discussion**

The photo current-voltage properties of the dye sensitized solar cell based ruthenium complexes using electrolyte containing iodine electrolyte. These complexes exhibited a short circuit photo current density of J_{SC} 0.766-3.48 mA cm^{-2} , with an open circuit voltage of Voc 0.53- 0.6 V and the fill factor (FF) of 0.46-0.6 respectively. The calculated conversion efficiency of these cells range from 0.207-1.05% under 1 sun 100 mW cm^{-2}, global air mass (AM) 1.5 illuminations.

Table 4.1: The photovoltaic parameters for the DSSCs

Anode(TiO_2)	Voc(V)	Jsc($mA.cm^{-2}$)	Fill factor (FF)	η(%)
[Ru(dsphen)(dcbpy)$(NCS)_2$]	0.56	2.79	0.5	0.84
[Ru(dcAldphen)(dcbpy)$(NCS)_2$]	0.53	0.78	0.45	0.207
[Ru(II)(dcbpy)(bpy)$(NCS)_2$]	0.63	3.478	0.597	1.06

4.7 **Calculations of solar cell conversion efficiency(η%)**

All substitution will be done, following the equations 1-4

$$J_{SC} = \frac{Isc(mA)}{A(cm^2)} \qquad (1)$$

$$J_{SC} = \frac{0.46}{0.6} = 0{,}766(mAcm^2)$$

$$FF = \frac{V_{MAX} \times J_{MAX}}{V_{OC} \times J_{SC}} \qquad (2)$$

Where FF is fill factor, Voc is an open circuit voltage; Jsc is a short circuit current density.

(i) *Calculation for [Ru(dcAldphen)(dcbpy)(NCS)$_2$]*

$$\eta(\%) = \frac{V_{MAX} \times J_{MAX}}{Pin} \qquad (3)$$

$$\eta(\%) = \frac{V_{OC} \times J_{SC} \times FF}{Pin} \times 100\% \qquad (4)$$ The above equation was adopted from the literature [3,4], and P_i is a light intensity 100 mWcm^{-2}

The final equation for overall conversion efficiency, will derived from the following equation, adopting the following literature [5,6]

$$\eta = \frac{0.766 mA cm^{-2} \times 0.53 V \times 0.51}{100 mW cm^{-2}} \times 100\%$$

= 0.207 %

(ii) *Calculations for [Ru(dcbpy)(bpy)(NCS)$_2$]*

$$J_{sc} = \frac{2.08 mA}{0.6 cm^{-2}}$$

$=3.466\ mA\ cm^{-2}$

$$\eta = \frac{3.466 mA cm^{-2} \times 0.5928 \times 0.6}{100 mW cm^{-2}} \times 100\%$$

$= 1.02\ \%$

(iii) *Calculation for [Ru(II)(dcbpy)(dsphen)(NCS)$_2$]*

$$J_{sc} = \frac{1.6762 mA}{0.6 cm^{-2}}$$

$= 2.793\ mAcm^{-2}$

$$\eta = \frac{2.793 mA cm^{-2} \times 0.53 \times 0.498}{100 mW cm^{-2}} \times 100\%$$

$= 0.82\ \%$

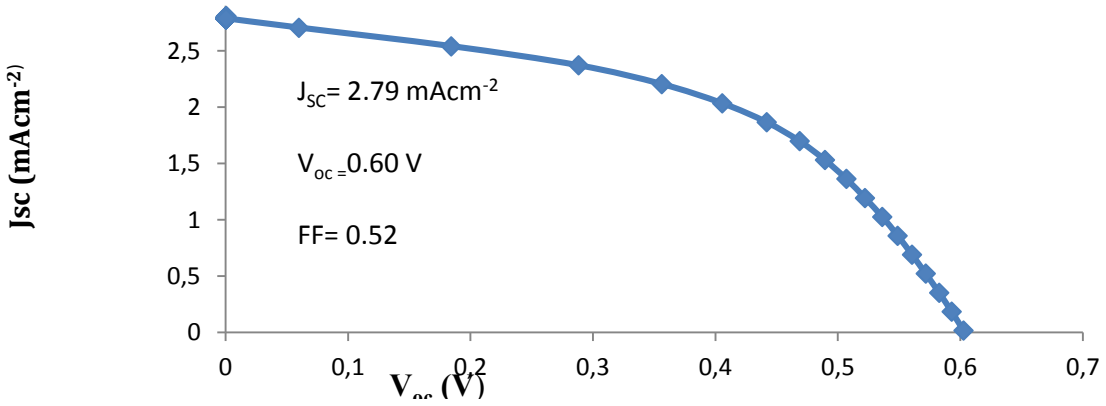

Figure 4.6: Photocurrent-voltage (J-V) curve for Ru-2 DSSC based on [Ru(dcbpy)(dsphen)(NCS)$_2$

The short-circuit photo current density (J_{sc}), open circuit voltage (V_{oc}) and the fill factor (FF) of the cell fabricated with Ru-2 are as follows 2.79 mA cm^{-2}, 0.60, and 0.52 respectively at 100 mW cm^{-2} intensity. The yield overall solar conversion efficiency η 0.82 % at with AM. 1.5 illumination. The low conversion efficiency of this dye-sensitized solar cell based on this ruthenium complex compared to dye-sensitized based on standard dye (N719) is probably due to hole-transporting material used in DSSCs, that is the liquid organic electrolyte is volatile, which give a low V_{OC}, resulting to low solar energy conversion efficiency.

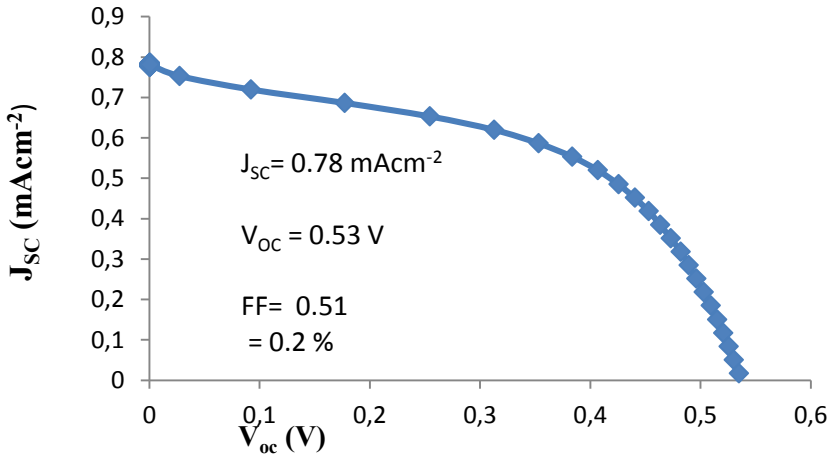

Figure 4.7: Photocurrent-voltage (J-V) curve for DSSC based on [Ru(dcAldphen)(dcbpy)$(NCS)_2$**.**

The photo-voltage curve (J-V) of dye-sensitized solar cell, based on Ru-3, exhibited a short photo current density of 0.766 mA cm^{-2}, open circuit voltage of 0.53 V, and fill factor 0.51 at A.M 1.5 illumination. This dye-sensitized solar cell based on this complex exhibited a low solar to electricity conversion efficiency of 0.207 %, this is might be due to set-backs from the volatile liquid electrolyte, short live excited state of this complex, making it lack of electron injection into the conduction band of semiconductor, and resulting to low photovoltaic effect [1,3,4].

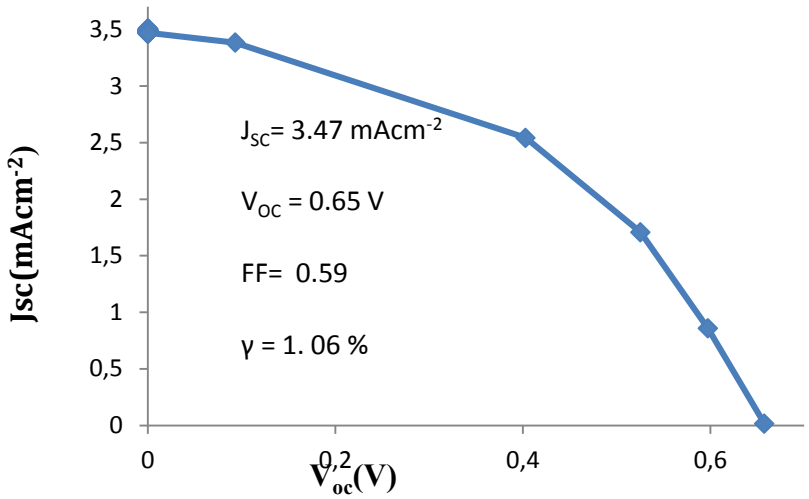

Figure 4.8: Photocurrent-voltage (I-V) curve for DSSC based on [Ru(bpy)(dcbpy)(NCS)$_2$

The above photocurrent-voltage curve of the dye-sensitized solar cell based on [Ru(bpy)(dcbpy)(NCS)$_2$]. The exhibited short-circuit photo current density (J_{sc}), open circuit voltage (V_{oc}) and the fill factor (FF) of the cell fabricated with [Ru(II)(bpy)(dcbpy)(NCS)$_2$] are as follows: 3.478 mAcm^{-2}, 0.65V, and 0.599 respectively at 100 mWcm^{-2} intensity. The yield overall solar conversion efficiency (η) 1.06 % at AM. 1.5 illumination. The low conversion efficiency of the solar cells from this complex compared to standard dye (N719) is probably due to hole transport property, that is the liquid organic electrolyte is volatile, which give a low V_{OC}, resulting to low solar energy conversion efficiency. However this complex is higher than other two complexes based sensitizers, this can be result of being N3 analogue and the simplicity of the structure, the presence of carboxylic acid group, that enhance the electron injection to conduction band of the semiconductor and better kinetics between hole transport material and oxidized dye. The high photo current density of this complex revealed that, there is a sufficient injection of electron to the conduction band of TiO_2 semiconductor, and the complex has a long time excited lifetime [8].

4.8 **References**

1. Erten-ela, S. Characterization and performance evaluation of dye sensitized solar Cell using nanostructured TiO_2 electrode. *Int. J. Photoenergy*. **2014**, *2014*, 1–6.

2. Giribabu, L.; Singh, V.K.; Kumar, C. V.; Soujanya, V. G. R.; Reddy, P.Y. Organic-ruthenium polypyridyl based sensitizer for dye-sensitized solar cell application. *Adv. Opt. Electronic,* **2011,** *2011,* 1-8.

3. Choi, S.; Cho, E.; Lee, S.; Kim, Y.; Lee, D. Evaluation of characteristics for dye-sensitized solar cell with reflector applied. *Optic. Express.* **2011***, 19,* 1-7

4. Soon, Y.; The development of novel Ru(II) polypyridyl complexes for application in dye sensitized solar cells. Ph.D. Thesis. Collage of Bowling Green. Dec, **2009**.

5. Nazeeruddin, M. K.; Bessho, T.; Cevey, L.; Ito, S.; Klein, C.; De Angelis, F.; Fantacci, S.; Comte, P.; Liska, P.; Imai, H.; Graetzel, M. A high molar extinction coefficient charge transfer sensitizer and its application in dye-sensitized solar cell. *J. Photochem. Photobiol. A Chem.* ***2007***, 185, 331-337.

6. Takagi, K.; S. Magaino, S.; Saito, H.; Aoki, T.; Aoki, D. Measurements and evaluation of dye-sensitized solar cell performance. *J. Photochem. Photobiol. C: Photochem. Rev.* **2013***, 14,* 1–12.

7. Ocakoglu, K.; Harputlu, E.; Guloglu, P.; Erten-Ela, S.; Design and synthesis of heteroleptic ruthenium (II) complexes and their applications in nanocrystalline TiO_2 solar cells. *Inorg. Chem. Commun.* **2012**, *24*, 118–124.

8. Nguyen, H. M.; Nguyen, D. N.; Kim, N. Improved performance of dye-sensitized solar cells by tuning the properties of ruthenium complexes containing conjugated bipyridine ligands. *Adv. Nat. Sci. Nanosci. Nanotechnol.* ***2010****, 1*. 1-6

CHAPTER 5

5.0 SUMMARY OF RESULTS CONCLUSION AND RECOMANDATION FOR FURTHER STUDIES

5.1 Summary of the results

We have managed to design and synthesize polypyridyl ligands based on 1,10-phenanthroline and 2,'2-bipyridine derivatives having different substituents on the ancillary ligands. The ligands were characterized by FT-IR, ^{1}H-NMR and melting point. The ligands showed a common peak at 2900-3300 cm^{-1} wich suggest the υ(-CH) stretch of the aromatic rings. ^{1}H-NMR of the ligands showed a prominent peaks at (σ) 6-8 ppm which suggests the doublets of the aromatic rings. Ruthenium complexes, heteroleptic and homoleptic were successfully synthesized and characterized by FT-IR, UV-Vis and fluorescence spectroscopy, there prominent peak at around 2100 cm^{-1} unique feature from the ligands. These complexes exhibited three shoulder absorption bands on UV-Vis spectra, at ultraviolet region 210-308 nm and at across the visible region 510-534 nm of the spectrum. The intense peak at ultraviolet region is (π-π*) transition within the polypyridyl ligands. The broad band absorption band across the visible region, is metal-to- ligands charge transfer (MLCT) transition. Also the meting point increase to ruthenium polypyridyl complexes may suggest the transformation of ligands to metal complexs. Some of these complexes showed an emission wavelength at around 699-700 nm, one has not intense enough and some that are not reported have low emission wave length. The metal-to-ligand charge transfer transition of these ruthenium polypyridyl complexes can at least confirms that the complexes were successfully synthesized, because there is strong, high intense peak at lower wavelength that common at all complexes and is due to (π-π*) (240-380 nm) and longer wavelength (490-533 nm) (MLCT) transitions that are due to intraligand charge transfer

and metal-to-ligand charge transfer respectively, and that is properties of (octahedral geometry) ruthenium complexes

The performance of the dye-sensitized solar cell based on ruthenium complexes were characterised by calculating open circuit voltage (V_{OC}), short circuit current density (J_{SC}), fill factor (FF) and overall electrical conversion efficiency using photo current-voltage (J-V) curve. The work also also reported the fabrication of the dye-sensitized solar cell based ruthenium(II) polypyridyl complexes using doctor blading technique. The dye sensitized solar cells were characterized using photo current- voltage (I-V) curve. The light to electricity conversion efficiency were 0.207-1.02 % which are lower than that of standard dye N719 dye sensitizer at standard global A.M 1.5 illumination all at constant $6x10^{-5}m^2$ area. The other obtained parameters were open circuit voltage (V_{OC}= 0.55-0.66 V), short circuit photo current J_{SC} (0.76-3.4 $mAcm^{-2}$), FF = 0.52-0.6 for ruthenium complexes coded as Ru-3, Ru-4 and Ru-6 in table 3.1.

The ruthenium complexes such as $[Ru(bpy)(dmbpy)(NCS)_2]$ showed a dark current, upon an illumination, the J-V curve observed was zigzag and zero efficiency. This could be probably the photo excited electron moved back ward without injection of electron, there is no anchoring group such as carboxylic group (-COOH) to anchored on TiO_2 interface

5.2 **Conclusion**

The prominent peak at 2100 cm^{-1} common in these complexes which are unique with to the features of ligands synthesised, confirms the N-coordination that is nitrogen of thiocyanate bonded to the Ru-metal centre, indicating the presence of metal. The metal-to- ligands charge

transfer (MLCT) transition which is the ruthenium polypyridyl complex properties, exhibited on UV-Vis spectra confirmed that ligands have bonded to the metal centre.

Based on the results, the ruthenium(II) complexes $[Ru(dsphen)(dcbpy)(NCS)_2]$, $[Ru(bpy)(dcbpy)(NCS)_2]$, using UV-Vis spectroscopy these complexes showed that can be used as dye-sensitizer in dye sensitized solar cells, because their absorption is at higher region of the electromagnetic spectrum λ_{max} = 520-530 nm, dominating the dominating the visible region of the spectrum. The emission properties of these complexes using photoluminiscence (PL) showed emission at high wavelength, suggesting that, their excited state life time is long enough, less chances to go for relaxation, before injection of electron to the conduction band of the TiO_2 semiconductor, which is the good requirement for dye-sensitized solar cells. The high intensity peak appeared on emission spectra suggest that have high molar extinction co-efficient and can harvest sunlight to convert into electricity. Therefore some of these ruthenium(II) polypyridyl complexes can qualify in dye-sensitized solar cells, because of the MLCT absorption across the visible region which is advantageous for solar light harvesting. This show they can harvest the ambient (sun) light. These complexes can also compete in the field or study of dye-sensitized solar, because some of them exhibit an appreciable absorption in the UV-Vis, and their MLCT absorption suppresses that of early reported complex N719 which have MLCT(λ_{nm} =528 nm).

Fabrication of dye-sensitized solar cells, based on the these complexes was successfully done, based on observation of the colour of the soaked TiO_2 thin film even after rinsed with ethanol,

this also showed that, these ruthenium complexes was successfully anchored on the TiO_2 interface with those carboxylic group (-COOH) and sulphonic ($-SO_3H$) groups of the ligands.

The photo current obtained from photon- to- current voltage (J-V) curve is 7.326-34 Am^{-2} suggest that, there current is generated, and there is charge separation and electron injection into the conduction band of the TiO_2 semiconductor. These complexes have low efficiency of only up to ~1.02 % than N719. The dye sensitized solar cells based on these sensitized solar cells are qualified for solar conversion into electricity, despite volatile liquid electrolyte that inhibits the solar cell performance.

Dye-sensitized solar cells fabrication done was environmentally friendly and convenient and they can replace the non-renewable and toxic fossil fuels.

The dye-sensitized solar cell based ruthenium complexes have a promising efficiency, and can be an alternative to conventional silicon based solar cells

5.3 **Recommendations**

These complexes need to be further synthesized, incorporate the more chromophoric groups into ancillary ligand, to increase the π-conjugation length, improving the absorption in visible to near IR region of solar spectrum. The high molar extinction coefficient can be obtained if complexes with high π-conjugated ligands and that are desirable property in dye-sensitized solar cells, because it increases the light harvesting efficiency.

The chromatography need to be employed into these complexes to purify, so that the both proton and carbon ^{1}H-NMR and mass spectroscopy could be easy to confirm or legitimatize the proposed structure.

The nonvolatile hole transporting material (HTM) that is electrolyte should be investigated because the volatile electrolyte lowers the dye-sensitized solar cell performance. The electrochemical impedance spectroscopy (EIS) needed to be used, to investigate the electron behavior on the surface of semiconductor and electrolyte solution, upon the photo excitation using the Nyquist plot.